SUPRAMOLECULAR DENDRIMER SELF-ASSEMBLIES BY COOPERATIVE BINDING

by

RONG JU

(Under the Direction of Yan Geng)

ABSTRACT

Cooperativity is a general principle that governs multivalent bindings in the supramolecular assemblies in nature, which is essential for a wide variety of biological structures and functions. Various model systems have been studied to reveal the energetics and mechanisms that underline cooperative bindings. However, not much effort has been made to maximize and utilize cooperative bindings towards constructing functional supramolecular assemblies. Dendrimers are nanometer-sized macromolecules with three-dimensional, highly-branched architectures, and can provide multivalent binding sites at the periphery. Here, we exploit the unique multivalency feature of dendrimers and their ability to maximize cooperative binding as a novel modular self-assembly approach to construct functional supramolecular structures.

First of all, we studied the self-assembly of spherical dendrimers via periphery cooperative salt-bridging. Dendrimers with carboxyl peripheral groups showed to form capsules in aqueous solutions with the addition of divalent metal ions. These capsules were tunable in size and thickness, and controllable in disassembly. To further exploit the cooperative feature of dendrimers, we revealed the ability of cooperative H-bonding in regulating supramolecular self-assemblies in highly-competitive solvents, *e.g.* water. These H-bonded dendrimer capsules have the advantage of the thermo-responsiveness to trigger controlled disassembly and release of encapsulated materials. Further more, emulsions were utilized to

template the cooperative self-assembly of dendrimers into a wide size range of capsules, which provides more versatility in the encapsulation of various materials.

To further advance the functionality of supramolecular dendrimer capsules, we explored the feasibility of combining π-π stacking at dendrimers' core with the periphery cooperative bindings. Dendrimers with an arene ring as the core self-assembled into capsules with dendrimers stack vertically in the membrane. This work provides the mechanistic foundation for incorporating functional micro-cycles into dendrimers core to generate capsules with sophisticated functionalities.

To explore the effect of shape symmetry in regulating supramolecular self-assemblies, the spatial symmetry of the dendrimer molecules are broken by coupling two different-sized but chemically identical dendritic fragments together. Asymmetric dendrimers assembled into cylindrical superstructures, either as parallel fibrillar bundles or supercoiled double-helices. This study provides new insights into supramolecular asymmetry, and offers a new systematic design principle for constructing novel asymmetrical supramolecular structures.

INDEX WORDS: supramolecular assembly, self-assembly, cooperativity, cooperative binding, dendrimer, dendron, electrostatic interactions, hydrogen bonding, π-π interactions, capsule, encapsulation, emulsion, symmetry, asymmetry, double helix

SUPRAMOLECULAR DENDRIMER SELF-ASSEMBLIES BY COOPERATIVE BINDING

by

Rong Ju

B.S., Peking University, China, 2006

A Dissertation Submitted to the Graduate Faculty of the University of Georgia in Partial Fulfillment of the Requirements for the Degree

DOCTOR OF PHILOSOPHY

ATHENS, GEORGIA

2011

SUPRAMOLECULAR DENDRIMER SELF-ASSEMBLIES BY COOPERATIVE BINDING

by

RONG JU

Major Professor:	Yan Geng
Committee:	George Majetich Jason Locklin

Electronic Version Approved:

Maureen Grasso
Dean of the Graduate School
The University of Georgia
May 2011

DEDICATION

I dedicate this dissertation to my loving family, especially ……

to my wonderful husband for his love, support and encouragement

to my loving mother for her love, support and encouragement

to the past ones. Your love and encouragement never left me.

ACKNOWLEDGEMENTS

The only thing I can think of right now is to express my sincerest gratitude to my wonderful husband, Jianfeng Zhou. You always stand by me for better or for worse. Your unconditional love and support encourage me to pursue my dream. To my parents, thank you for loving me, supporting me and always encouraging me to do better. I couldn't have achieved this without any you. To all my family membranes, I'm so fortunate to having all you loving ones.

I would like to express my thanks to my advisor, Dr. Yan Geng. I'm honored to become your PhD student and start my research under your instructions. You not only taught me the necessary knowledge, but the most importantly imparted me how to do research: how to question thoughts and express ideas. Your excellent guidance, caring and patience provided me an excellent atmosphere for developing my professional career.

I also would like to acknowledge my supportive and knowledgeable committee members, Dr. George Majetich and Dr. Jason Locklin. I own my special appreciation to both of you for support me through a lot of challenges. I sincerely thank Dr. Majetich for your support and encouragement, which helped me go through a lot of tough times. Your class "Organic Synthesis" is the most difficult class I ever took, but the abundant knowledge benefit me throughout my research. I also want to thank Dr. Locklin. You not only taught me a wonderful "Softer Matter" class, but also advised me on how to develop my professional career.

I am so fortunate to have the opportunity to work with so many kind and brilliant peoples. Jennifer Haley, you are the best lab mate anyone can think of. You are like a sister for me and I'm so happy we went through these together. Dr. Robert Woods and Matthew Tessier thank you

for your computational simulation work. Dr. Anne Summers and Dr. Lynda Ollif, thank you for your input on the ITC studies. I also offer my thanks to Dr. Jeffery Urbauer and Dr. Remona Urbauer for your tremendous help. I'll never forget that you even stay late just to wait for me finish experiments. Dr. John Shields, Dr. Jianguo Fan thank you for all the instrument guidance.

TABLE OF CONTENTS

Page

LIST OF TABLES

Page

LIST OF FIGURES

Page

CHAPTER 1

INTRODUCTION AND LITERATURE REVIEW

1.1 Supramolecular assembly

Supramolecular assembly is a complex but structurally well-defined chemical system constituted by a large number of assembled molecular subunits through noncovalent interactions.[1-3] Although the concept "supramolecular assembly" was first applied in 1976, nature has mastered the magic skill to create the most delicate supramolecular assemblies all along. More importantly, these structures and their assembly process are responsible for many critical biological functions:[4] (1) the formation of DNA double helix is essential for the replication, transcription and translation[5,6]; (2) the assembly and dis-assembly of protein subunits in cytoskeletons, *e.g.* microtubules and microfilaments, play important roles in both intracellular transport and cellular division[6,7]; (3) virus, *e.g.* polyhedron-shaped HIV virus and rod-shaped tobacco mosaic virus, are constituted by RNA and thousands of protein subunits, which execute protein synthesis.[8]

Supramolecular assemblies have been attracting tremendous attentions, mainly because of two reasons:

(1) By study the existing biological supramolecular assembly systems and the synthetic model structures, people can better understand the structural functionalities and energetic properties that underline the complicate biological processes, and possibly design and synthesize assembling systems to mimic these biological functions.

(2) Supramolecular assembly permits an access to manufacture nanometer-scaled functional structures using a bottom-up approach. By encoding information into the design of molecule entities, these building blocks could spontaneously assemble into functional structures, such as targeted drug/DNA delivery systems, fuel cell, or molecular electronics on the nanometer scale.

Because of the profound impact of supramolecular assembly studies, the most important goal is always to explore new building blocks and self-assembly mechanisms that can be applied in new and emerging fields.[3] With tremendous efforts, a variety of building blocks have been exploited in this field. There are nature existing polymeric structures, like peptide[9-12], RNA[13], DNA[14,15] and protein[16], as well as some small molecules[17,18], polymers/copolymer[19-25], and dendrimer/dendritic structures[26-32], and colloidal nanoparticles[33-37]. Various supramolecular assembly morphologies have been reviewed, such as sphere, polyhedron, cage rod, helix, sheet-like structures, toroids, vesicles, et.al., and they often have dimensions ranging from nanometers to micrometers.[38]

Supramolecular assemblies are usually formed via non-covalent interactions. As thermodynamic controlled systems, these relatively weak interactions allows forming, breaking, and reforming until the system find the lowest energy state-the final assembled structures. Several weak interactions have been utilized in the generation of supramolecular assemblies, including hydrophobic interactions, van der Waals interactions, electrostatic interactions, hydrogen bonding, π-π interactions, and metal coordination.[3,4] Especially, as the more directed interactions, hydrogen bonding, π-π interactions, and metal coordination are generally exploited to define the architectural specificities.[39-41]

1.2 Cooperativity in supramolecular self-assembly

Supramolecular assemblies are built up by relatively weak interactions, such as hydrophobic interactions, van der Waals interactions, electrostatic interactions, hydrogen bonding, π-π interactions, and metal coordination. When multiple weak interactions are combined together, they can lead to affinities that are strong enough to assemble molecules together. However, during this process, the final interaction does not simply equal the sum of all the weak interactions. This phenomenon is described as cooperativity.[3] When the final interaction is stronger than the simple sum of all the individual interactions, it is referred to as positive cooperativity, which can also be described as the Gibbs free energy of assembly is more negative than the sum of Gibbs free energy changes for individual interactions. When the opposite is true, negative cooperativity is informed.[3]

Cooperativity is a general principle that facilitates multivalent bindings between two entities, *e.g.* multivalent ligand-receptor interactions, as well as subunit binding in self-assembly processes. It is essential for a wide variety of biological assembling structures and functions.[42-45] The multivalent cooperative ligand-receptor binding is responsible for various proteins' and enzymes' functions,[46-49] such as the positive cooperative binding between hemoglobin and oxygen.[44,50] Subunit cooperativity is another commonly seen phenomenon, such as the folding and unfolding of proteins,[43] collective base pairing in DNA double-helix formation,[51-53] assembling of protein subunits into viral capsid,[54,55] clathrin cage and cytoskeleton superstructures[56,57].

Because of the importance of cooperativity, a lot of effort have been made to reveal the energetics and mechanisms that underline these multivalent cooperative bindings.[58-63] So far, various molecular recognition, guest-host and dimer complexation systems have been well

studied. Hunter and Tomas and co-workers studied the cooperative assembly of supramolecular ladder complexes composed of metalloporphyrin oligomers and showed that the origin of the beneficial free energy in positive cooperativity is only entropic without any enthalpic effects.[62] By studying the interactions between guanidinium and Cu(II) containing hosts for polycarboxylate guests in water, Anslyn and co-workers discovered a rarely seen positive cooperativity in the synthetic guest-hosts assembly in water.[59] The polyvalency of interactions in biological systems have been well studied, and utilized to design new targets and new strategies for pharmaceutical agents.[60]

To study the relatively weak energy in these cooperative bindings, various experimental techniques have been applied, *e.g.* UV-Vis, fluorescence spectroscopies, NMR and isothermal calorimetry. Both UV-Vis and Fluorescence spectroscopies are very sensitive, but they are limited to the systems with desirable spectroscopic groups. NMR is used to observe the signal shift associated with binding. The advantage of NMR is that that it can also provide structural information about binding. UV-vis, fluorescence spectroscopies and NMR can measure the binding constant by directly monitoring the concentration, and then Gibbs free energy change can be determined. However, in order to distinguish the contribution between enthalpy and entropy, multiple experiments at different temperatures have to be carried. Compared with the above techniques, isothermal calorimetry is much more efficient. By titrating one part of the binding system to the other, the heat released or absorbed in each step is measured, which allow us to directly determine the binding constant and enthalpy change, and then the Gibbs free energy change and entropy change can be obtained.

With the assistance of these techniques, cooperativity is becoming better understood and recognized. However, a very limited effort has been made to utilize and maximize multivalent

and subunit cooperative binding to construct functional supramolecular assemblies from large numbers of subunits.

1.3 Dendrimers: historical perspectives, properties and preparation methods

In this dissertation, we explored the unique features of dendrimers as nano-sized macromolecules with highly-branched peripheral binding sites, and their ability to maximize cooperative binding as a novel self-assembly approach to construct functional supramolecular assemblies.

Dendriemrs are macromolecules with roughly globular topology, monodispersed in size, and nanometers in dimension (1~10nm).[64,65] As described by the origin of its name - Greek word "tree", dendrimer has a repeatedly and highly branched architecture emanating from the core. The number of repeated branching cycles is referred to as a generation. Compared with traditional linear macromolecules, dendrimers have attracted broad interest due to their unique architectures and interesting properties. Typically, a dendrimer often appears roughly spherical with multiple functional groups on the molecular surface. The cavity inside the dendrimer allows for encapsulation of small functional molecules, which can be utilized to fabricate supramolecular assemblies with sophisticated functions. The multiple interaction sites makes them great candidate for cooperative bindings. A dendrimer's solubility and functionality are largely depended on the periphery functional groups. Therefore, dendrimers' properties can be easily modified from periphery for desired applications. The size of a dendrimer and the number of peripheral functional groups can be controlled via their generations, which further enhance the versatility of dendrimers as building blocks for supramolecular assembly.

There are two general synthetic methods to prepare dendrimers; the divergent approach and the convergent approach. In the divergent approach, the dendrimer grows from a core with

multifunctional groups, and a series of repetitive reactions will be applied to produce new generations. In the convergent approach, the dendrimer is assembled starting from small molecules that will eventually appear on the surface of dendrimer. Several rounds of reactions will be used to reach the desired generation until finally elaborated to a core.[64,65] The first dendritic structure was synthesized by Vögtle in 1978 using a divergent approach.[66] Seven years later, Tomalia and Newkome developed the first several dendrimers in 1985.[67-69] In 1990, Fréchet introduced the convergent approach[70]; for dendrimer formation, the convergent approach is more advantageous on increasing the monodispersity of the final dendrimers, because it is easier to remove the defected side products. However, due to the larger steric effects, it is very difficult to prepare large generation dendrimers through convergent approach. Recently a lot of new reactions and synthetic methods have been used to benefit dendrimer synthesis, such as click chemistry, solid phase synthesis, which greatly improves the purity and efficiency of dendrimer synthesis.[71,72]

Because of their unique properties, dendrimers, dendritic structures and their derivatives are also widely explored as building blocks in supramolecular assemblies, which will be discussed in detail next.

1.4 Current researches on dendrimer self-assemblies

One of the goals of supramolecular chemistry is to precisely control the structure and functionality of supramolecular assemblies by tuning the molecule structures. Because of the unique architectural properties, dendrimers and their derivatives have been vigorously pursued as versatile building blocks towards fabrication of a wide variety of functional supramolecular assemblies, particularly molecular recognition and self-assembly systems.[30,73-77]

In molecular recognition, two of a dendrimer's structural features, multiple periphery groups and inside cavity, are generally utilized. The active species, such as a dye, imaging particles, or pharmaceutically active compound, can be conjugated onto dendrimers' surface to make a dendrimer function as a detecting agent, an imaging agent, or as a drug targeting and delivery systems. [30,73,75-79] The inside cavities can also be utilized as a nano-sized container to encapsulate hydrophobic drugs, DNA/RNA, as well as reaction vessel to benefit the synthesis of products. Studies in this field have lead dendrimers into a wide range of potential applications, ranging from drug delivery, imaging agents, catalysts, sensors, remedidiation of industrial pollution, and nanosized reaction vectors, which have been subjected in numerous reviews.[30,73,75-79]

Other than molecular recognition, dendrimers are also utilized in self-assembly systems in bulk, in solution or on the surface. The self-assembly of dendrimers in bulk showed liquid-crystalline properties, and have been broadly and extensively reviewed.[75,78,80-82] Dendrimers can also assemble on surface to form monolayers, multilayers or surface patterns, which have been applied as sensosr, molecular printboards, and catalysts. The progresses in this field have also been reviewed.[83,84] As unique building blocks, dendrimers and dendritic structures also show the ability to self-assemble into various superstructures in solution, ranging from dimmers, oligomers, megamer clusters, rotaxane complexes to large assemblies such as vesicles, fibers and gels.[29,85-92] Tremendous effort has been made to design, synthesize new dendrimers, and study their self-assembly behaviors in solution. So far, the self-assemblies of dendrimer in solution were largely depended on traditional amphiphile hydrophobic interactions, dimeric/oligomeric linages via hydrogen bonding, metal complexation or electrostatic interactions, which will be reviewed below.

1.4.1 Hydrophobic interactions

Hydrophobic interactions are very important driving force for supramolecular assemblies in Nature. It also has been drastically exploited to construct functional assembly systems. In order to utilize this interaction, typically the molecule has to have a hydrophobic domain and a hydrophilic domain, as called an amphiphile. When an amphiphile is added to water, the hydrophobic domain will be excluded by the water molecules and will organize together to minimize their contact with the water.

A large amount of dendrimer assembly systems are based on hydrophobic interactions. These dendrimer structures are designed with both hydrophobic and hydrophilic domains. One commonly seen amphiphilic dendrimer class is the dendritic bolamphiphiles. Two hydrophilic dendritic structures are linked through a hydrophobic spacer. Newkome and co-workers developed a series of dendritic bolamphiphiles by linking two dendritic polyols with simple alkyl, alkyne chains, biphenyl units, or tetrathiafulvalene spacers.[67,93-95] These dumbbell-shaped bolamphiphiles form gels in water. Further detailed morphological studies and computational simulation showed that these molecules stack orthogonally via the hydrophobic interaction between the spacers, while the dendritic ends interact with each other through hydrogen bonding and get exposed to water. Fréchet and co-workers synthesized bolamphiphiles with hydrophobic 3,5-benzyl ether dendritic ends and hydrophilic PEO linker, and explored their solvent depended self-assembly behavior.[96-98] Another commonly seen amphiphilic dendrimer class is conjugating the dendrimer with linear polymers having different polarity. Meijer and co-works developed amphiphiles with polystyrene and poly (propylene imine) dendrimers and revealed that dendrimer generation and solvent can effect their self-assembly morphologies.[91] Percec and co-workers synthesized amphiphiles by conjugating 3,5-benzyl ether dendritic block onto a

dipeptides and they can self-assembles into helical porous structures.[99] Diblock codendrimers are also well studied. Wegner, Wei Wang and co-workers synthesized diblock coderdrimers of poly(benzyl ether) and poly(methallyl dichloride), which can self-assemble into vesicles with double layer membranes.[100] These vesicles are very soft, due to the loose packing of the dendrimers. Percec and co-workers recently developed a library of amphiphilic Janus dendrimers by coupling hydrophilic and hydrophobic dendritic building blocks.[29] These dendrimers can self-assemble into a wide variety of morphologies in water, including bilayer vesicles, disks, tubular vesicles, and helical ribbons. The resulting bilayer vesicles were called dendrimersomes. These dendrimersomes show great stability, permeability and mechanical stress. More impressively, unlike other classic amphiphiles, such as lipids, surfactants, and diblock copolymers, dendrimersomes have very low dispersity due to the unified molecule structures.

Amphiphilic dendrimers greatly enriched the amphiphile family, and are a versatile and powerful structure-directing building block for the construction of precise and functionalized supramolecular assemblies. However, there are also drawbacks for using amphiphilicity as the self-assembly driving force: (1) amphiphiles usually assemble into structures with bilayered membrane, which lacks the capability for tuning the thickness and then the permeability for more sophisticated functionalities and (2) the self-assembly of certain amphiphiles largely depends on the polarity of solvent, which realistically does not provide enough flexibility in controlling disassembly. In order to achieve the stimuli-responsive disassembly, molecules have to be specially designed with complicated stimuli-responsive domains.

1.4.2. Dimeric/oligomeric linages via hydrogen bonding

Among different non-covalent forces, hydrogen bonding is one of the most important binding interactions, which is not only essential to biological systems and processes, such as in

DNA double-helix formation and protein folding,[101] but also widely pursued in the fabrication of synthetic supramolecular assemblies.[38,102-105] However, a single hydrogen bond is weak. In order to organize molecules into discrete, ordered structures, multiple hydrogen bonds through encoded pre-organized arrays of complementary hydrogen bond donors and acceptors, combined with sterically constrained, well-defined molecular geometry, has been widely used in molecular design.[38,103,104]

Many elegant and inspiring examples of this classic approach have been reported, which has advanced our understanding of molecular recognition, host-guest complexation and supramolecular chemistry. One of the most well known examples of using hydrogen bonding in dendrimer self-assembly was developed by Zimmerman and co-workers.[86,106,107] Because of the carboxylic acid dimmer formation, isophthalic acid itself self-assemble into cyclic hexamers or linear, zigzag polymeric aggregates. By linking two isophthalic acid units with a rigid spacer, and then attaching Fréchet type 3,5-benzyl ether dendrons onto this tetraacid core, these dendrimers self-assembled into cyclic hexamers in organic solvent. By controlling the generation of the attached dendron, the stability of these cyclic hexamers could be controlled. Other core structures which can also form complementary hydrogen bonding arrays were used to construct hexametric, linear dendrimer self-assemblies. For example, Meijer and co-workers functionalized the periphery of poly(propylene imine) dendrimers with adamantylurea,[108] upon the addition of PEO containing ureido-acetic acid ends, they self-assembled into supramolecular dendrimer networks through hydrogen bonding between adamantylurea and ureido-acetic acid. Other than these complex self-assembly morphologies, hydrogen bondings are also used to link dendrons together into dendrimers.[109,110]

While hydrogen bonding provides precise control over the assembly architectures, this strategy is largely limited to making dimers and cyclic oligomers, and is difficult to use to fabricate more complex assemblies from large numbers of molecular subunits. Another great challenge for hydrogen bonding is that it is strongly solvent dependent and prone to be disrupted in competitive solvents. For example, water is the exclusive solvent in nature yet one of the most difficult media for intermolecular hydrogen bonding.[101] How to strategically construct robust and functional molecular self-assembly by hydrogen bonding in aqueous solution represents a formidable yet important task.

1.4.3. Metal complexation

Metal complexation is an essential part in supramolecular chemistry, as well as dendrimer chemistry, and has been the subject of numerous reviews.[111-113] The metal ion can be used to assemble two or three dendrons together. The assembly of dendrimers via metal coordination was first reported by Newkome and co-workers, where by two different dendrons having a terpyridine core are linked together by ruthenium ion.[114] Chow and co-workers studied the properties of dendrimers with ruthenium and iron ions as models of redox proteins.[115] Fréchet and co-workers reported the assembly of three identical dendrons linked together by the coordination of a lanthanide cation.[116,117] Other than locating coordination center in the dendrimers' core, metal ions can be found throughout all layers. Balzani and co-workers developed a dendrimer construction method using ruthenium ion at all of the branch points to connect all of the subunits together.[118,119] Astruc and co-workers showed that by coupling dicyclopentadienyl iron onto dendrimer's periphery, dendrimer can function as electrochemical sensor to recognize both oxo-anions and late transition-metals cations.[120-122] The utilization of metal coordination in dendrimer supramolecular chemistry has been explored as catalysts,

photochemical devices and molecular electronics. However, this design strategy is limited to making dendrimers from dendritic subunits, and it is difficult to use for the production of more complex assemblies.

1.4.4. Electrostatic interaction

Electrostatic interactions have also been exploited as the design strategy for dendrimer self-assemblies. Dendrimers with cationic terminal groups showed to bind with DNA or oligonucleotides via electrostatic interactions. Dendrimer-loaded DNA microarrays and biosensors have been the subject of several reviews.[123-126] Newkome and co-workers reported the formation of superstructures by the multi-ion pairing between dendrimer and metallomacrocycle.[90] The stable nanofibers were produced by the ion-promoted, automorphogenic and stoichiometric self-assembly utilizing the negatively charged, first generation dodeca carboxylate-terminated dendrimers and positively charged, rigid Ru-containing hexameric macrocycle. When 3rd generation dendrimers were used, spheres were obtained. Recently, Aida and co-workers reported the formation of high-water-content mouldable hydrogels by mixing clay and a very small proportion of dendritic molecules. Basically, the positively charged dendritic molecules served as binders to crosslink the clay nano-sheets together into a supramolecular network via salt-bridging.[127]

1.5 Challenges in current research

In the past few decades, dendrimers have been used to construct functionalized supramolecular assemblies. However, there are still many challenges remain unsolved.

First of all, the controllable fabrication of nanometer-scale functional structures is one of the central issues in supramolecular studies.[128] Because of the disadvantages of the current design strategies, the development of alternative approaches is indispensable. As we have

discussed previously, cooperativity is essential for a wide variety of biological assembling structures and functions. However, little work has been done to combine and maximize multivalent and subunit cooperative binding towards constructing supramolecular self-assemblies from large numbers of subunits. On the other hand, dendrimer self-assemblies, however, were largely based on traditional amphiphile hydrophobic effect, guest-host complexation, or dimeric/oligomeric linkages via H-bonding or metal coordination. The unique features of dendrimers as molecular spheres with highly-branched peripheral binding sites hasn't been fully explored in supramolecular self-assembly.

Secondly, constructing functional supramolecular assemblies are always difficult in competitive solvents-water, since these competitive solvent would interrupt the weak interactions-hydrogen bonding. That's why the traditional strategies of utilizing the more directed interactions, *e.g.* hydrogen bonding, π-π interactions, and metal coordination, are largely limited to making dimers and cyclic oligomers in solution. The less specific and directional hydrophobic interactions are widely utilized in aqueous solution to provide strong enough driving force to hold molecules together. However, hydrophobic interactions' nature decides they wouldn't provide sufficient architectural specificities. In order to utilize the more directed interactions to fabricate delicate assemblies from large numbers of molecular subunits, the new self-assembly approaches are needed to overcome the energy barrier from solvent interruption.

Thirdly, one of the greatest achievements of supramolecular chemistry is that it provides a convenient bottom-up approach to fabricate nano-scaled capsules. These capsules have been widely applied in many technologies, ranging from drug delivery, food processing, waste removal, to catalysis, artificial enzyme reactors and protein/cell transplantations. However, efficient and selective encapsulation is always challenging. Many different approaches have been

engineered to achieve the desired encapsulation. Among these approaches, using emulsion as templates to direct capsule formation has the advantages of simplicity, effectiveness and versatility, and has attracted lots of interest. Nanometer- to micrometer- sized spherical particles were shown to spontaneously adsorb onto the emulsion surface. However, treatments have to be performed to interlock these particles together into solid capsules. Despite the tremendous success with solid nanoparticles and colloidal particles, little attention has been given to applying this general emulsion adsorption mechanism to molecules. This is probably because most molecules are not suitable for this application, since they are below nanometer in size and highly dynamic in molecular conformations. Dendrimers have the unique nanometer size and spherical architecture. However, the ability of dendrimers to spontaneously adsorb onto emulsion droplet surface – just as solid nanoparticles- has not been explored.

Fourthly, symmetry is an important structural property that influences the functions and properties of objects at all scales, ranging from molecules and nano/micro-particles to macroscopic matters. Considerable effort has been made to construct chiral supramolecular structures that maybe of interest for optoelectronic applications, or as templates for functional nanoparticle self-assemblies for chiral catalysis and sensor applications. The most popular design strategy is by incorporating chiral centers within the molecular subunits to generate asymmetric supramolecular complexes. However, the asymmetric components are not limited to chiral center. Little efforts has been made to reveal how the simple shape non-symmetry of molecules subunits can impact their supramolecular self-assembly processes.

1.6 The goal and organization of this dissertation

1.6.1. Overall goal

As introduced above, cooperativity is a general principle that facilitate multivalent binding in the functional self-assembly process, which is essential for a wide variety of biological assembling structures and functions. However, cooperativity has not been fully utilized for generating synthetic functional supramolecular assemblies. The existing challenges supramolecular chemistry facing would further lead us to search for new ways to utilize and maximizing cooperativity to fabricate functional supramolecular assemblies. Dendrimers are nanometer-sized macromolecules with three-dimensional, highly-branched architectures. The multivalent binding sites on dendrimers' surface make them ideal candidates for maximize cooperativity. Therefore, the overall goal of my Ph.D study is to explore the unique feature of dendrimers and their ability to maximize cooperative binding as a novel self-assembly approach to construct functional supramolecular structures.

1.6.2. Organization of this thesis

In Chapter 2, we demonstrated that the unique features of dendrimers can maximize cooperative binding and enable their self-assembly into capsules via electrostatic interactions. Dendrimers with carboxyl peripheral groups self-assembled into capsules in aqueous solution with the addition of divalent metal ions. These supramolecular capsules are tunable in size and thickness, controllable in disassembly, and can be potentially used for a wide variety of encapsulation applications.

In Chapter 3, we further exploit the cooperative feature of dendrimers and reveal the intriguing ability of cooperative H-bonding in regulating supramolecular self-assembled capsules in highly-competitive solvents. Such cooperatively H-bonded dendrimer capsules can

conveniently encapsulate guest materials into their cavity, and have the advantage of the thermo-responsive functionality to trigger controlled disassembly of the capsules and release of the encapsuslant.

In Chapter 4, emulsion template assembly was utilized to direct the cooperative self-assembly of dendrimers into a wide size range of supramolecular capsules. The unique feature of dendrimer and the flexibility of emulsification in the encapsulation of various materials allows for generating more sophisticated encapsulation systems, which can be potentially used for a wide variety of applications.

In Chapter 5, we explored the feasibility of combining other more directed interactions, ***e.g.*** hydrogen bonding, π-π interactions at dendrimers' core with the periphery cooperative bindings. Dendrimers with an arene ring as the core self-assembled into capsules via periphery cooperative bindings, meanwhile the π-π interactions at dendrimers' core help stack them co-facially in membrane. This work provide the foundation for further incorporating functional groups into dendrimers core to generate dendrimer capsules with built-in pores/channels, which can spontaneously and selectively encapsulate or release certain materials.

In Chapter 6, the effect of shape symmetry in regulating the supramolecular self-assembly will be discussed. By coupling two different-sized but chemically identical dendritic fragments together, the spatial symmetry of dendrimer molecules are broken. Asymmetric dendrimers showed to assemble into cylindrical superstructures, from parallel fibrillar bundles to supercoiled double-helices. This study provides new insights into supramolecular asymmetry, and offers a new systematic design principle for constructing novel asymmetrical supramolecular structures that maybe of interest for optoelectronic applications, or as functional nanoparticle templates for chiral catalysis and sensor applications.

1.7 References

(1) Lehn, J. M. *Supramolecular chemistry : concepts and perspectives : a personal account built upon the George Fisher Baker lectures in chemistry at Cornell University and the Lezione Lincee, Accademia nazionale dei Lincei, Roma*; VCH: Weinheim ; New York, 1995.

(2) Lehn, J. M. *Science* **1993**, *260*, 1762-1763.

(3) Anslyn, E. V.; Dougherty, D. A. *Modern physical organic chemistry*; University Science: Sausalito, Calif., 2006.

(4) Cragg, P. J.; SpringerLink (Online service) *Supramolecular chemistry from biological inspiration to biomedical applications*; Springer: Dordrecht ; London.

(5) Berg, J. M.; Tymoczko, J. L.; Stryer, L. *Biochemistry*; 6th ed.; W. H. Freeman: New York, 2007.

(6) Alberts, B. *Molecular Biology of the Cell*; 4th ed.; Garland Science: New York, 2002.

(7) Frixione, E. *Cell Motil. Cytoskeleton* **2000**, *46*, 73-94.

(8) Society for General Microbiology. Symposium (60th : 2001 : Heriot-Watt University); Smith, G. L.; Society for General Microbiology. *New challenges to health: the threat of virus infection*; Cambridge University Press: Cambridge, 2001.

(9) Ghadiri, M. R.; Granja, J. R.; Buehler, L. K. *Nature* **1994**, *369*, 301-304.

(10) Ghadiri, M. R.; Granja, J. R.; Milligan, R. A.; Mcree, D. E.; Khazanovich, N. *Nature* **1993**, *366*, 324-327.

(11) Nowak, A. P.; Breedveld, V.; Pakstis, L.; Ozbas, B.; Pine, D. J.; Pochan, D.; Deming, T. J. *Nature* **2002**, *417*, 424-428.

(12) Cui, H. G.; Pashuck, E. T.; Velichko, Y. S.; Weigand, S. J.; Cheetham, A. G.; Newcomb, C. J.; Stupp, S. I. *Science* **2010**, *327*, 555-559.

(13) Chworos, A.; Severcan, I.; Koyfman, A. Y.; Weinkam, P.; Oroudjev, E.; Hansma, H. G.; Jaeger, L. *Science* **2004**, *306*, 2068-2072.

(14) Douglas, S. M.; Dietz, H.; Liedl, T.; Hogberg, B.; Graf, F.; Shih, W. M. *Nature* **2009**, *459*, 414-418.

(15) He, Y.; Ye, T.; Su, M.; Zhang, C.; Ribbe, A. E.; Jiang, W.; Mao, C. D. *Nature* **2008**, *452*, 198-U141.

(16) Diehl, M. R.; Zhang, K. C.; Lee, H. J.; Tirrell, D. A. *Science* **2006**, *311*, 1468-1471.

(17) MacGillivray, L. R.; Atwood, J. L. *Nature* **1997**, *389*, 469-472.

(18) Engelkamp, H.; Middelbeek, S.; Nolte, R. J. M. *Science* **1999**, *284*, 785-788.

(19) Greef, T. F. A.; Meijer, E. W. *Nature* **2008**, *453*, 171-173.

(20) Hirschberg, J. H. K. K.; Brunsveld, L.; Ramzi, A.; Vekemans, J. A. J. M.; Sijbesma, R. P.; Meijer, E. W. *Nature* **2000**, *407*, 167-170.

(21) Cornelissen, J. J. L. M.; Fischer, M.; Sommerdijk, N. A. J. M.; Nolte, R. J. M. *Science* **1998**, *280*, 1427-1430.

(22) Discher, B. M.; Won, Y. Y.; Ege, D. S.; Lee, J. C. M.; Bates, F. S.; Discher, D. E.; Hammer, D. A. *Science* **1999**, *284*, 1143-1146.

(23) Pochan, D. J.; Chen, Z. Y.; Cui, H. G.; Hales, K.; Qi, K.; Wooley, K. L. *Science* **2004**, *306*, 94-97.

(24) Discher, D. E.; Eisenberg, A. *Science* **2002**, *297*, 967-973.

(25) Geng, Y.; Discher, D. E.; Justynska, J.; Schlaad, H. *Angew. Chem., Int. Ed.* **2006**, *45*, 7578-7581.

(26) Percec, V.; Glodde, M.; Bera, T. K.; Miura, Y.; Shiyanovskaya, I.; Singer, K. D.; Balagurusamy, V. S. K.; Heiney, P. A.; Schnell, I.; Rapp, A.; Spiess, H. W.; Hudson, S. D.; Duan, H. *Nature* **2002**, *419*, 862-862.

(27) Zeng, X. B.; Ungar, G.; Liu, Y. S.; Percec, V.; Dulcey, S. E.; Hobbs, J. K. *Nature* **2004**, *428*, 157-160.

(28) Frechet, J. M. J. *Proc. Natl. Acad. Sci. U. S. A.* **2002**, *99*, 4782-4787.

(29) Percec, V.; Wilson, D. A.; Leowanawat, P.; Wilson, C. J.; Hughes, A. D.; Kaucher, M. S.; Hammer, D. A.; Levine, D. H.; Kim, A. J.; Bates, F. S.; Davis, K. P.; Lodge, T. P.; Klein, M. L.; DeVane, R. H.; Aqad, E.; Rosen, B. M. *Science* **2010**, *328*, 1009-1014.

(30) Zeng, F. W.; Zimmerman, S. C. *Chem. Rev.* **1997**, *97*, 1681-1712.

(31) Percec, V.; Ahn, C. H.; Ungar, G.; Yeardley, D. J. P.; Moller, M.; Sheiko, S. S. *Nature* **1998**, *391*, 161-164.

(32) Percec, V.; Dulcey, A. E.; Balagurusamy, V. S. K.; Miura, Y.; Smidrkal, J.; Peterca, M.; Nummelin, S.; Edlund, U.; Hudson, S. D.; Heiney, P. A.; Hu, D. A.; Magonov, S. N.; Vinogradov, S. A. *Nature* **2004**, *430*, 764-768.

(33) Dinsmore, A. D.; Hsu, M. F.; Nikolaides, M. G.; Marquez, M.; Bausch, A. R.; Weitz, D. A. *Science* **2002**, *298*, 1006-1009.

(34) Zerrouki, D.; Baudry, J.; Pine, D.; Chaikin, P.; Bibette, J. *Nature* **2008**, *455*, 380-382.

(35) Chiruvolu, S.; Walker, S.; Israelachvili, J.; Schmitt, F. J.; Leckband, D.; Zasadzinski, J. A. *Science* **1994**, *264*, 1753-1756.

(36) Li, M.; Schnablegger, H.; Mann, S. *Nature* **1999**, *402*, 393-395.

(37) Manoharan, V. N.; Elsesser, M. T.; Pine, D. J. *Science* **2003**, *301*, 483-487.

(38) Lawrence, D. S.; Jiang, T.; Levett, M. *Chem. Rev.* **1995**, *95*, 2229-2260.

(39) Hoeben, F. J. M.; Jonkheijm, P.; Meijer, E. W.; Schenning, A. P. H. J. *Chem. Rev.* **2005**, *105*, 1491-1546.

(40) Holliday, B. J.; Mirkin, C. A. *Angew. Chem., Int. Ed.* **2001**, *40*, 2022-2043.

(41) Prins, L. J.; Reinhoudt, D. N.; Timmerman, P. *Angew. Chem., Int. Ed.* **2001**, *40*, 2382-2426.

(42) Ben-Naim, A. *Cooperativity and regulation in biochemical processes*; Kluwer Academic/Plenum Publishers: New York, 2001.

(43) Perutz, M. F. *Mechanisms of cooperativity and allosteric regulation in proteins*; Cambridge University Press: Cambridge [England] ; New York, 1990.

(44) Weissbluth, M. *Hemoglobin : cooperativity and electronic properties*; Chapman and Hall ;Springer Verlag: London&New York, 1974.

(45) Hill, T. L. *Cooperativity theory in biochemistry : steady-state and equilibrium systems*; Springer-Verlag: New York, 1985.

(46) Kuo, L. C. *Proc. Natl. Acad. Sci. U. S. A.* **1983**, *80*, 5243-5247.

(47) Qian, H.; Shi, P. Z. *J. Phys. Chem. B* **2009**, *113*, 2225-2230.

(48) Koshland, D. E.; Hamadani, K. *J. Biol. Chem.* **2002**, *277*, 46841-46844.

(49) Lindberg, D.; Revenga, M. D.; Widersten, M. *Biochemistry* **2010**, *49*, 2297-2304.

(50) Tsai, C. H.; Fang, T. Y.; Ho, N. T.; Ho, C. *Biochemistry* **2000**, *39*, 13719-13729.

(51) Ivanov, V.; Piontkovski, D.; Zocchi, G. *Phys. Rev. E* **2005**, *71*, 8.

(52) Groebke, K.; Hunziker, J.; Fraser, W.; Peng, L.; Diederichsen, U.; Zimmermann, K.; Holzner, A.; Leumann, C.; Eschenmoser, A. *Helv. Chim. Acta* **1998**, *81*, 375-474.

(53) Krueger, A.; Protozanova, E.; Frank-Kamenetskii, M. D. *Biophys. J.* **2006**, *90*, 3091-3099.

(54) Zlotnick, A. *J. Mol. Biol.* **1994**, *241*, 59-67.

(55) Wruss, J.; Runzler, D.; Steiger, C.; Chiba, P.; Kohler, G.; Blaas, D. *Biochemistry* **2007**, *46*, 6331-6339.

(56) Wakeham, D. E.; Chen, C. Y.; Greene, B.; Hwang, P. K.; Brodsky, F. M. *Embo J.* **2003**, *22*, 4980-4990.

(57) Badley, R. A.; Woods, A.; Rees, D. A. *J. Cell Sci.* **1981**, *47*, 349-363.

(58) Jencks, W. P. *Proc. Natl. Acad. Sci. U. S. A.* **1981**, *78*, 4046-4050.

(59) Hughes, A. D.; Anslyn, E. V. *Proc. Natl. Acad. Sci. U. S. A.* **2007**, *104*, 6538-6543.

(60) Mammen, M.; Choi, S. K.; Whitesides, G. M. *Angew. Chem., Int. Ed.* **1998**, *37*, 2755-2794.

(61) Silva, J. L.; Verjovskialmeida, S. *Braz. J. Med. Biol. Res.* **1981**, *14*, 199-199.

(62) Camara-Campos, A.; Hunter, C. A.; Tomas, S. *Proc. Natl. Acad. Sci. U. S. A.* **2006**, *103*, 3034-3038.

(63) Ercolani, G. *J. Am. Chem. Soc.* **2003**, *125*, 16097-16103.

(64) Newkome, G. R.; Moorefield, C. N.; Vogtle, F. *Dendritic Macromolecules: Concepts, Synthesis, Perspectives*; VCH, Wenheim, Germany, 2001.

(65) Frechet, J. M. J.; Tamalia, D. A. *Dendrimers and Other Dendritic Polymers*; Whiley,: Chichester, UK, 2001.

(66) Buhleier, E.; Wehner, W.; Vogtle, F. *Synthesis-Stuttgart* **1978**, 155-158.

(67) Newkome, G. R.; Baker, G. R.; Saunders, M. J.; Russo, P. S.; Gupta, V. K.; Yao, Z. Q.; Miller, J. E.; Bouillion, K. *J. Am. Chem. Soc.,Chem. Commun.* **1986**, 752-753.

(68) Newkome, G. R.; Yao, Z. Q.; Baker, G. R.; Gupta, V. K.; Russo, P. S.; Saunders, M. J. *J. Am. Chem. Soc.* **1986**, *108*, 849-850.

(69) Tomalia, D. A.; Baker, H.; Dewald, J.; Hall, M.; Kallos, G.; Martin, S.; Roeck, J.; Ryder, J.; Smith, P. *Polym. J.* **1985**, *17*, 117-132.

(70) Hawker, C. J.; Frechet, J. M. J. *Macromolecules* **1990**, *23*, 4726-4729.

(71) Lebreton, S.; Monaghan, S.; Bradley, M. *Aldrichimica Acta* **2001**, *34*, 75-83.

(72) Franc, G.; Kakkar, A. *Chem. Commun.* **2008**, 5267-5276.

(73) Emrick, T.; Frechet, J. M. J. *Curr. Opin. Colloid Interface Sci.* **1999**, *4*, 457-457.

(74) Matthews, O. A.; Shipway, A. N.; Stoddart, J. F. *Prog. Polym. Sci.* **1998**, *23*, 1-56.

(75) Rosen, B. M.; Wilson, C. J.; Wilson, D. A.; Peterca, M.; Imam, M. R.; Percec, V. *Chem. Rev.* **2009**, *109*, 6275-6540.

(76) Smith, D. K.; Diederich, F. *Dendrimers Ii* **2000**, *210*, 183-227.

(77) Smith, D. K.; Hirst, A. R.; Love, C. S.; Hardy, J. G.; Brignell, S. V.; Huang, B. Q. *Prog. Polym. Sci.* **2005**, *30*, 220-293.

(78) Astruc, D.; Boisselier, E.; Ornelas, C. *Chem. Rev.*, *110*, 1857-1959.

(79) Fischer, M.; Vogtle, F. *Angew. Chem., Int. Ed.* **1999**, *38*, 885-905.

(80) Donnio, B.; Buathong, S.; Bury, I.; Guillon, D. *Chem. Soc. Rev.* **2007**, *36*, 1495-1513.

(81) Marcos, M.; Martin-Rapun, R.; Omenat, A.; Serrano, J. L. *Chem. Soc. Rev.s* **2007**, *36*, 1889-1901.

(82) Donnio, B.; Guillon, D. In *Supramolecular Polymers Polymeric Betains Oligomers*; Springer-Verlag Berlin: Berlin, 2006; Vol. 201, p 45-155.

(83) Zimmerman, S. C.; Lawless, L. J. In *Dendrimers Iv*; Springer-Verlag Berlin: Berlin, 2001; Vol. 217, p 95-120.

(84) Smith, D. K.; Diederich, F. In *Dendrimers Ii*; Springer-Verlag Berlin: Berlin, 2000; Vol. 210, p 183-227.

(85) Giles, M. D.; Liu, S. M.; Emanuel, R. L.; Gibb, B. C.; Grayson, S. M. *J. Am. Chem. Soc.* **2008**, *130*, 14430-+.

(86) Zimmerman, S. C.; Zeng, F. W.; Reichert, D. E. C.; Kolotuchin, S. V. *Science* **1996**, *271*, 1095-1098.

(87) Tomalia, D. A.; Brothers, H. M.; Piehler, L. T.; Durst, H. D.; Swanson, D. R. *Proc. Natl. Acad. Sci. U. S. A.* **2002**, *99*, 5081-5087.

(88) Stevelmans, S.; vanHest, J. C. M.; Jansen, J.; vanBoxtel, D.; vandenBerg, E.; Meijer, E. W. *J. Am. Chem. Soc.* **1996**, *118*, 7398-7399.

(89) Amabilino, D. B.; Ashton, P. R.; Balzani, V.; Brown, C. L.; Credi, A.; Frechet, J. M. J.; Leon, J. W.; Raymo, F. M.; Spencer, N.; Stoddart, J. F.; Venturi, M. *J. Am. Chem. Soc.* **1996**, *118*, 12012-12020.

(90) Wang, P.; Moorefield, C. N.; Jeong, K. U.; Hwang, S. H.; Li, S.; Cheng, S. Z. D.; Newkome, G. R. *Adv. Mater.* **2008**, *20*, 1381-+.

(91) Vanhest, J. C. M.; Delnoye, D. A. P.; Baars, M. W. P. L.; Vangenderen, M. H. P.; Meijer, E. W. *Science* **1995**, *268*, 1592-1595.

(92) Ungar, G.; Liu, Y. S.; Zeng, X. B.; Percec, V.; Cho, W. D. *Science* **2003**, *299*, 1208-1211.

(93) Newkome, G. R.; Baker, G. R.; Arai, S.; Saunders, M. J.; Russo, P. S.; Theriot, K. J.; Moorefield, C. N.; Rogers, L. E.; Miller, J. E.; Lieux, T. R.; Murray, M. E.; Phillips, B.; Pascal, L. *J. Am. Chem. Soc.* **1990**, *112*, 8458-8465.

(94) Newkome, G. R.; Moorefield, C. N.; Baker, G. R.; Behera, R. K.; Escamillia, G. H.; Saunders, M. J. *Angew. Chem., Int. Ed. in English* **1992**, *31*, 917-919.

(95) Newkome, G. R.; Lin, X. F.; Chen, Y. X.; Escamilla, G. H. *J. Org. Chem.* **1993**, *58*, 7626-7626.

(96) Gitsov, I.; Wooley, K. L.; Frechet, J. M. J. *Angew. Chem., Int. Ed. in English* **1992**, *31*, 1200-1202.

(97) Gitsov, I.; Wooley, K. L.; Hawker, C. J.; Ivanova, P. T.; Frechet, J. M. J. *Macromolecules* **1993**, *26*, 5621-5627.

(98) Frechet, J. M. J.; Gitsov, I. *Macromol. Symp.* **1995**, *98*, 441-465.

(99) Percec, V.; Dulcey, A. E.; Peterca, M.; Ilies, M.; Nummelin, S.; Sienkowska, M. J.; Heiney, P. A. *Proc. Natl. Acad. Sci. U. S. A.* **2006**, *103*, 2518-2523.

(100) Yang, M.; Wang, W.; Yuan, F.; Zhang, X.; Li, J.; Liang, F.; He, B.; He, B.; Minch, B.; Wegner, G. *J. Am. Chem. Soc.* **2005**, *127*, 15107-15111.

(101) Jeffrey, G. A.; Saenger, W. *Hydrogen Bonding in Biological Structures*; Springer-Verlag: Berlin, 1991.

(102) Whitesides, G. M.; Mathias, J. P.; Seto, C. T. *Science* **1991**, *254*, 1312-1319.

(103) Whitesides, G. M.; Mathias, J. P.; Seto, C. T. *Science* **1991**, *254*, 1312-1319.

(104) Krische, M. J.; Lehn, J. M. *Molecular Self-Assembly* **2000**, *96*, 3-29.

(105) Dong, W. Y.; Zhou, Y. F.; Yan, D. Y.; Li, H. Q.; Liu, Y. *Phys. Chem. Chem. Phys.* **2007**, *9*, 1255-1262.

(106) Corbin, P. S.; Lawless, L. J.; Li, Z. T.; Ma, Y. G.; Witmer, M. J.; Zimmerman, S. C. *Proc. Natl. Acad. Sci. U. S. A.* **2002**, *99*, 5099-5104.

(107) Ma, Y. G.; Kolotuchin, S. V.; Zimmerman, S. C. *J. Am. Chem. Soc.* **2002**, *124*, 13757-13769.

(108) Versteegen, R. M.; van Beek, D. J. M.; Sijbesma, R. P.; Vlassopoulos, D.; Fytas, G.; Meijer, E. W. *J. Am. Chem. Soc.* **2005**, *127*, 13862-13868.

(109) Rudzevich, Y.; Rudzevich, V.; Moon, C.; Schnell, I.; Fischer, K.; Bohmer, V. *J. Am. Chem. Soc.* **2005**, *127*, 14168-14169.

(110) Wang, Y.; Zeng, F. W.; Zimmerman, S. C. *Tetrahedron Lett.* **1997**, *38*, 5459-5462.

(111) Mery, D.; Astruc, D. *Coord. Chem. Rev.* **2006**, *250*, 1965-1979.

(112) Reek, J. N. H.; Arevalo, S.; Van Heerbeek, R.; Kamer, P. C. J.; Van Leeuwen, P. In *Advances in Catalysis, Vol 49*; Elsevier Academic Press Inc: San Diego, 2006; Vol. 49, p 71-151.

(113) Hwang, S. H.; Shreiner, C. D.; Moorefield, C. N.; Newkome, G. R. *New J. Chem.* **2007**, *31*, 1192-1217.

(114) Newkome, G. R.; Guther, R.; Moorefield, C. N.; Cardullo, F.; Echegoyen, L.; Perezcordero, E.; Luftmann, H. *Angew. Chem., Int. Ed. in English* **1995**, *34*, 2023-2026.

(115) Chow, H. F.; Chan, I. Y. K.; Chan, D. T. W.; Kwok, R. W. M. *Chem.-Eur. J.* **1996**, *2*, 1085-1091.

(116) Kawa, M.; Frechet, J. M. J. *Thin Solid Films* **1998**, *331*, 259-263.

(117) Kawa, M.; Frechet, J. M. J. *Chem. Mater.* **1998**, *10*, 286-296.

(118) Serroni, S.; Campagna, S.; Puntoriero, F.; Juris, A.; Denti, G.; Balzani, V.; Venturi, M. In *Inorganic Syntheses, Vol 33*; John Wiley & Sons Inc: New York, 2002; Vol. 33, p 10-18.

(119) Venturi, M.; Serroni, S.; Juris, A.; Campagna, S.; Balzani, V. In *Dendrimers*; Springer-Verlag Berlin: Berlin 33, 1998; Vol. 197, p 193-228.

(120) Camponovo, J.; Ruiz, J.; Cloutet, E.; Astruc, D. *Chem.-Eur. J.* **2009**, *15*, 2990-3002.

(121) Ornelas, C.; Aranzaes, J. R.; Cloutet, E.; Alves, S.; Astruc, D. *Angew. Chem., Int. Ed.* **2007**, *46*, 872-877.

(122) Astruc, D.; Blais, J. C.; Cloutet, E.; Djakovitch, L.; Rigaut, S.; Ruiz, J.; Sartor, V.; Valerio, C. In *Dendrimers Ii*; Springer-Verlag Berlin: Berlin, 2000; Vol. 210, p 229-259.

(123) Rosi, N. L.; Mirkin, C. A. *Chem. Rev.* **2005**, *105*, 1547-1562.

(124) Caminade, A. M.; Turrin, C. O.; Majoral, J. P. *New J. Chem. 34*, 1512-1524.

(125) Caminade, A. M.; Turrin, C. O.; Majoral, J. P. *Chem.-Eur. J.* **2008**, *14*, 7422-7432.

(126) Caminade, A. M.; Padie, C.; Laurent, R.; Maraval, A.; Majoral, J. P. *Sensors* **2006**, *6*, 901-914.

(127) Wang, Q.; Mynar, J. L.; Yoshida, M.; Lee, E.; Lee, M.; Okuro, K.; Kinbara, K.; Aida, T. *Nature*, *463*, 339-343.

(128) Ariga, K.; Hill, J. P.; Lee, M. V.; Vinu, A.; Charvet, R.; Acharya, S. *Sci. Technol. Adv. Mater.* **2008**, *9*-10.

CHAPTER 2

SUPRAMOLECULAR DENDRIMER CAPSULES BY COOPERATIVE BINDING

Rong Ju, Matthew Tessier, Lynda Olliff, Robert Woods, Anne Summers, Yan Geng. 2011. *Chemical Communications*. 47:268-270. Reprinted here with permission of The Royal Society of Chemistry, 2011. http://pubs.rsc.org

2.1 Abstract

We exploit the unique features of dendrimers as molecular nanospheres with many peripheral binding sites to show that maximizing cooperative binding enables a novel modular self-assembly approach to construct supramolecular capsules.

2.2 Introduction

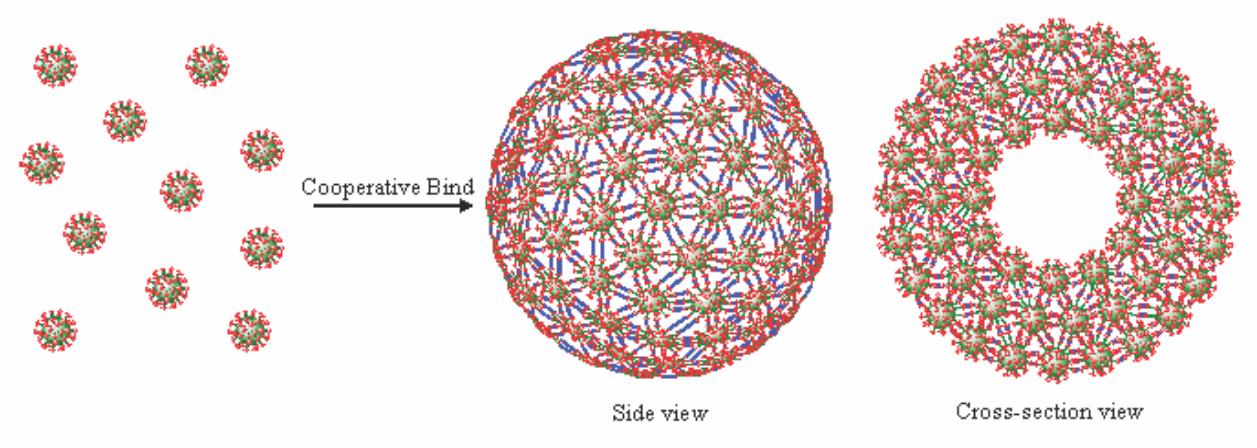

Figure 2.1 Schematic illustration of the cooperative binding of dendrimers into supramolecular capsules.

Cooperativity is a general principle that governs multivalent binding between two entities, *e.g.* multivalent ligand-receptor interactions, as well as subunit binding in self-assembly processes, *e.g.* collective base pairing in DNA double-helix formation and assembling of protein subunits into viral capsid or cytoskeleton superstructures.[1-3] Cooperative multivalent binding in molecular recognition has been well studied.[1-3] However, limited effort has been made to combine and maximize multivalent and subunit cooperative binding towards constructing functional supramolecular self-assemblies from large numbers of subunits. Here, we explore

dendrimers as molecular nanospheres with highly-branched peripheral binding sites to show a new concept that maximizing cooperative binding enables a novel modular self-assembly approach to construct functional supramolecular capsules, as shown in Figure 2.1.

Dendrimers have a highly branched architecture emanating from the core, thus can provide many binding sites at the periphery. They are globular in topology, monodispersed in size, and nanometers in dimension (1~10nm).[4-6] Dendrimers and their conjugates are not only of great interest to molecular recognition studies, but have also been vigorously pursued in the fabrication of supramolecular self-assemblies, ranging from dimers, oligomers, megamer clusters, rotaxane complexes, to large assemblies such as vesicles, fibers, gels and liquid crystals. [7-13] Despite tremendous achievements, such dendrimer self-assemblies, however, were largely based on traditional amphiphile hydrophobic effect, guest-host complexation, or dimeric/oligomeric linkages via H-bonding or metal coordination. The unique features of dendrimers as molecular nanospheres with highly-branched binding sites are yet to be fully exploited.

2.3 Results and Disscussion

To demonstrate the generality of the cooperative binding concept, here we studied two types of dendrimers that differ significantly in composition, branching motif and rigidity - Fréchet-type dendrimers with 1→2 aryl branching motif and ether connectivity, and Newkome-type dendrimers with 1→3 C-branching motif and amide connectivity, Figure 2.2A, 2.3A. Each dendrimer was functionalized with carboxyl peripheral groups to allow for potential electrostatic interactions in water. The benzyl ether interior of the Fréchet dendrimers is rather rigid and highly hydrophobic, whereas the Newkome dendrimers have much more conformational freedom around sp^3-C branching points, and their amide rich interior is much more hydrophilic. Consistently, our molecular Dynamics (MD) simulations on the Newkome dendrimers

demonstrated a large degree of conformational flexibility and revealed water penetration into their amide-rich interior, Figure 2.3A(II). The distinct difference between these two types of dendrimers was also confirmed by solubilization of hydrophobic fluorescent dyes inside the Fréchet dendrimers, but not by the Newkome dendrimers.

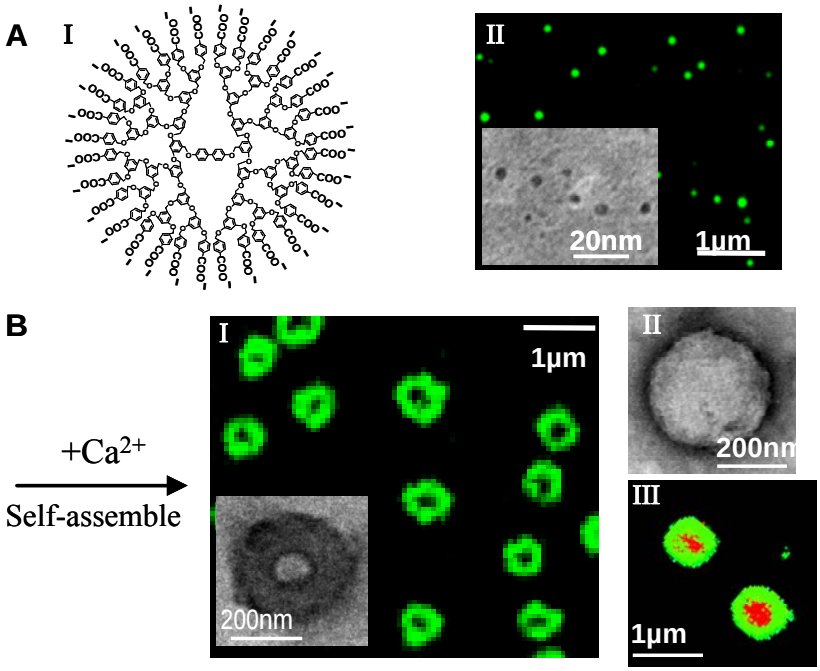

Figure 2.2. Ca^{2+} induced self-assembly of Fréchet-COO^- dendrimers into supramolecular capsules in water. (**A**) I. Molecular structure; II. FM and cryo-TEM (inset) imaging on dispersed Fréchet-COO^- dendrimers; (**B**) I. Cross-section projection of the Ca^{2+} induced capsules imaged by FM and TEM (inset); II. Surface topology of the capsules imaged by negatively-stained TEM; III. Encapsulation of red-fluoresecentl Dox by the capsules.

The carboxyl peripheral groups can completely dissociate into carboxylate anions (-COO^-) at neutral pH in aqueous solution, and both types of dendrimers dispersed as individual

molecules upon dissolution in water, Figure 2.2A(II), 2.3A(III). Although the Fréchet dendrimers have highly hydrophobic benzyl ether interiors, their hydrophobic associations into bilayer vesicles are unlikely due to their conformational rigidity. In fact, such Fréchet dendrimers are well known as unimolecular micelles in water, where the hydrophobic benzyl ether interior collapses into a rigid core surrounded by closely packed polar groups at the surface.[14] Direct Fluorescent Microscopy (FM) imaging of dye-labeled Fréchet-COO^- dendrimers revealed their Brownian motion in water as dispersed individual molecules, Figure 2.2A(II). Cryogenic-Transmission Electron Microscopy (Cryo-TEM) with resolution in nanometers showed similar results to those obtained by FM, Figure 2.2A (II, inset), where the diameters of the fourth-generation-(G4)-Fréchet-COO^- dendrimers (with 32 peripheral groups) and second-generation-(G2)-Fréchet-COO^- dendrimers (with 8 peripheral groups) were measured as 5 nm and 3 nm respectively. Cryo-TEM studies on Newkome- COO^- dendrimers showed that they are also dispersed molecular nanospheres with average diameters of 4 nm and 2.5 nm for G2 (with 36 peripheral groups) and G1 (with 12 peripheral groups) respectively.

Regardless of core composition and hydrophobicity, branching motif or generations, upon the addition of divalent Ca^{2+}, the dendrimer-COO^- nanospheres spontaneously assembled into submicron hollow capsules, Figure 2.2B (I), 2.3B. Both FM and TEM imaging of these capsules revealed the projection of hollow cavities and dense membranes. Negative staining in TEM, Figure 2.2B (II), further resolved the enclosed, ragged surface topology of these capsules, which appear to be composed of large numbers of tightly bound dendrimer nanospheres. The enclosed capsule structure was further confirmed by their ability to encapsulate guest materials into their cavity, as demonstrated in Figure 2.2B (III), using red-fluoresecent anti-cancer drug Doxorubicin. Based on the membrane volumes of the capsules and the sizes of the dendrimer

nanosphere molecules, we estimate these dendrimer capsules to contain hundreds to more than tens of thousands of dendrimer nanosphere units. These capsules were also observed to be robust and stable against shear and rupture stress.

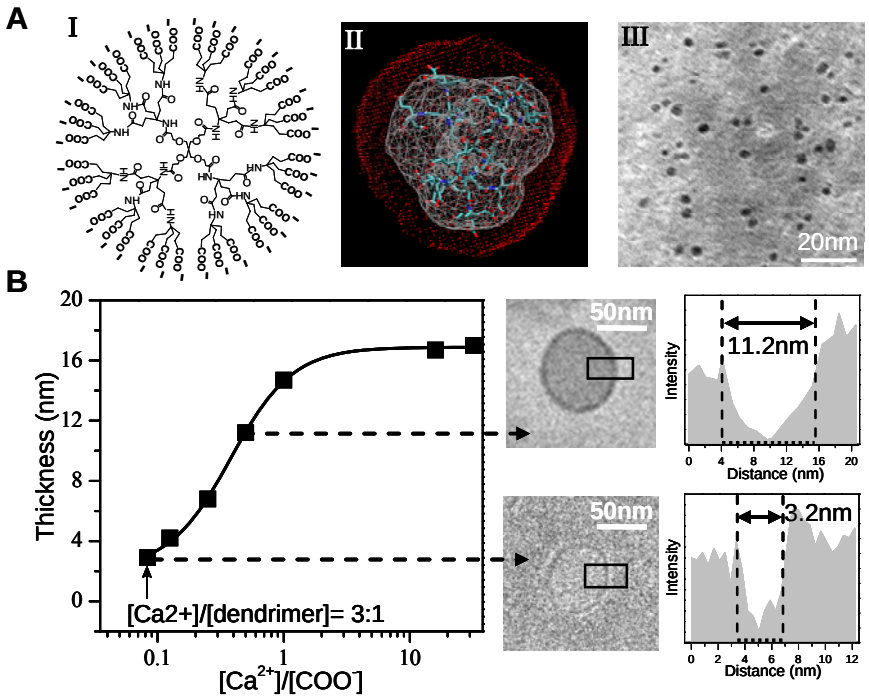

Figure 2.3. Ca^{2+} induced self-assembly of Newkome-COO^- dendrimers into supramolecualr capsules in water. (**A**) I. Molecular structure; II. MD simulation; Grey/red contour – deviation in conformations; III. Cryo-TEM imaging on dispersed Newkome-COO^- dendrimers in water; (B) Scaling and illustration of the capsule thickness with the Ca^{2+}/carboxylate molar ratio.

Although both types of dendrimers formed capsules with Ca^{2+}, they differed distinctively in their response to Ca^{2+}. Fréchet-COO^- dendrimers required excess Ca^{2+} than total carboxylates to assemble, *i.e.* Ca^{2+}:COO^-≥4, whereas Newkome-COO^- dendrimers, regardless of generations, began to form monolayer capsules at Ca^{2+}:Dendrimer~3:1, where the Ca^{2+} stoichiometry is far

below carboxylates, *i.e.* Ca^{2+}:COO^{-} = 1:8 for G2, Figure 2.3B. Newkome dendrimers also tend to form smaller and thinner capsules than Fréchet-COO^{-} dendrimers. Capsules from G4-Fréchet-COO^{-} dendrimers have average cavity sizes around 100nm and their membrane thickness can grow up to 100nm at high Ca^{2+} concentrations, whereas G2-Newkome dendrimers with comparable number of peripheral groups formed capsules with average cavity sizes around 50nm

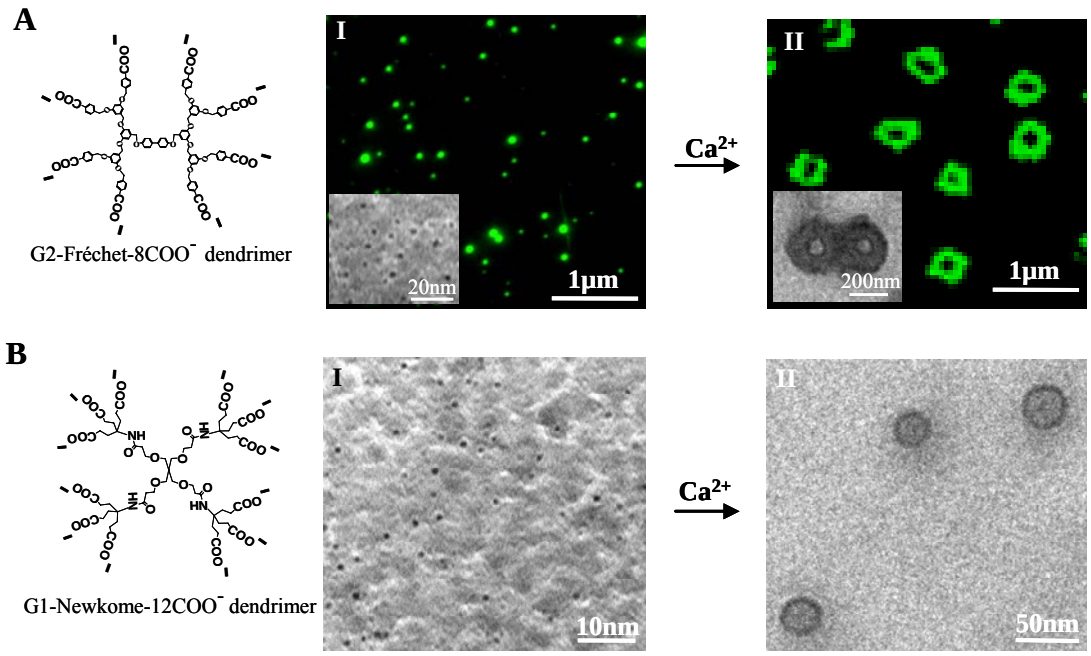

Figure 2.4. Ca^{2+} induced supramolecular capsule formation from the smaller lower generation of carboxylate-dendrimers. **A.** Capsules from G2-Fréchet-$8COO^{-}$ dendrimers; The average cavity size is around 70nm, and the membrane thickness can grow up to 80nm. **B.** Capsules from G1-Newkome-$12COO^{-}$ dendrimers; The average cavity size is around 30nm, and the membrane thickness can grow up to 12nm.

and their thickness can grow from monolayer to a maximum of 20nm with increasing Ca^{2+} concentrations, Figure 2.3B. The size and thickness of the capsules also depended on the

generation of the dendrimers. For both types of dendrimers, the smaller lower-generation dendrimers formed smaller cavities with thinner membranes, Figure 2.4.

Such Ca^{2+} induced capsule formation is distinctively different from the classical amphiphile hydrophobic-effect driven bilayer vesicles, as this process is independent of hydrophobicity and the membrane thickness can grow from monolayer to far beyond bilayers. Although Ca^{2+} is commonly used for inducing coil and aggregation of carboxylate based polyelectrolytes,[15,16] the formation of the ordered hollow capsules here is surprising. Hollow capsule formation, such as in viral capsid, generally proceeds by nucleation and growth pathway, where an oligomeric patch forms first followed by bending and expansion into a shell to minimize the surface energy.[17,18] The dendrimers here share some common features with proteins, as they are nanometers in size and spherical in shape with many binding sites at periphery. Divalent Ca^{2+} can not only bind with $-COO^-$ as counterion, but can also form COO^--Ca^{2+}-COO^- salt-bridges linking between dendrimer nanospheres. The highly branched feature of dendrimers would also allow for multiple Ca^{2+} salt-bridges between dendrimers, as well as three-dimensional binding into multiple layers with sufficient Ca^{2+}, consistent with the observed capsule thickening with the increasing Ca^{2+}.

To better understand the Ca^{2+}/COO^- binding that underlies the capsule formation, we used isothermal titration calorimetry (ITC) to study the energetics of the binding process. Ca^{2+} was added incrementally into the aqueous solution of the more sensitive Newkome-COO^- dendrimers. The heat changes of the titration and the integrated heat per mole of added Ca^{2+} versus the molar ratio of Ca^{2+}:Dendrimer were plotted in Figure 2.5. Interestingly, the titration was multiphasic and was best fitted with the two independent binding site model. The most obvious distinction among sites possible in this system is between individual Ca^{2+}-COO^-

counterion binding and COO^{-}-Ca^{2+}-COO^{-} salt-bridge forming to join two dendrimers. The parameters reported by ITC for two processes were $K_1 = 3.1\times10^3\ M^{-1}$, $\Delta H_1 = 7.5$ kcal/mol, $T\Delta S_1 = 12.2$ kcal/mol, $\Delta G_1 = -4.7$ kcal/mol; and $K_2 = 4.8 \times 10^4\ M^{-1}$, $\Delta H_2 = -3.4$ kcal/mol, $T\Delta S_2 = 1.7$ kcal/mol, $\Delta G = -5.1$ kcal/mol. Both binding events are spontaneous processes with release of free energy. The first process is endothermic and entropically driven, consistent with disruption of the ordered water solvation shell upon individual counterion binding.[19] Average binding constant K_1 is also similar to the previously reported Ca^{2+}-COO^{-} counterion binding constant[20]. In contrast, the second Ca^{2+} binding process is exothermic and enthalpically driven with the

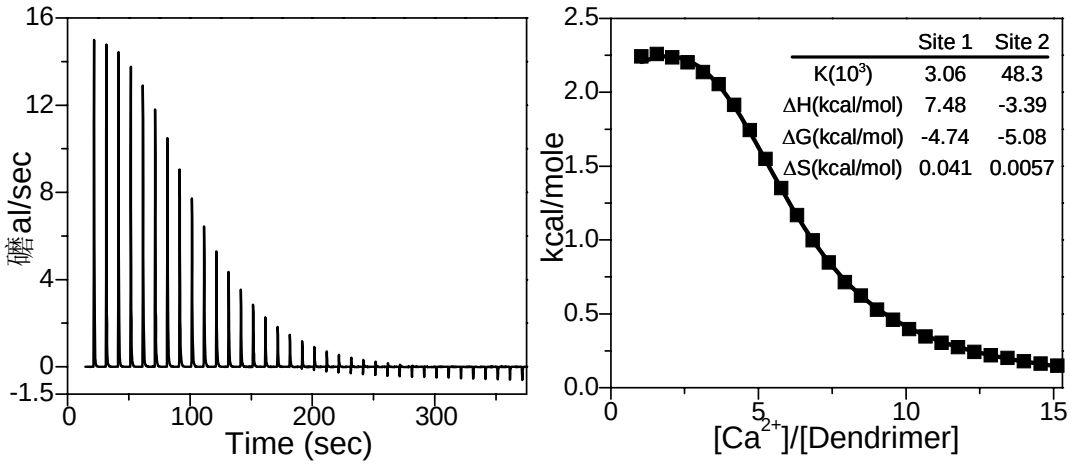

Figure 2.5. ITC analysis on Ca^{2+} binding to Newkome-COO^{-} dendrimers. Left panel shows the calorimetric titrations; Right panel displays the integrated heat values as a function of molar ratio. The solid line represents the curve fit to a two independent binding site model.

average K_2 ten times greater than K_1. The isotherm is also sigmoidal, indicating a positive cooperative effect. The second process is likely the COO^{-}-Ca^{2+}-COO^{-} salt-bridge binding that

assembles dendrimers into capsules, where the formation of the highly ordered dendrimer nanosphere lattices would yield exothermic lattice energy and entropy loss. In addition, as two dendrimers are brought together by the first Ca^{2+} salt-bridge formation, their proximity would facilitate the subsequent formation of Ca^{2+} salt bridges between them and maximize the cooperativity. Multiple bonding in turn can enhance the binding strength between dendrimers, and stabilize the self-assembly structure and account for the robustness of these capsules.

The Ca^{2+} induced cooperative binding of dendrimers also explains for the observed differences between Fréchet- and Newkome-COO^- dendrimers. As rigid spheres with tightly packed carboxylate groups at the surface, Fréchet dendrimers require addition of more Ca^{2+} to bind and screen the densely negative surface charges first, before they can be brought to proximity to form Ca^{2+} salt-bridges.[21] In contrast, the carboxylate groups in the highly flexible Newkome dendrimers are more like independent point charges, which can extend to form Ca^{2+} salt-bridges much more freely. The flexibility of Newkome dendrimers would also enable bending into much smaller shells as observed. Quantitatively, since at least one Ca^{2+} salt-bridge is needed to link between every two Newkome dendrimers and each dendrimer sphere would be surrounded by six neighbors in close-packing, a minimum ratio of Ca^{2+}:Dendrimer = 6/2 (3:1) would be required to induce the capsule formation for Newkome dendrimers, which is consistent with our experimental finding.

Cooperative binding not only allows for flexible supramolecular dendrimer capsule fabrication, but also possesses the advantage of ease in controlling disassembly towards release. Since the capsules are bound by Ca^{2+} salt-bridges, removal of Ca^{2+} would cause the capsules to disassemble into dendrimer monomers. Figure 2.6 shows that as EDTA, an effective Ca^{2+}

chelator that can withdraw Ca^{2+} from the capsules, was added to Frèchet-COO^{-}/Ca^{2+} capsule solutions, the capsules quickly disassembled within time, which was directly observed by FM.

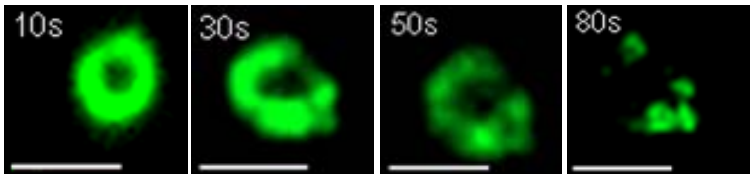

Figure 2.6. FM imaging on the disassembly of the Fréchet-COO^{-}/Ca^{2+} capsule by the addition of EDTA. Scale bar: 1 μm.

2.4 Conclusion

In summary, we have exploited the unique features of dendrimers as molecular nanospheres with highly-branched binding sites and demonstrated their ability to maximize cooperative binding, which enables a novel modular self-assembly approach to construct supramolecular capsules. Such capsules by cooperative binding are tunable in size and thickness, controllable in disassembly, and can be potentially used for a wide variety of encapsulation applications.

2.5 Experimental Information

2.5.1 Materials

*G2-Fréchet-8COOH and G4-Fréchet-32COOH***,** were synthesized by the reported convergent route[14], using 3,5-dihydroxybenzyl alcohol as the monomer unit and step-wise growth process consisting of activation by bromination and coupling by alkylation, Figure 2.7. In the final step, two dendritic fragments were coupled with difunctional core, 4,4'-dihydroxy-

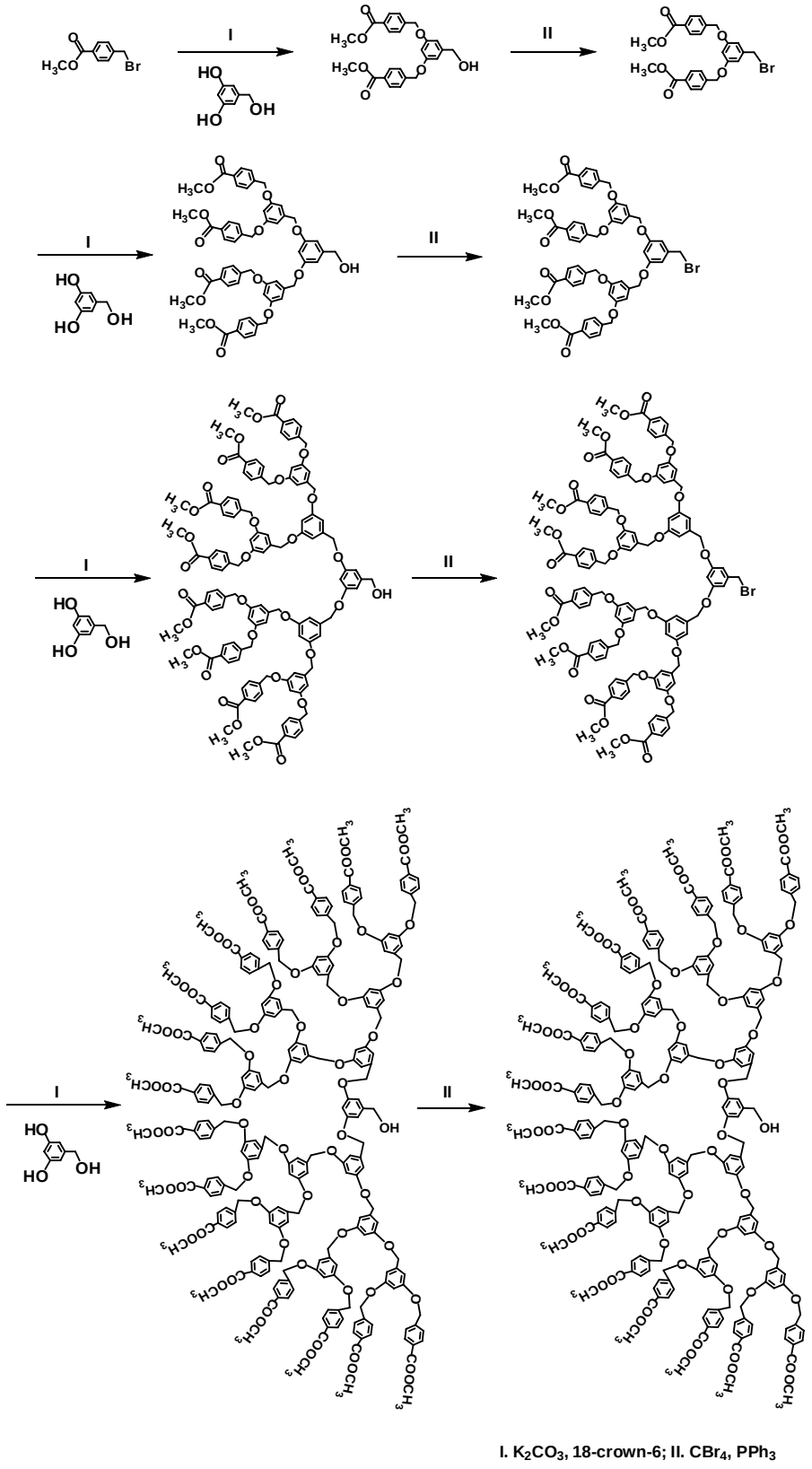

Figure 2.7 Reaction scheme for the preparation of dendritic benzyl ether fragments.

biphenyl, and followed by hydrolysis of the methyl ester protecting groups, Figure 2.8, 2.9. All synthesized dendrimers were characterized by NMR before use. ^{1}H NMR([H_6]-DMSO) of the synthesized G2-Fréchet-8COOH: δ(ppm) = 4.94 and 5.05 (s,24H,OCH_2), 6.4-6.7(m, 18H, ArH), 6.91(m,4H, core ArH) and 7.44 and 8.00(m, total 36H, 32 PhH and 4 core ArH). ^{1}H NMR([H_6]-DMSO) of the synthesized G4-Fréchet-32COOH: δ(ppm) = 4.95 and 5.10 (s,124H,OCH_2), 6.49-6.70 (m,90H,ArH), 6.91(m,4H,core ArH), 7.50 and 7.98 (m, total 132H, 128PhH and 4 core ArH).

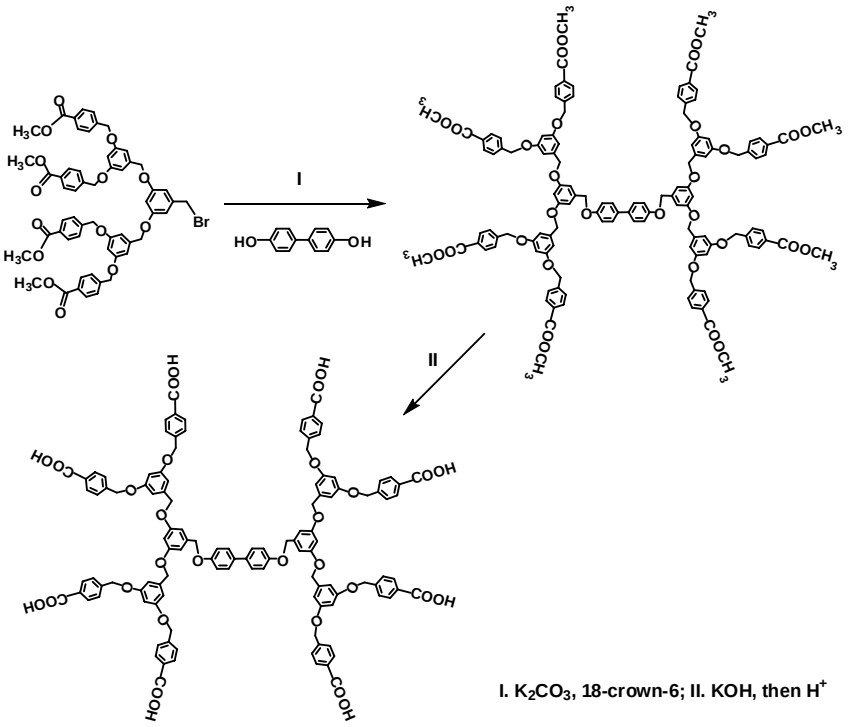

Figure 2.8 Reaction scheme for the preparation of G2-Fréchet-8COOH.

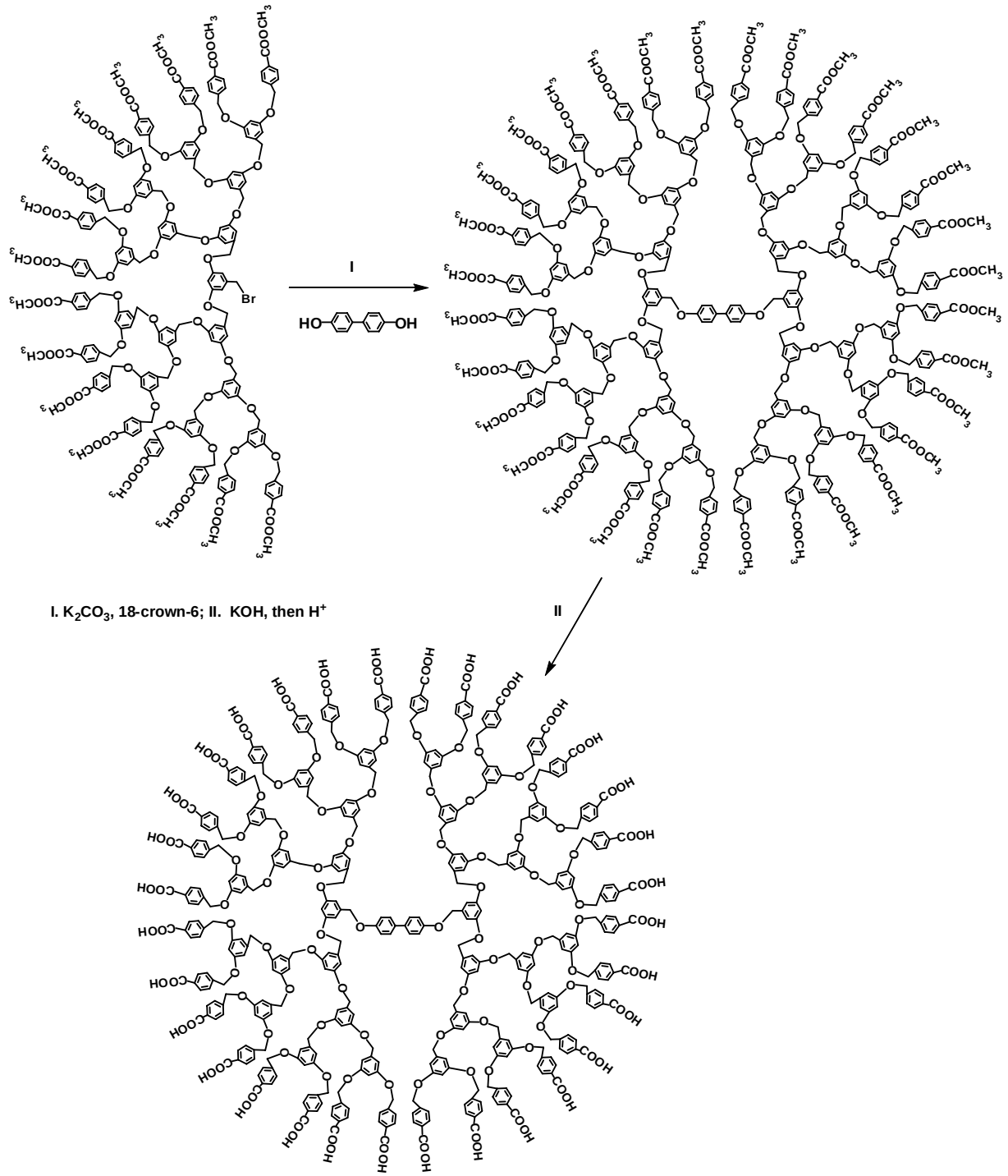

Figure 2.9. Reaction scheme for the preparation of Frechet-G4-32COOH.

G1-Newkome-12COOH and G2-Newkome-36COOH, were synthesized by the reported divergent approach. The tri-branched amine monomer was synthesized by the addition of nitromethane to t-butylacrylate, followed by Raney-nickel reduction[22], Figure 2.10, and the tetraacid core was prepared by Michael addition of acrylonitrile to pentaerythritol[23,24], Figure 2.11. The different dendrimers were synthesized by using the tetraacid core and stepwise growth consisting of DCC/1-HBT peptide coupling with the tri-branched amine monomer, and activation by facile removal of the t-Butyl protecting group,[23,25] Figure 2.12, 2.13.

^{1}H NMR(D_2O) of the synthesized G1-Newkome-12COOH: δ(ppm) = 1.76 (t,24H,C**H**$_2$$CH_2COO$), 1.98 (t,24H,$CH_2COO$), 2.32(br,8H,$CH_2CONH$) and 3.15(br,8H,$CH_2O$) and 3.52(br,8H,$OCH_2$).

^{1}H NMR(D_2O) of the synthesized G2-Newkome-36COOH: δ(ppm) = 1.75 and 1.95 (br, 192H, CH_2CH_2CO), 2.38 (br,8H,CH_2CONH), 3.24(br,8H,CH_2O) and 3.50(br,8H,OCH_2).

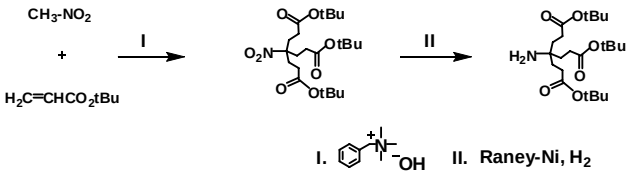

Figure 2.10. Reaction scheme for the preparation of tri-branched amine monomer.

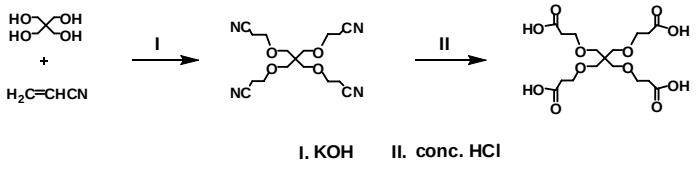

Figure 2.11. Reaction scheme for the preparation of tetraacid core.

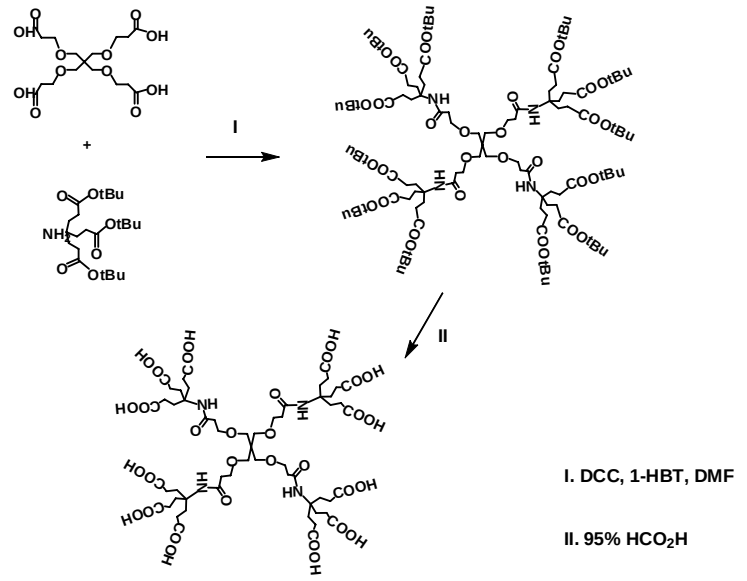

Figure 2.12. Reaction scheme for the preparation of G1-Newkome-12COOH.

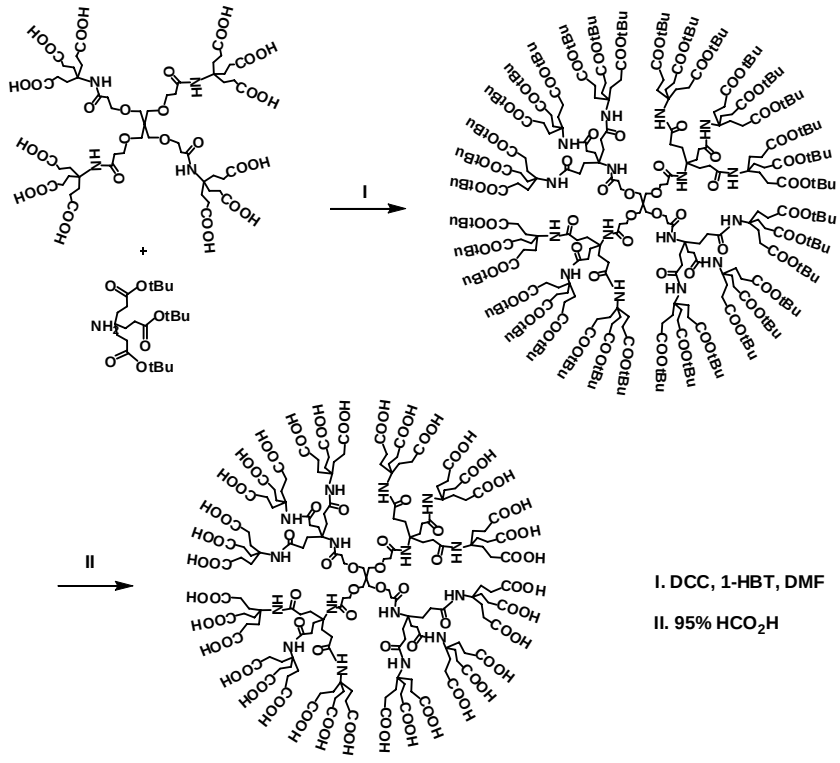

Figure 2.13. Reaction scheme for the preparation of G2-Newkome-36COOH.

2.5.2 Methods

Fluorescent and Light Microscopy Imaging was taken by labeling the Fréchet-type dendrimers in aqueous solution with a hydrophobic fluorophore dye (PKH 26). The dipersed dendrimers and their self-assembled supramolecular capsules by the addition of Ca2+ in water were directly observed on an Olympus IX71 inverted fluorescence microscope with a 60X objective and a Cascade CCD camera. 2 μL samples were used in the chamber formed between glass slide and cover slip for imaging.

Cryo-Transmition Electron Microscopy (TEM) imaging on the dispersed carboxylate-decorated dendrimers in aqueous solutions was carried by pipetting 3μL of the sample solution onto a carbon coated copper grids. A piece of filter paper was then used to quickly remove the excess liquid, and the sample copper grid was quickly plunged into liquid nitrogen to ensure vitrification. The specimen was stored under liquid nitrogen, and then transferred to a cryogenic sample holder (Gatan 626) in a FET TECNAI 20G TEM operating at -177°C for imaging.

Regular-TEM, negatively-stained TEM imaging on the Ca^{2+} induced capsules, the specimens were freeze dried before imaging. The surface topology was obtained by negative staining. A droplet of 2% uranyl acetate was placed onto the freeze dried specimen for 60 seconds and the excess liquid was removed by filter paper before imaging. TEM images were obtained on a FET TECNAI 20G Transmission Electron Microscopy operating at an acceleration voltage of 200kV and at ambient temperature.

Encapsulation of Doxorubicin was carried by first dissolving Doxorubicin, a spontaneously red-fluorescent anti-cancer drug, in aqueous solution. Fréchet-COO^- dendrimers and then Ca^{2+} were added to Dox solution to form capsules and encapsulate Dox. The Dox-loaded Fréchet-COO^-/ Ca^{2+} capsules were then collected by centrifuge and re-dispersed in water.

Fréchet-COO^- dendrimers were then green fluorescently-labeled for FM imaging, which demonstrated the encapsulation of the red-fluorescent Dox within the cavity of the green-fluorescent Fréchet-COO^- dendrimer capsules.

Isothermal Titration Calorimetery (ITC) measurements were recorded on a VP-ITC MicroCalorimeter (MicroCal, Inc). Aqueous solution of 0.344 mM G2-Newkome-36COO^- dendrimer at pH 7.4 was loaded into the titration cell, and the reference cell was filled with deionized water. Fifty successive injections of 50 mM Ca^{2+} were made into the dendrimer sample cell in 5 μL increments at 10 min interval with stirring at 300 rpm to ensure complete equilibration. Control experiments to determine the heat of dilution were carried out by making identical injections in the absence of dendrimers. The net binding reaction heat was obtained by subtracting the heat of dilution from the measured total heat of reaction. The titration data were then fitted using the MicroCal Origin software and least-square algorithm, and these data were best fit to a two independent binding site model. The binding enthalpy ΔH, binding constant K, and the binding stoichiometry n were permitted to float during the least-square minimization process and taken as the best-fit value.

Molecular dynamics (MD) simulations on the conformations of the Newkome-carboxylate(COO^-) dendrimers in water were performed with the GLYCAM06 force field with the Sander module of the AMBER 9 simulation package[26]. Molecular dynamics (MD) simulations was done by Matthew Tessier and Dr. Robert Woods, and is included as an important result in this chapter. Detailed simulation procedures can be found in the following webpage: http://www.glycam.com/supporting_info.html. Briefly, Newkome-COO^- dendrimers were built from the angles and torsions obtained from HF/6-31++g** optimized fragments which were used to generate the partial charge models. These initial structures were then subjected to a

gas-phase minimization using a 5,000 step minimization with a dielectric of 1.0 and a non-bonded cutoff of 12.0 Å. Before solvating the dendrimer molecule, it was neutralized by 18 Ca^{2+} ions[27] to allow for Particle Mesh Ewald simulations[28]. The optimized dendrimer models were then solvated using a minimum of edge to solute distance of 8.0 Å to form a cubic box of water. Each solvated complex was minimized using 5,000 steps of steepest descent and up to 15,000 steps of conjugate gradient minimization with a 8.0 Å non-bonded cutoff and a dielectric constant of 1.0. Following minimization, the dendrimer was subjected to a series of constant pressure (NPT) simulations using a 2 fs timestep, non-bonded scaling factors set to unity, an 8.0 Å non-bonded cutoff, a pressure of 1.0 atm, and a compressibility equivalent to water, 44.6 10^{-11} $m\ kg^{-1}\ s^{2}$. Since the dendrimers were developed from small fragments, it was necessary to equilibrate the system using 100 ps of heating from 5 K to 300 K followed by 10,000 ps at 300 K and annealing from 300 K back to 5 K over 600 ps. A standard heat/cooling scheme was used to disorder and relax the dendrimers into different conformations. The first heating/cooling scheme consists of heating from 5 K to 300 K over 50 ps followed by 50 ps of heating to 1,000 K and 500 ps of simulation time at 1,000 K. The system was then cooled to 300 K over 100 ps and 50 ps of simulation time was obtained at 300 K and re-heated once more from 300 K to 1000 K over 50 ps and a 1000 K simulation time of 500 ps followed by cooling back to 300 K over 100 ps. In subsequent heating schemes, the simulation is heated from 5 K to 300 K for 50 ps and the simulation is not annealed to 5 K between cycles. Ten sequential heating/cooling schemes are performed where structures are extracted after each scheme finishes and these structures were each subjected to a 10 ns production run at 300 K yielding ten distinct production simulations of 10 ns each. The solvent accessible surface area (SASA) was obtained from the MM_PBSA module in AMBER. An estimation of the diameter of the solvated dendrimers was also

performed using the average maximum cross-distance from the heavy atoms at the ends of each finger to each finger on the branch opposite it. The two maximum distances from both pairs of opposite branches are then averaged together to get an approximate diameter. The average diameter for G2- and G1-Newkome-COO^- dendrimers were calculated as 4.1 nm and 2.7 nm respectively, consistent with the cryo-TEM measurements.

2.6 References

(1) Jencks, W. P. *Proc. Natl. Acad. Sci.U. S. A.* **1981**, *78*, 4046-4050.

(2) Hughes, A. D.; Anslyn, E. V. *Proc. Natl. Acad. Sci.U. S. A.***2007**, *104*, 6538-6543.

(3) Mammen, M.; Choi, S. K.; Whitesides, G. M. *Angew. Chem., Int. Ed.* **1998**, *37*, 2755-2794.

(4) Newkome, G. R.; Moorefield, C. N.; Vogtle, F. *Dendritic Macromolecules: Concepts, Synthesis, Perspectives*; VCH, Wenheim, Germany, 2001.

(5) Frechet, J. M. J.; Tamalia, D. A. *Dendrimers and Other Dendritic Polymers*; Whiley,: Chichester, UK, 2001.

(6) Zeng, F. W.; Zimmerman, S. C. *Chem. Rev.* **1997**, *97*, 1681-1712.

(7) Giles, M. D.; Liu, S. M.; Emanuel, R. L.; Gibb, B. C.; Grayson, S. M. *J. Am. Chem. Soc.* **2008**, *130*, 14430-+.

(8) Zimmerman, S. C.; Zeng, F. W.; Reichert, D. E. C.; Kolotuchin, S. V. *Science* **1996**, *271*, 1095-1098.

(9) Tomalia, D. A.; Brothers, H. M.; Piehler, L. T.; Durst, H. D.; Swanson, D. R. *Proc. Natl. Acad. Sci.U. S. A.* **2002**, *99*, 5081-5087.

(10) Amabilino, D. B.; Ashton, P. R.; Balzani, V.; Brown, C. L.; Credi, A.; Frechet, J. M. J.; Leon, J. W.; Raymo, F. M.; Spencer, N.; Stoddart, J. F.; Venturi, M. *J. Am. Chem. Soc.* **1996**, *118*, 12012-12020.

(11) Wang, P.; Moorefield, C. N.; Jeong, K. U.; Hwang, S. H.; Li, S.; Cheng, S. Z. D.; Newkome, G. R. *Adv. Mater.* **2008**, *20*, 1381-+.

(12) Vanhest, J. C. M.; Delnoye, D. A. P.; Baars, M. W. P. L.; Vangenderen, M. H. P.; Meijer, E. W. *Science* **1995**, *268*, 1592-1595.

(13) Ungar, G.; Liu, Y. S.; Zeng, X. B.; Percec, V.; Cho, W. D. *Science* **2003**, *299*, 1208-1211.

(14) Hawker, C. J.; Wooley, K. L.; Frechet, J. M. J. *J. Chem. Soc., Perkin Trans. 1* **1993**, 1287-1297.

(15) Sondjaja, H. R.; Hatton, T. A.; Tam, K. C. *Langmuir* **2008**, *24*, 8501-8506.

(16) Li, Y.; Gong, Y. K.; Nakashima, K. *Langmuir* **2002**, *18*, 6727-6729.

(17) Caspar, D. L. D. *Biophys. J.* **1980**, *32*, 103-138.

(18) Kim, D.; Kim, E.; Kim, J.; Park, K. M.; Baek, K.; Jung, M.; Ko, Y. H.; Sung, W.; Kim, H. S.; Suh, J. H.; Park, C. G.; Na, O. S.; Lee, D. K.; Lee, K. E.; Han, S. S.; Kim, K. *Angew. Chem., Int. Ed.* **2007**, *46*, 3471-3474.

(19) Linton, B. R.; Goodman, M. S.; Fan, E.; van Arman, S. A.; Hamilton, A. D. *J. Org. Chem.* **2001**, *66*, 7313-7319.

(20) Joseph, N. R. *J. Biol. Chem.* **1946**, 529-541.

(21) Israelachvili, J. In *Academic Press* London, 1992.

(22) Cruz-Morales, J. A.; Guadarrama, P. *J. Mol. Struct.* **2005**, *779*, 1-10.

(23) Newkome, G. R.; Weis, C. D. *Org. Prep. Proced. Int.* **1996**, *28*, 242-244.

(24) Worl, R.; Koster, H. *Tetrahedron* **1999**, *55*, 2941-2956.

(25) Young, J. K.; Baker, G. R.; Newkome, G. R.; Morris, K. F.; Johnson, C. S. *Macromolecules* **1994**, *27*, 3464-3471.

(26) Case, D. A.; Darden, T. A.; Cheatham III, T. E.; Simmerling, C. L.; Wang, J.; Duke, R. E.; Luo, R.; Merz, K. M.; Pearlman, D. A.; Crowley, M.; Walker, R. C.; Zhang, W.; Wang, B.; Hayik, S.; Roitberg, A.; Seabra, G.; University of California: San Francisco, 2006.

(27) Humphrey, W.; Dalke, A.; Schulten, K. *J. Mol. Graphics* **1996**, *14*, 33-&.

(28) Essmann, U.; Perera, L.; Berkowitz, M. L.; Darden, T.; Lee, H.; Pedersen, L. G. *J. Chem. Phys.* **1995**, *103*, 8577-8593.

CHAPTER 3

DENDRIMER SELF-ASSEMBLY THROUGH COOPERATIVE HYDROGEN BONDING

Rong Ju, Jennifer Haley, Yan Geng.

To be submitted to *Soft Matter*

3.1 Abstract

Hydrogen bonding is one of the most important interactions for constructing supramolecular assemblies. However, because hydrogen bonding is strongly solvent dependent and prone to be disrupted in competitive solvents, *e.g.* water, strategically construct robust and functional molecular self-assembly by hydrogen bonding in aqueous solution by hydrogen bonding is yet to be explored. Here, we demonstrate that despite lack of directionality and specificity, highly cooperative hydrogen bonding enables dendrimers spontaneously self-assemble into stable hollow capsules in not highly-competitive organic and aqueous solution. Such cooperatively H-bonded dendrimer capsules are thermo-responsive in nature, and we found a narrow and facile temperature window can be used to trigger controlled disassembly and release.

3.2 Introduction

Molecular self-assembly through non-covalent bonding is the cornerstone towards advancing the complexity in structure and function of matter. In the course of molecular self-assembly processes, cooperativity plays an important role. Cooperativity is a general principle that applies to not only multiple binding between two entities, but also processes that involve multiple subunits, where multi-valent or multi-unit binding can be collectively enhanced than corresponding monovalent or single unit interactions.[1-3] Both of the multi-valent and multi-unit cooperativity are ubiquitous in biology – *e.g.* the multi-valent cooperative binding between ligands and receptors is commonly seen in substrate-enzyme association, cell adhesion, signal transduction and gene regulation,[4] whereas the subunit cooperativity is reflected in collectively base pairing in DNA double-helix formation, folding of protein polyamide backbones into secondary structures, and assembling of protein subunits into viral capsid and cytoskeleton

superstructures.[1-3] Cooperativity is not only essential to biological structures and functions, but also crucial to the design of synthetic molecular self-assembly. Since non-covalent forces are generally weak by nature, cooperative multiple binding, *i.e.* multi-valent cooperativity, between molecules can create sufficient bonding strength for assembly to occur. The subunit cooperativity, on the other hand, can help achieve self-directing, self-recognizing, and self-correcting in self-assembly processes.[5-7] Although multivalent cooperativity between the two entities has been extensively studied in molecular recognition, little effort has been made to use both multi-valent and subunit cooperativity in molecular self-assembly to enhance one another and thus maximize cooperative binding. Such an approach will greatly enhance the control and ease in orchestrating molecular self-assembly process, and provide a new conceptual design platform towards constructing complex, robust and functional supramolecular self-assemblies.

Among different non-covalent forces, hydrogen bonding is one of the most important binding interactions, which is not only commonly employed in biological systems and processes, such as in DNA double-helix formation and protein folding,[8] but also widely pursued in the fabrication of synthetic supramolecular assemblies.[9-13] However, a single hydrogen bond is rather weak. To achieve sufficient bonding strength, directionality and specificity between molecules, especially in order to organize molecules into discrete, ordered structures, multiple hydrogen bonding through encoded pre-organized arrays of complementary hydrogen bond donors and acceptors, combined with sterically constrained, well-defined molecular geometry, has been widely used in molecular design.[10-12] Many elegant and inspiring examples by this classical approach have been reported to advance our understanding in molecular recognition, host-guest complexation and supramolecular chemistry. This strenuous design strategy, however, is largely limited to making dimers and cyclic oligomers, and is difficult to apply to fabricating

more complex assemblies from large numbers of molecular subunits. Another limitation of hydrogen bonding is that it is strongly solvent dependent and prone to be disrupted in competitive solvents. For example, water is the exclusive solvent in nature yet one of the most difficult media for intermolecular hydrogen bonding.[8] How to strategically construct robust and functional molecular self-assemblies by hydrogen bonding in aqueous solution represents a formidable yet important task.

Previously, we have exploited the unique features of dendrimers as highly-branched molecular nanospheres, and revealed their ability to combine and maximize multi-valent and multi-unit cooperative binding in the self-assembly process. In Chapter 2, we demonstrated that maximizing cooperative binding enables dendrimers to self-assemble in large numbers into discrete, close-packed capsules via ionic salt-bridge interactions.[14] Ionic interactions, however, are a much stronger force than hydrogen bonding and are much less influenced by solvents. Whether cooperativity would be powerful enough to allow self-assembly through weak and solvent-sensitive hydrogen bonding in different solvents, including water, is an intriguing and challenging question.

3.3 Results and Discussion

Two types of dendrimers that differ significantly in composition, branching motif and rigidity were examined – *i.e.* rigid aryl-branched Fréchet-type dendrimers and more flexible C-branched Newkome-type dendrimers, Figure 3.1A. Dendrimers were then functionalized with simple carboxyl (-COOH) or hydroxyl (-OH) peripheral groups to allow for potential H-bonding. The spherical geometry of dendrimers does not impart directionality, and no predefined H-bond recognition pattern at the dendrimer periphery has been programmed either.

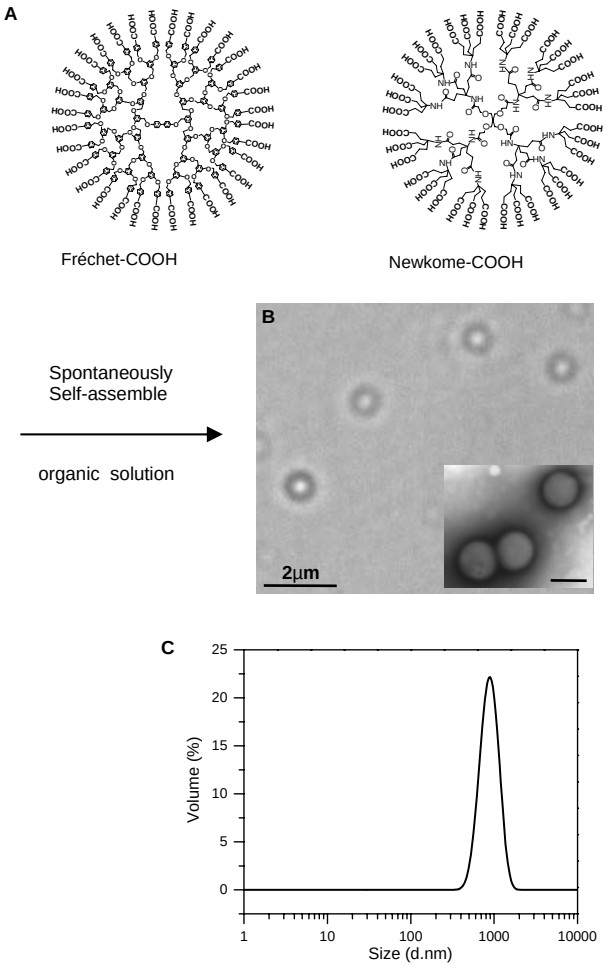

Figure 3.1 Spontaneous self-assembly of carboxyl-terminated dendrimers into capsules in organic solvents. (**A**) Molecular structure. (**B**) Cross-section projection of the capsules by light microscopy. Inset: Surface topology imaged by negatively-stained TEM, scale bar:500nm. (**C**) DLS measurements of Fréchet dendrimer capsules in THF.

Upon dissolution in less polar organic solvents, such as chloroform and THF, both Fréchet and Newkome-COOH dendrimers, regardless of their structural differences, immediately self-assembled into submicron hollow capsules, Figure 3.1B. These capsules remained suspended in solution without precipitation, due to their submicron colloidal sizes. Direct

imaging in solution by light microcopy revealed the projection of the hollow cavities and dense membranes of these capsules. Negative staining in TEM (inset) further resolved the enclosed surface. Dynamic Light Scattering (DLS) measurements revealed fairly narrow size distribution of these capsules, consistent with the TEM imaging, Figure 3.1C. It seems nearly all dendrimer molecules had assembled into capsule structures, since no free dendrimer monomers were detected by TEM imaging or DLS measurements. Since individual dendrimer molecules have a diameter of 3-5 nm,[14] we estimated that each capsule to be hundreds-of-nanometers in size and to contain tens of thousands of dendrimer molecule units. These dendrimer capsules are highly stable, and robust against shear and rupture stress, as well as the drying processes.

FT-IR analysis on these dendrimer capsules showed a strong carbonyl stretching vibrational absorption band at ~ 1690 cm^{-1}, Figure 3.2, which was revealed to compose two peaks from the second derivative analysis (inset). The peak at the shorter wavenumber of 1685 cm^{-1} confirmed the formation of H-bonded carboxyl dimers, whereas the small peak at 1704 cm^{-1} was attributed to the free, non H-bonded carboxyl groups.[13,15,16] Hollow capsule formation, such as in viral capsid, generally proceeds by nucleation and growth pathway, where the protein subunits with complementary binding domains bind into oligomeric patches first followed by expansion and bending into a closed shell to minimize the surface energy.[17] It appears for dendrimer macromolecules, despite the lack of directionality and specificity, they can nonetheless self-recognize each other and cooperatively self-assemble via H-bonds into stable capsules in less polar organic solvents.

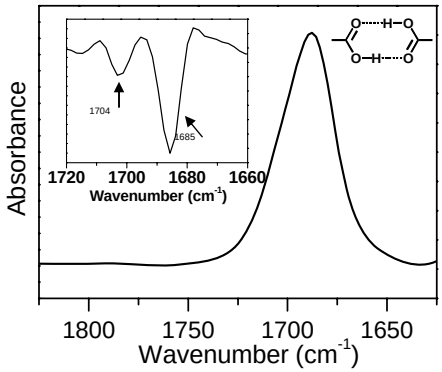

Figure 3.2 FT-IR analysis on capsules assembled by carboxyl-terminated dendrimers in THF.

Compared to less polar organic solvents, intermolecular H-bonding in competitive and disruptive solvents, such as water, would be much more difficult. To explore the possibility of using cooperative H-bonding to assemble dendrimers even in the highly challenging aqueous environment, we studied hydroxyl functionalized dendrimers, which will remain neutral for a wide range of pH and are capable of forming weak O–H---O hydrogen bonds. At first glance, it seems rather unlikely that weak O–H---O hydrogen bonds would be able to assemble molecules into stable structures in highly disruptive aqueous solutions. Indeed, Fréchet-OH dendrimers remained dispersed as monomers in water without further assembly. Surprisingly, Newkome-OH dendrimers spontaneously formed hollow capsules upon dissolution in water, Figure 3.3B. H-bonding formation from the hydroxyl groups of the Newkome dendrimers was further confirmed by FT-IR analysis, Figure 3.3C. In the FT-IR analysis, in order to avoid any interference from water moisture in the air, Newkome-OH dendrimer capsules were prepared in D_2O to exchange hydrogen with deuterium before drying. As temperature was increased from 25°C to 65°C, the IR absorption intensity significantly decreased in both of the O-D stretching vibrational region of

3000–3500 cm^{-1} and the O-D bending vibrational region of 1300–1500 cm^{-1}. This observation was resulted from the weakening of hydrogen bonds with increasing temperature, which demonstrates the presence of O-D hydrogen bonding in these dendrimer capsules.

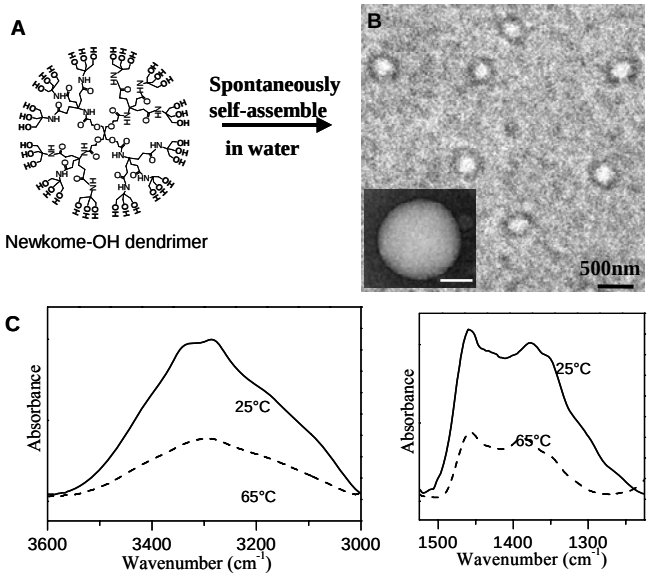

Figure 3.3 Spontaneous self-assembly of Newkome-OH dendrimers into hollow capsules in water. (**A**) Molecular structure. (**B**) Cross-section projection of the dendrimer capsules by TEM. Inset: Surface topology imaged by negatively-stained TEM, scale bar:100 nm. (**C**) FT-IR analysis on the dendrimer capsules.

To gain further insight into the hydroxyl H-bonding in the Newkome dendrimer self-assembly process, we used quantum mechanical (QM) simulation to study potential interactions between the trident(-CH_2-OH) peripheral branches of the Newkome dendrimers in gas phase. QM optimization showed that instead of interacting as individually hydroxyl groups, the trident(-CH_2-OH) branches interact as flexible clusters to cooperatively generate a polyhedron H-bond network, Figure 3.4. Each oxygen atom participates in two H-bonding formation, *i.e.* one with a

neighboring hydroxyl hydrogen within the same branch and one with a hydroxyl hydrogen from another branch, giving rise to a deformed trigonal antiprism network with a total of twelve hydrogen bonds. Although individual O–H---O hydrogen bonds are weak, the cooperative formation of the multiple H-bond polyhedron network can significantly enhance the strength and stability of the H-bonding between dendrimers and thus enable their assembly. It is also possible that in aqueous solutions, the trident(-CH_2-OH) peripheral branches interdigitate with each other to create a hydrophobic environment that can facilitate as well as further stabilize the hydroxyl H-bond network formation. The cooperative H-bonding between the peripheral hydroxyl groups, nonetheless, must be crucial to the dendrimer self-assembly in water. Otherwise, as in rigid Fréchet dendrimers with comparable -CH_2-CH_2-OH peripheral groups but lack the flexibility and sufficiently high cooperativity as in Newkome dendrimers, self-assembly would be unable to proceed as observed.

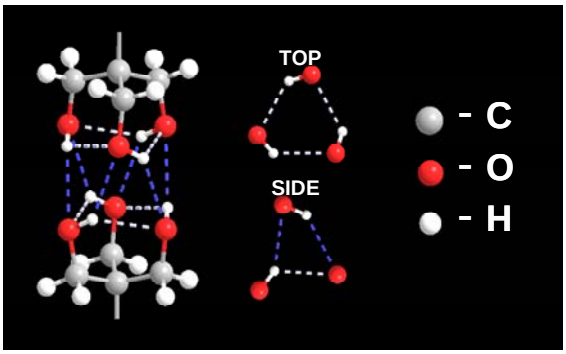

Figure 3.4 H-bonding network formation between tris(-CH_2-OH) branches by Quantum mechanical simulations.

The spontaneous self-assembly of dendrimer macromolecules into discrete hollow capsules by cooperative H-bonding allows for the encapsulation of guest materials into the

enclosed cavity. Moreover, since H-bonding is sensitive to temperature, such cooperatively H-bonded dendrimer capsules are expected to be thermo-responsive in nature, Figure 3.5 A. We then used Dynamic Light Scattering to track the changes of the Newkome-OH dendrimer capsules in aqueous solution with the increasing temperature, Figure 3.5B. At the initial room temperature, the average particle diameter in solution was measured by DLS as ca. 180nm, consistent with the predominant presence of submicron capsule structures, as visualized by TEM in Figure 3.3B. However, as the temperature was increased to a critical value of 45 – 55°C, DLS measurements showed that the size of particles in solution quickly plunged to below 5nm. This observation indicates that the capsule structures of hundreds-of-nanometers in size had completely disassembled into nanometer sized individual dendrimer monomeric units. TH This temperature and heat triggered capsule disassembly further confirmed H-bonding as the major binding force for these dendrimer capsules. More importantly, such a narrow and facile temperature window can be exploited as a convenient controlled release mechanism for practical usages in drug delivery and sensor application. To further illustrate the temperature triggered release, the red-fluoresecent anti-cancer drug Doxorubicin was encapsulated as a model guest material. At room temperature, Dox was encapsulated inside the capsules' cavity, as shown in Figure 3.5B inst. While, when temperature was increased above 50°C, capsules quickly disassembled into free dendrimers and Dox was released, shown as reddish background in Figure 3.5B inset. The release kinetics of Dox at different temperatures was also studied. The Dox-loaded capsules were trapped in a dialysis cassette and the internal solution was sampled at different time intervals for monitoring the 485nm absorption peak of Dox, Figure 3.5C. At 25°C,

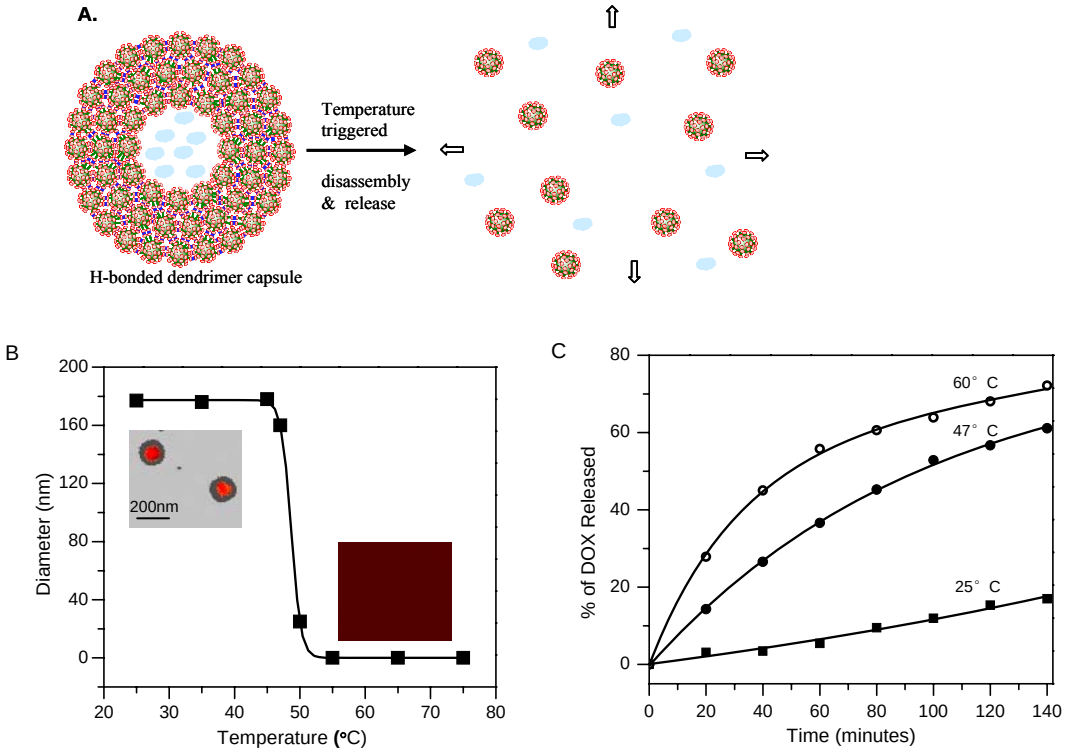

Figure 3.5 Temperature triggered disassembly and release of the H-bonded Newkome-OH dendrimer capsules. **(A)** Schematic representation; **(B)** Measurements by Dynamic Light Scattering with increasing temperature. Inset: Encapsulation of red-fluorescent Doxorubincin in to the capsule cavity; Dox after release. **(C)** Release kinetics of encapsulated Dox at 25°C, 47°C and 60°C. Line is provide to help the visualization.

the encapsulated Dox showed great stability and less than 20% Dox was released after 140min. As comparison, at 47°C, 17% encapsulated Dox was released after the first 20min and more than 50% was released after 140min. When the temperature was further increased to 60°C, Dox was released even faster. About 30% was released during the first 20min and 70% after 140 min. The swift growth of the releasing speed is due to the temperature and heat triggered capsule

disassembly. These studies further demonstrate the disassembly and release of these H-bonding based capsules can be conveniently controlled by managing temperature.

3.4 Conclusion

In summary, we showed that despite lack of directionality and specificity, the high cooperativity imparted by dendrimer macromolecules enable their spontaneously self-assemble via H-bonds into stable hollow capsules in the common less polar organic solvents. More interestedly, we revealed the potential cooperative formation of multiple H-bond polyhedron network that can significantly enhance the strength and stability of H-bonding, which allows for dendrimer self-assembly into capsules even in highly competitive and disruptive aqueous solutions. Such cooperatively H-bonded dendrimer capsules are thermo-responsive in nature, and we found a narrow and facile temperature window can be used to trigger controlled diassembly and release. Our finding demonstrates the intriguing ability of using cooperative H-bonding in regulating molecular self-assembly process and property, and we expect this finding will lead to new strategies for designing functional supramolecular materials.

3.5 Experimental information

3.5.1 Materials

G4-Fréchet-32COOH, G2-Newkome-36COOH: The detailed synthesis was described in Chapter 2. 1H NMR (D2O) G2-Newkome 36COOH: δ(ppm) = 1.72 (br, 72H, a, CH2CH2COO), 1.94 (br, 72H, b, CH2COO), 2.33 (br, 8H, c, CH2CONH), 3.21(br, 8H, d, CH2CH2O) and 3.47(br, 8H, e, OCH2), Figure 3.6.

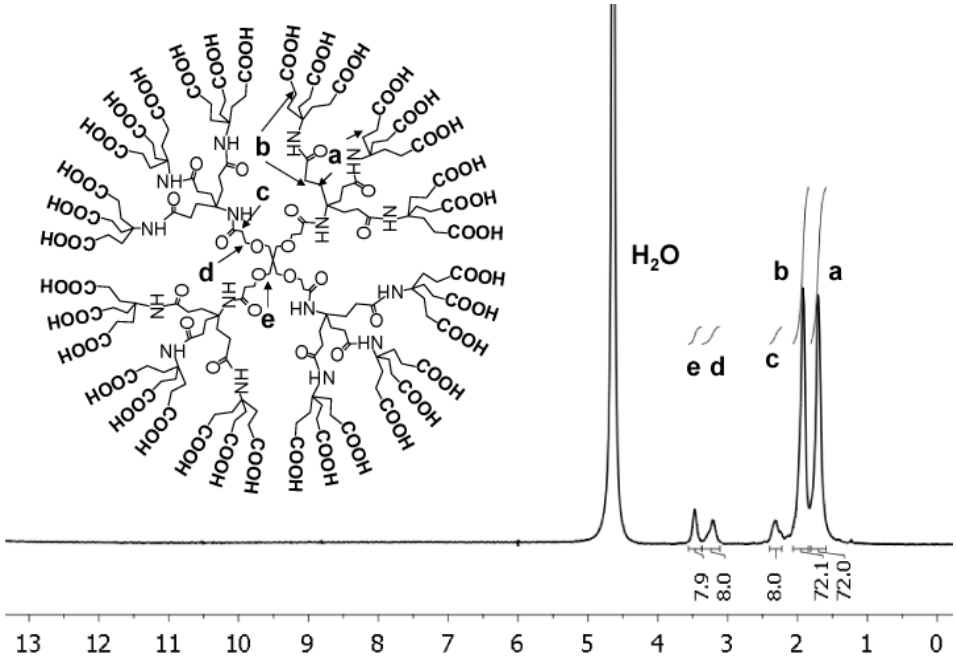

Figure 3.6 NMR spectra of synthesized G2-Newkome-36COOH.

G2-Newkome-36OH were then prepared by reacting the corresponding ester intermediates with tris(hydroxymethyl)aminomethane in DMSO, using K2CO3 as catalyst [18,19], Figure 3.7. 1H NMR (D2O) of the synthesized G2-Newkome-36OH: δ(ppm) = 1.77 (br, 24H, a, CH2CH2CONH), 2.01 (br, 24H, b, CH2CONH), 2.40 (br, 8H, c, CH2CH2O), 3.29 (br, 8H, d, CH2CH2O), 3.40 (s, 72H, e, CH2OH) and 3.58 (br, 8H, f, OCH2), Figure 3.8.

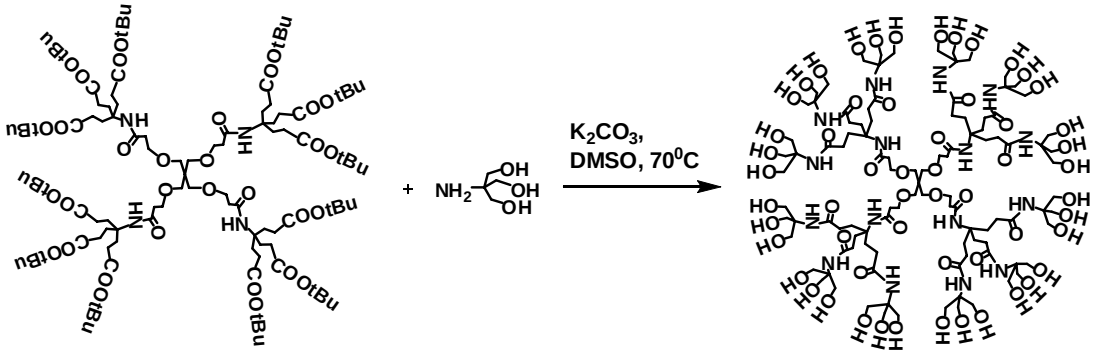

Figure 3.7 Reaction scheme for the preparation of G2-Newkome-36OH.

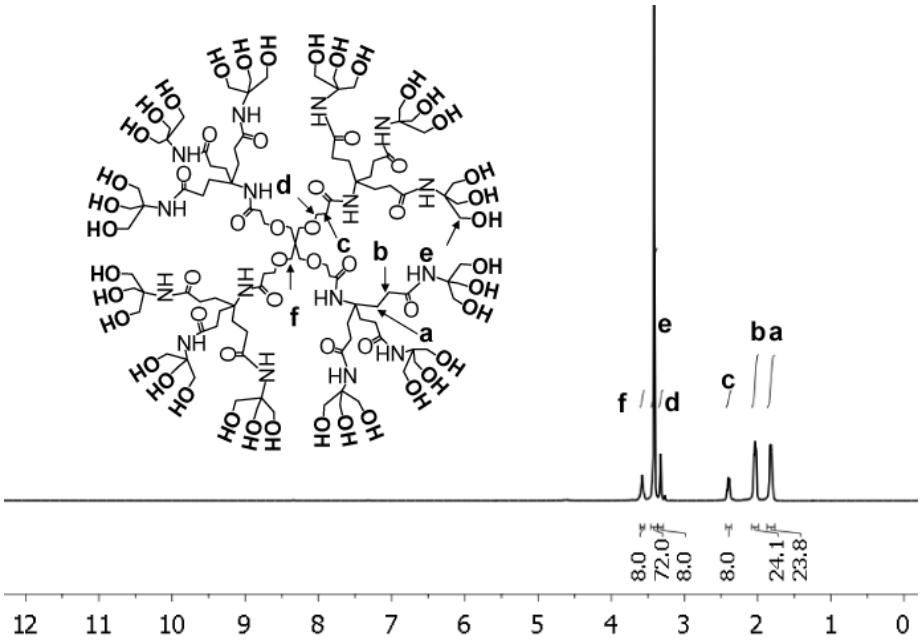

Figure 3.8 NMR spectra of synthesized G2-Newkome-36OH.

G4-Fréchet-32OH were prepared by esterification of the corresponding G4-Fréchet-COOH dendrimers with ethanediol, HOCH2CH2OH, using a mixture of MeSO3H and Al2O3.[20] 1H NMR ([H6]-DMSO) of G4-Fréchet-32OH: δ(ppm) = 3.88 (t, 64H, a, CH2OH), 4.44 (t, 64H, b, OCH2CH2OH), 4.78-5.21 (m, 124H, c, OCH2), 6.25-6.70 (m, 90H, d, ArH), 6.72-6.80 (m, 4H, e, core ArH), 7.12-7.98 (m, total 132H, f, 128PhH and 4 core ArH)

Dendrimer Capsule Preparation: Tetrahydrofuran (THF) (CHROMASOLV PLUS, for HPLC, ≥99.9%, inhibitor free) and Chloroform (CHROMASOLV PLUS, for HPLC, ≥99.9%, contains 0.5-1.0% ethanol as stabilizer) were purchased from Sigma-Aldrich and were used as received. Water was purified by PURELAB Plus® High Purity Water Polishing System (U.S.Filter), and then filtrated through syringe filters with 0.45μm sized pore (polypropylene filter media, Whatman®). Dendrimers were added into proper solvent following the

concentrations listed in Table 3.1., and then stirred for 2h followed by placing still for another 2h before further testing.

Table 3.1. H-bonded dendrimer capsule solution preparation

Dendrimer	G4-Fréchet-32COOH		G2-Newkome-36COOH		G2-Newkome-36OH	
Solvent	THF	Chloroform	THF	Chloroform	H_2O	D_2O
Concentration	1mg/mL	1mg/mL	1mg/mL	1mg/mL	1mg/mL	1mg/mL

3.5.2 Methods

Light and Fluorescent Microscopy Imaging: Capsules formed by dendrimers Fréchet-G4-32COOH and Newkome-G2-36COOH in THF or Chloroform, were imaged by Olympus IX71 inverted microscope with a 60X objective and a Cascade CCD camera. 3μL dendrimer capsule solution was pipetted onto a glass slide (3″×1″×1mm, Premium Microscope Slides, Fisher) and the coverslip(25×25×0.13~0.17mm, Premium Cover Glass, Fisher) was carefully placed on. The sample was then directly visualized under bright-field light microscope. The encapsulated and released Dox were imaged by using an Olympus IX71 inverted fluorescence microscope with a 60X objective and a Cascade CCD camera. The Dox-encapsulated capsules were obtained by overlapping the light microscopy image of capsules and the fluorescence microscope image of the encapsulated Dox with *Image-Pro® Plus* version 6.2. The glass slides and coverslips were rinsed with ethanol and dried with N_2 before using.

Cryo-Transmition Electron Microscopy (TEM) measurements: The capsules formed by G2-Newkome-36OH in aqueous solution were imaged by Cryo-TEM. The Cryo-TEM specimen was prepared by pipetting 3μL capsules solution onto a lacey carbon copper grid (ESI) for 30s, followed by removal excess liquid with a piece of filter paper, leaving a thin film of solution spanning the grid. The specimen was then quickly plunged into liquid nitrogen. The specimen was stored in liquid nitrogen, and then transferred to a cryogenic sample holder (Gatan 626) in a FET TECNAI 20G TEM operating at -177°C for imaging.

Negatively-stained TEM measurements: Surface topologies of dendrimer capsules were imaged by negatively-stained TEM. 3μL dendrimer capsule solution was pipetted onto a carbon coated formvar copper grids. A piece of filter paper was then used to quickly remove the excess liquid, leaving a thin film of solution spanning the grid. The sample copper grids were then quickly dried under vacuum. For negative staining, a droplet of 2% uranyl acetate in ethanol was placed onto the dried specimen for 30 seconds and the excess liquid was removed by filter paper before imaging. TEM images were obtained on a FET TECNAI 20G TEM operating at an acceleration voltage of 200kV and at ambient temperature.

FT-IR Spectroscopy measurements of dendrimers capsules were obtained on a Digilab (Cambridge, MA) FT-7000 Fourier Transform Infrared spectrometer, equipped with a MCT detector, ZnSe crystal sample stage and continuously purging with dry filtered air. 10μL of 1mg/mL dendrimers capsules solution were pipetted onto the crystal and dried before testing. The FT-IR spectra of dis-assembled Newkome-OH dendrimers aqueous solution was taken at 65°C by heating ZnSe crystal sample stage with a heating and cooling thermostat (Lauda Brinkmann). The dendrimers solution was incubated at 65°C for 1h before pipetted onto the 65°C crystal sample stage, followed by drying with filtered air. Interferograms were collected at

4cm^{-1} resolution and apodized with a NB(Norton-Beer) Function. Second derivative spectra were obtained with the use of a 9 point Savitsky-Golay algorithm from the Digilab software.

Dynamic Light Scattering (DLS) measurement: The hydrodynamic radius and the size distribution of the dendrimer capsules in solution were measured by ZETASIZER Nano-S90, Malvern, with a 633nm laser and scattering angle fixed at 90°. The cuvette was filled with dendrimer capsule solution and was equilibritated at set temperature for 10min before measurement. The dis-assembly of Newkome-OH dendrimer capsules in aqueous solution was record at 25°C, 35°C, 45°C, 47°C, 50°C, 55°C, 65°C, 75°C.

Sample preparation for release kinetics: Dox loaded dendrimer capsule solution was prepared by first dissolving Dox in purified water as 100μg mL^{-1}. G2-Newkome-36OH was added into a certain volume of Dox aqueous solution to reach the concentration as 1mg mL^{-1}. The solution was then stirred for 4h at 25°C in dark, and dialyzed against purified water at 25°C in dark for 1h. To ensure a complete remove of the free Dox, the concentration of Dox was monitored by UV-Vis every 20mins until it was constant.

UV-Vis spectrometry measurement for release kinetics was carried on a Cary 100 UV-Vis spectrophotometer. The 485nm absorption intensity of Dox was monitored as an indication of concentration. The absorption of 1mg/mL dendrimer aqueous solution was also measured, and subtracted as background. In order to obtain the release kinetics, 3mL Dox-loaded capsule solution was injected into a cassette (molecular weight cut-off 2000g mol^{-1}, 3mL capacity, Thermo Scientific), and then dialyzed against 200mL purified water at 25°C, 47°C, or 55°C. 150μL internal solution was taken from the dialysis cassette every 20min, and placed into a 4X2mm quartz microcuvette. The solution was injected right back after UV-Vis testing. The

total solution volume was measured after the test, and no volume increase was observed, so the dilution did not contribute to the concentration decrease.

Computational Simulation: A model of the HF/6-31++G(2d,2p) optimized structure of the end of G2-Newkome-36OH dendrimer was developed to determine the relative stability of a simple dendrimer-dendrimer interaction in solvent. Two monomeric tri-hydroxyl clusters were then combined together to develop the dimer-interaction model. Both the monomer and dimer-interaction models were subjected to single point energy calculations with HF/6-31++G(2d,2p) and the Gaussian 03 implicit water model[21] to determine the solvation energy contribution. This part of work was done by Matthew Tessier and Dr. Robert Woods.

3.6 References

(1) Jencks, W. P. *Proc. Natl. Acad. Sci. U. S. A.* **1981**, *78*, 4046-4050.

(2) Mammen, M.; Choi, S. K.; Whitesides, G. M. *Angew. Chem., Int. Ed.* **1998**, *37*, 2755-2794.

(3) Hughes, A. D.; Anslyn, E. V. *Proc. Natl. Acad. Sci. U. S. A* **2007**, *104*, 6538-6543.

(4) Scrutton, N. S.; Deonarain, M. P.; Berry, A.; Perham, R. N. *Science* **1992**, *258*, 1140-1143.

(5) Gnichwitz, J. F.; Wielopolski, M.; Hartnagel, K.; Hartnagel, U.; Guldi, D. M.; Hirsch, A. *J. Am. Chem. Soc.* **2008**, *130*, 8491-8501.

(6) Ercolani, G. *J. Am. Chem. Soc.* **2003**, *125*, 16097-16103.

(7) Garrett, T. M.; Koert, U.; Lehn, J. M. *J. Phys. Org. Chem.* **1992**, *5*, 529-532.

(8) Jeffrey, G. A.; Saenger, W. *Hydrogen Bonding in Biological Structures*; Springer-Verlag: Berlin, 1991.

(9) Whitesides, G. M.; Mathias, J. P.; Seto, C. T. *Science* **1991**, *254*, 1312-1319.

(10) Lawrence, D. S.; Jiang, T.; Levett, M. *Chem. Rev.* **1995**, *95*, 2229-2260.

(11) Whitesides, G. M.; Mathias, J. P.; Seto, C. T. *Science* **1991**, *254*, 1312-1319.

(12) Krische, M. J.; Lehn, J. M. *Molecular Self-Assembly* **2000**, *96*, 3-29.

(13) Dong, W. Y.; Zhou, Y. F.; Yan, D. Y.; Li, H. Q.; Liu, Y. *Phys. Chem. Chem. Phys.* **2007**, *9*, 1255-1262.

(14) Ju, R.; Tessier, M.; Olliff, L.; Woods, R.; Summers, A.; Geng, Y. *Chem. Commun.* **2011**, *47*, 268-270.

(15) Kumar, U.; Kato, T.; Frechet, J. M. J. *J. Am. Chem. Soc.* **1992**, *114*, 6630-6639.

(16) Kato, T.; Frechet, J. M. J. *J. Am. Chem. Soc.* **1989**, *111*, 8533-8534.

(17) Caspar, D. L. *Biophys. J.* **1980**, *32*, 103.

(18) Newkome, G. R.; Baker, G. R.; Saunders, M. J.; Russo, P. S.; Gupta, V. K.; Yao, Z. Q.; Miller, J. E.; Bouillion, K. *J. Chem. Soc., Chem. Commun.* **1986**, 752-753.

(19) Halabi, A.; Strumia, M. C. *J. Org. Chem.* **2000**, *65*, 9210-9213.

(20) Sharghi, H.; Hosseini, M.; Sarvari *Tetrahedron* **2003**, *59*, 3627-3633.

(21) Frisch, M. J.; Trucks, G. W.; Schlegel, H. B.; Scuseria, G. E.; Robb, M. A.; Cheeseman, J. R.; Montgomery, J., J. A.; Vreven, T.; Kudin, K. N.; Burant, J. C.; Millam, J. M.; Iyengar, S. S.; Tomasi, J.; Barone, V.; Mennucci, B.; Cossi, M. *et al.*; Gaussian, Inc.: Wallingford, CT, 2004.

CHAPTER 4

EMULSION-TEMPLATED DENDRIMER CAPSULES

Rong Ju, Yan Geng.

To be submitted to *Soft Matter*

4.1 Abstract

Previously, we exploited the unique features of dendrimers as highly-branched, nanometer sized molecular spheres and demonstrate their ability to maximize cooperative binding, which allows for spontaneous self-assembly into submicron capsules in solution via salt bridge or H-bonding. Here, we applied dendrimers as molecular nanospheres to spontaneously adsorb onto emulsion droplet surface. The multiple periphery binding sites of dendrimers allows them to cooperatively bind into multiple-layered capsules. Such emulsion-templated dendrimer self-assembly advanced the capsule formation to a broad range of micron sizes, which enables versatile and efficient encapsulation of a wide variety of materials. These dendrimer capsules also have the advantages of ease in controlling disassembly and release of the encapsulant with external stimuli, such as the addition of EDTA or heat.

4.2 Introduction

Dendrimers are highly-branched, three-dimensionally spherical and nanometer-sized macromolecules, which have attracted broad interest due to their unique architecture and interesting properties.[1-9] Previously, we exploited the unique features of dendrimers and demonstrated their ability to maximize cooperative binding, which allows for spontaneous self-assembly into submicron capsules in solution via salt bridge or H-bonding.[10,11] The spontaneous formation of hollow capsules provides a convenient method for the direct encapsulation of materials, however, passive enclosure is generally associated with significant material loss and their submicron sizes also limit the range of materials that can be encapsulated. In order to overcome these drawbacks in spontaneously formed dendrimer capsules, more active fabrication approach need to be explored.

Efficient encapsulation is important to many technologies, ranging from drug delivery, food processing, waste removal, to catalysis, artificial enzyme reactors and/or protein/cell transplantations.[12-22] Among many different approaches, using emulsions as templates to direct capsule formation has the advantages of simplicity, effectiveness and versatility, and is a very active area of research.[23-25] Since the target material will be directly emulsified and contained within the liquid emulsion droplets, minimal material loss is expected. Moreover, emulsification allows for the production of capsule sizes ranging from submicrons, microns to even millimetres, which makes encapsulation of a wide variety of materials possible. In the earlier studies on emulsions, the surface of emulsion droplets is typically modified with ionic surfactants to introduce charge, and oppositely charged polyelectrolytes or particles are then used to adsorb onto the emulsion surface via electrostatic interactions. Recently, a more general adsorption mechanism has been revealed.[26,27] Due to the surface energy difference between the emulsion interface and the particle in two fluids, if particles fall in the nanometer to micrometer size range, their adsorption onto the emulsion surface is energetically favored and can proceed spontaneously without any surface pre-treatment.[28-30] This general mechanism has significantly advanced the applicability of emulsions, and intensive effort has been made to exploit emulsions for nanoparticle or micron-sized colloidal particle assembly, where solid particles spontaneously adsorb onto the surface of emulsion droplets to form a close-packed layer and subsequently be interlocked together by sintering or other treatments into solid capsules.

Despite the tremendous success with solid nanoparticles and colloidal particles, little thoughts have been given to applying this general emulsion adsorption mechanism to molecules. This is probably because most molecules are below nanometer in size and have large degree of freedom in molecular conformation and dynamics. At the molecular level, the concept of

molecule adsorbing onto the emulsion surface has been traditionally limited to surfactants, due to their amphiphilic nature. Here, based on the unique nanometer size and spherical architecture of dendrimers, we hypothesize that dendrimers as molecular nanospheres-just like solid nanoparticles-will also be able to spontaneously adsorb onto emulsion droplet surface. We also expect that once adsorbed, the highly-branched periphery of dendrimers will allow them to spontaneously bind cooperatively into stable shells. If so, using emulsification as the template to assemble dendrimer molecules into capsules will enhance the encapsulation versatility and loading efficiency. Moreover, it will extend the emulsion-templated self-assembly approach into the molecular regime and bring forth molecular-leveled functions, controls and advantages into capsule fabrication.

4.3 Results and Discussion

4.3.1 Emulsion-templated dendrimer self-assembly

To explore the general applicability of emulsification in templating dendrimer self-assembly, dendrimers that differed significantly in composition, branching motif and rigidity were investigated, Figure 4.1. The Fréchet-type dendrimers are composed of rather rigid and highly hydrophobic benzyl ether interior, whereas the Newkome-type dendrimers have much more conformational freedom around the sp^3-C branching points, and their amide rich interior is much more hydrophilic. Since the size of a dendrimer is determined by the number of layer of branches, different generations of dendrimers were also examined. The terminal of each dendrimer molecule was then functionalized with carboxyl (-COOH) or hydroxyl (-OH) groups to achieve different potential peripheral binding.

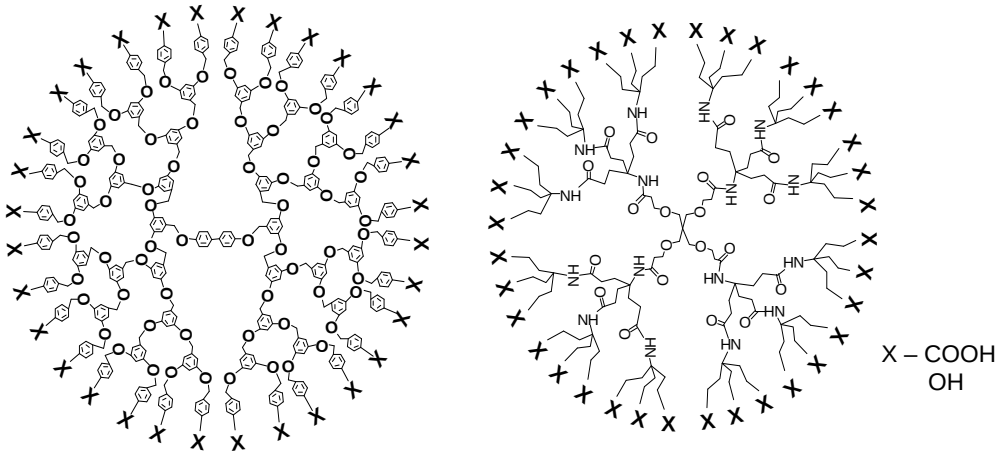

Fréchet-type dendrimer Newkome-type dendrimer

Figure 4.1. Molecular structure of Fréchet-type and Newkome-type dendrimers functionalized with either carboxyl or hydroxyl peripheral groups (-X).

Upon the addition of dendrimer molecules into emulsion solutions that contain micron-sized oil-in-water or water-in-oil droplets, dendrimer molecules, regardless of composition, spontaneously adsorb onto the surface of emulsion droplets and form stable capsules, Figure 4.2. Direct light microscopy imaging on these capsules in solution revealed the projection of their hollow micron-sized cavities and dense membranes, Figure 4.2A. The capsule membrane can also be labelled by fluorescent dyes and visualized by fluorescent microscopy, Figure 4.2B. The contour of these dendrimer capsules suggests that they are elastic and deformable. The surface topology of these micron-scaled dendrimer capsules was then visualized by scanning electron microscopy (SEM) after drying, Figure 4.2C. Due to the elastic nature, some deformed capsules could also be found, Figure 4.2D. The fact that these capsules remained enclosed and intact without breakage after drying indicates that they are highly robust and can provide sufficient mechanical strength as protective coatings.

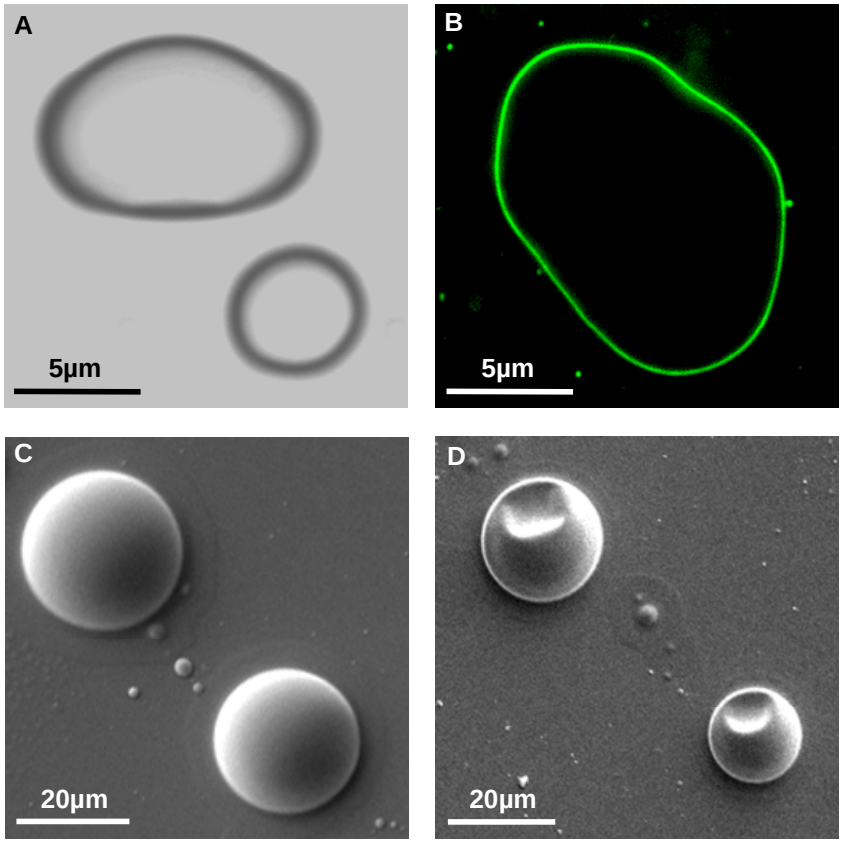

Figure 4.2 Imaging of emulsion-templated dendrimer capsules by light microscopy (**A**); Fluorescent microscopy (**B**); and scanning electron microscopy (**C** & **D**).

The mechanism that underlines the formation of emulsion-templated dendrimer capsule formation is schematically illustrated in Figure 4.3. In the first step, dendrimers as molecular nanospheres spontaneously adsorb onto the surface of emulsion droplets, Figure 4.3A, B. For particles with sizes in the nanometer to micrometer range, the surface energy between the two immiscible fluids, $\sigma_{i,e}$, generally exceeds the difference of the surface energies between the particle and the fluid, $\sigma_{p,i}$, and between the particle and the external fluid, $\sigma_{p,e}$, *i.e.* $\sigma_{i,e} > | \sigma_{p,i} - \sigma_{p,e} |$. This principle has been widely applied to solid nanoparticles and micron-sized colloidal particles. Our studies demonstrated that this surface energy driven adsorption principle also

applies to nanometer-sized, spherical-shaped molecules, such as dendrimers, and is independent of dendrimer compositions and terminal functionalities.

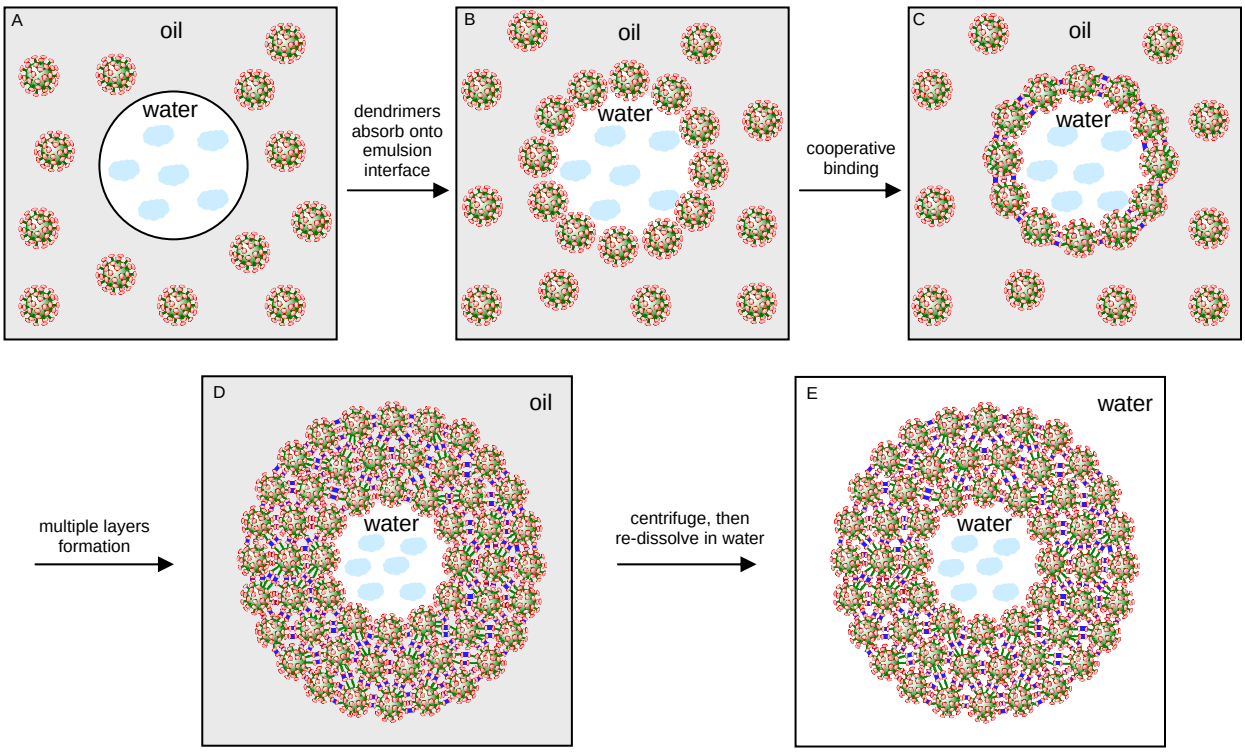

Figure 4.3. Schematic illustration of the emulstion-templated self-assembly process of dendrimers into capsules.

After the emulsion droplet surface is completely covered by dendrimer nanospheres, a layer of close-packed dendrimer shell is formed and the dendrimer molecules are brought to close proximity which enables direct binding with each other at the periphery, Figure 4.3C. Unlike solid nanoparticle or colloidal particles, which require sintering or other treatment, the cooperative binding between close-packed dendrimer molecules will spontaneously interlock them into a shell. The large numbers of terminal binding sites of dendrimer molecules will also enable multiple intermolecular bonding, which further enhance the stability and robustness of the

shell. The binding mechanism between dendrimers can be quite versatile, depending on the terminal functional groups that are already encoded in the dendrimer molecular design. For example, carboxyl terminal groups will give rise to stable intermolecular dimeric-carboxyl hydrogen bonding in less polar oil phase, whereas in aqueous solutions, the dissociated carboxylate terminal anions allow for intermolecular COO^{-}-M^{2+}-COO^{-} ionic salt-bridging with the addition of divalent M^{2+} counterion. The hydroxyl terminal groups, on the other hand, remain neutral in both oil and aqueous solutions and are able to form intermolecular O–H---O hydrogen bonds. However, individual O–H---O hydrogen bonds are rather weak, and our previous studies show that in order to generate sufficiently strong and stable intermolecular binding force, the dendrimers needed to be flexible enough to cooperatively form multiple H-bonding polyhedron networks. Rigid dendrimers, such as Fréchet-type dendrimers, lack this capability and are not able to bind strongly with hydroxyl terminal groups. In this study, we also found that with hydroxyl terminal groups, although both Newkome and Fréchet-OH dendrimers can readily adsorb onto the emulsion surface, stably bound shells were only found with flexible Newkome-OH dendrimers.

One notable difference between dendrimer molecules and solid particles in the emulsion-templated self-assembly process is their ability to form multiple layers. Once the initial close-packed dendrimer shell is formed at the emulsion surface, the highly-branched feature of dendrimer molecules allow them to continue to bind into the next layer, Figure 4.3D. The total number of dendrimer shell layers determines the membrane thickness of the capsule formed, and is influenced by many factors. With ionic dendrimers in bulk aqueous media, the capsule membrane thickness increases with the amount of divalent cation added, which is responsible for the inter-dendrimer salt-bridge formation, before reaching a maximum value. With dendrimer

capsules driven by spontaneous H-bonding, the membrane thickness is mostly affected by the amount of dendrimers added to a certain volume of emulsion solutions. The maximum capsule thickness of different dendrimer molecules appears to be innately determined by the curvature of the emulsion droplets and the size of the dendrimer molecule. Dendrimers in fewer generation and smaller in size tends to generate thicker capsules compared to their larger counterparts, presumably due to easier packing of smaller particles around the same curvature. The typical maximum capsule thickness for the dendrimers used in this study ranges from 200nm to 500nm, depending on the binding motifs and the dendrimer generation, which suggests more than a hundred layers of close-packed dendrimer spheres, can be achieved at the surface of the emulsion droplets. The ability of dendrimers to form multiple layers of close-packed shells can not only be used to enhance the mechanical strength of the capsules, but also provide a convenient method used to adjust the permeability of these dendrimer capsules.

After the final formation of dendrimer capsules at the emulsion droplet surface, these highly-robust capsules can be collected using a centrifuge and then re-suspended in a different media, *e.g.* the same media as the internal phase, Figure 4.3E. This eliminates the phase difference between the interior and exterior of these dendrimer capsules, or when a more bio- or environmental compatible media is required.

4.3.2 Versatile encapsulation by emulsion-templated dendrimer self-assembly

The emulsion-templated self-assembly of dendrimers expands the potential capsule size to a broad range beyond nanometers, which will allow for versatile encapsulation of a wide variety of different materials. This method also provides an active and convenient approach that leads to highly efficient encapsulation of target materials. In this method, target material pre-dissolved in a select solvent will be emulsified with an immiscible fluid and is expected to be

confined within the emulsion droplet throughout the process. Minimal material loss can thus be achieved. Moreover, the versatility in dendrimer molecular design in the aspects of terminal groups, branching motif and generation further allows for control of the interlocking mechanism and flexible adjustment of the capsule properties, such as permeability.

In Figure 4.4, we demonstrated the encapsulation of small drugs, bio-macromolecular proteins and living cells, respectively, by using emulsification and different dendrimers. A dual drug loading by emulsion-templated dendrimer capsules is shown in Figure 4.4A, using two anti-cancer drugs – Doxorubicin, which is automatically red fluorescent, and green-fluorescently labelled Taxol. Efficient drug loading is the critical first step for drug delivery, and lots of effort has been made to achieve this goal. The common approach of passive enclosure of drugs followed by removing the excess free drugs, however, is intrinsically associated with significant material loss. Many active methods developed to enhance loading also have their limitations. For example, a pH gradient across the membrane is commonly used to help the anti-cancer drug Doxorubicin permeate through membranes and load into the lumen of liposomes and polymersomes. However, due to its crystalline nature, the passage of Doxorubicin through membranes is difficult and leads to low loading efficiency. Here, water-soluble Dox was directly dissolved in a small amount of aqueous solution before emulsification in oil and will be confined within the water droplets throughout the process. Fréchet-COOH dendrimers were subsequently added to form capsules enclosing the Dox containing water droplets. To remove the oil phase, the Dox loaded dendrimer capsules were spin down by centrifuge and re-suspended in biocompatible aqueous solution that contains Ca^{2+} to interlock dendrimers. Since most drugs are small molecules, e.g. Dox has MW ~ 500, Fréchet-type dendrimers that are tightened in conformation and highly hydrophobic in nature are more suitable for drug encapsulation

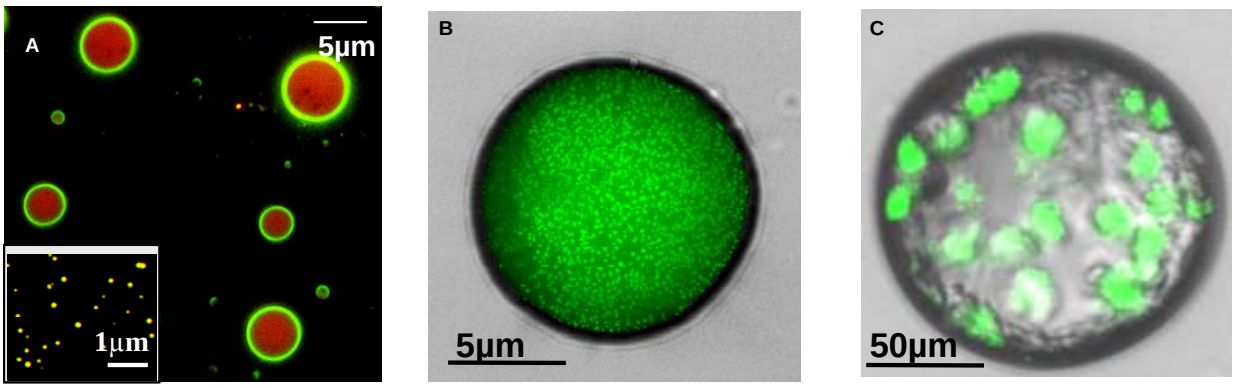

Figure 4.4 Encapsulation of target materials by emulsification. (**A**) Dual drug loading. Red fluorescent: Doxorubicin; Green fluorescent: Taxol. Inset: Extrusion of micron-sized dendrimer capsules into 100nm size. (**B**) Encapsulation of green-fluorescently labelled streptavidin. (**C**) Encapsulating of living human embryonic kidney cells marked by green-fluorescent Calcein.

purpose, which can effectively prevent the undesirable leakage of the loaded small drug molecules. The molecular feature of Fréchet dendrimers that constitute the capsule membrane can be further exploited to achieve multi-functionality. For example, each Fréchet- dendrimer of the capsule membrane can function as an unimolecular micelle to load with a hydrophobic drug inside its hydrophobic core. Thus, in addition to encapsulation of a water-soluble drug inside the cavity, the capsule membrane can load another hydrophobic drug to achieve dual drug loading, as shown in Figure 4.4A. Moreover, these elastic, micron-sized, dual-drug loaded dendrimersomes can be further extruded into much smaller sizes without leakage. This ability allows us to flexibly control the final size of these dendrimer capsules and make mono-dispersed nanoscale capsules, if required. For drug delivery applications, nanometer sized particles would be more advantageous since smaller particle size can prolong circulation and enhance cell internalization. In the inset of Figure 4.4A, we show the extrusion of initial tens-of-microns sized dual-drug loaded dendrimer capsules in size into ca. 100nm sized capsules.

Other than encapsulating small molecules, using dendrimers for emulsification also provides a convenient and efficient method for encapsulating proteins and enzymes, which is important for many biotechnological applications, such as in bioreactors, sensors and protein implantations. Here, by using green-fluorescently labelled streptavidin as a model protein, we have demonstrated the encapsulation of biomacromolecules by using dendrimers and emulsification, Figure 4.4B. Following similar procedures, streptavidin was dissolved in a small amount of aqueous solution and emulsified into droplets in oil, and Newkome-OH dendrimers were then added to the emulsion solution, which spontaneously adsorbed onto the streptavidin-containing water droplets and interlock into stable capsules via H-bonding. The dendrimer capsules with streptavidin enclosed inside were then collected by centrifuge and re-dispersed in biocompatible aqueous media.

Beyond molecular targets, this approach is also applicable to encapsulating much larger objects, such as living cells, which are typically around 10μm in size. With the rapid development of cell and tissue engineering, there is an increasing need in encapsulating living cells in recent years. However, due to their large size, as well as conditions required to support living cells, nano-sized capsules as well as many traditional encapsulation techniques, such as coating, are not suitable for encapsulating living cells. Here, we successfully encapsulated living human embryonic kidney cells as an example, using emulsification and Newkome-OH dendrimers, Figure 4.4C. The cells were stained with Calcein, *i.e.* a viability marker to allow only viable cells emit green fluorescence, and the viability of these cells encapsulated in the Newkome-OH dendrimer capsules was observed to maintain beyond twelve hours. Other than protecting the cells from the surrounding environment, the tightly bound dendrimer capsule

membranes are also likely to provide a robust and biocompatible scaffold that supports the living cells and enhances their viability.

In these encapsulation studies, different dendrimers were selected for different purposes. By changing the terminal groups of dendrimers, different peripheral binding and interlocking mechanism via either salt-bridge or hydrogen-bonding can be allowed. Different interior of dendrimers, on the other hand, will have a strong impact on the permeability of the formed capsules. Unlike colloidosomes, where the permeability is defined by interstice holes between micron-sized colloidal particles, here dendrimers are molecular spheres of several nanometers in size and their tight binding and close-packing is unlikely to generate substantial interstice holes. However, the permeability of the dendrimer capsules can be conveniently adjusted by many other factors, such as the thickness of the capsule membrane as well as the molecular feature of dendrimer units. Since Fréchet-type dendrimers have tightened highly hydrophobic interior, the capsules that they generate are expected to have low permeability. Newkome-type dendrimers with a large hydrophilic interior, on the other hand, will enhance the permeability of the capsules and allows the passage of water, gas and/or small molecules. Depending on the desired usage of capsules, the right choice of dendrimers can be selected. For example, in the encapsulation of small molecule drugs, Fréchet-type dendrimers would efficiently prevent leakage of the encapsulated drugs, which is important for drug delivery applications. In contrast, for the encapsulation of larger materials, such as biomacromolecules and living cells, the leakage is a much less concern. Instead, it is more useful for the capsules to allow passage of water, gases and nutrients in many biotechnological applications, and the Newkome-type dendrimers would be more suitable for such applications.

Other than providing versatile peripheral binding motifs and flexible adjustment of the permeability of the capsules, using dendrimers as the building blocks also offers opportunities for incorporating molecular functions into the capsule membrane. In the drug encapsulation study, we took advantage of Fréchet-type dendrimers as unimolecular micelles to load a second drug into the dendrimer membrane.

4.3.3 Controlled disassembly and release mechanism of the emulsion-templated capsules

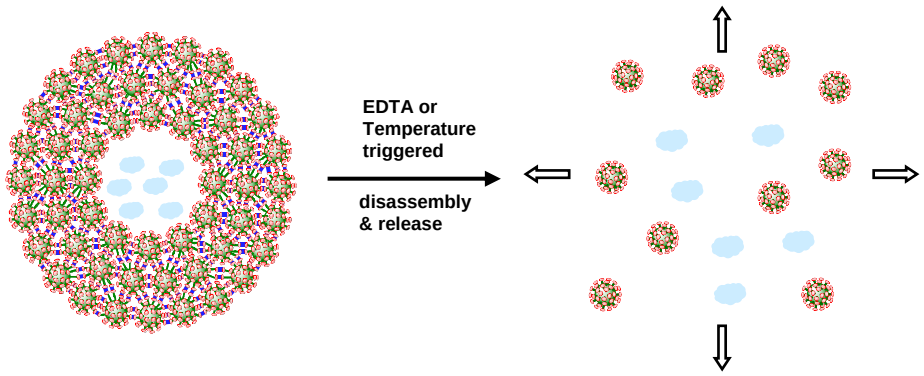

Figure 4.5 Schematic illustration of the controlled disassembly of the dendrimer capsules into dendrimer units and release of the contents.

In addition to versatile and efficient encapsulation, these micron scaled emulsion-templated dendrimer capsules also have the advantage of ease in controlling disassembly and release, just like the previously reported submicron denderimer capsules formed by spontaneous self-assembly. Although the fabrication process here starts with using emulsion droplets as template to assemble dendrimer molecules at the interface, the subsequent interlocking between dendrimer units into stable capsules is nonetheless based on cooperative peripheral binding forces, either via salt-bridge ionic interactions or hydrogen-bonding. Previously, we showed that with spontaneously self-assembled dendrimer capsules via COO^{-}-M^{2+}-COO^{-} salt-bridges,

removal of the M^{2+} sources would break down the capsules. The spontaneously self-assembled dendrimer capsules via hydrogen-bonding, on the other hand, are thermo-responsive in nature and would disassemble with increasing temperatures as hydrogen-bonding breaks down. In this study, we found similar strategies also apply to these micron-scaled, emulsion-templated dendrimer capsules, Figure 4.5.

In Figure 4.6A, we demonstrated the disassembly of salt-bridge bound, emulsion-templated dendrimer capsules with the addition of EDTA, *i.e.* an efficient Ca^{2+} chelator that can withdraw Ca^{2+} from the capsules. The tens-of-microns sized capsules made of Fréchet-COOH dendrimers were labelled with green fluorescent dyes, and their changes with the addition of EDTA were directly monitored in solution by Fluorescent Microscopy. Pores around the capsule membrane were observed to develop in tens of seconds. Eventually, the capsule membrane completely broke down into dispersing nanometer-sized dots, *i.e.* dendrimer units. In Figure 4.6B, we used Dynamic Light Scattering (DLS) to track the changes of hydrogen-bonded emulsion-templated dendrimer capsules with the increasing temperature. At the initial room temperature, the average particle radius in solution was measured by DLS as ca. 900nm, consistent with the predominant presence of submicron capsule structures, as visualized by TEM. However, as the temperature was increased to a critical value of 50 – 65°C, DLS measurements showed that the size of particles in solution quickly plunged to below 5nm, Figure 4.6B. This observation indicates that the capsule structures of micronmeter in size had completely disassembled into nanometer sized individual dendrimer molecular units. This temperature and heat triggered capsule disassembly further confirmed H-bonding as the major binding force for these dendrimer capsules. More importantly, such a narrow and facile temperature window can be exploited as a convenient controlled release mechanism for practical usages in drug delivery and sensor application.

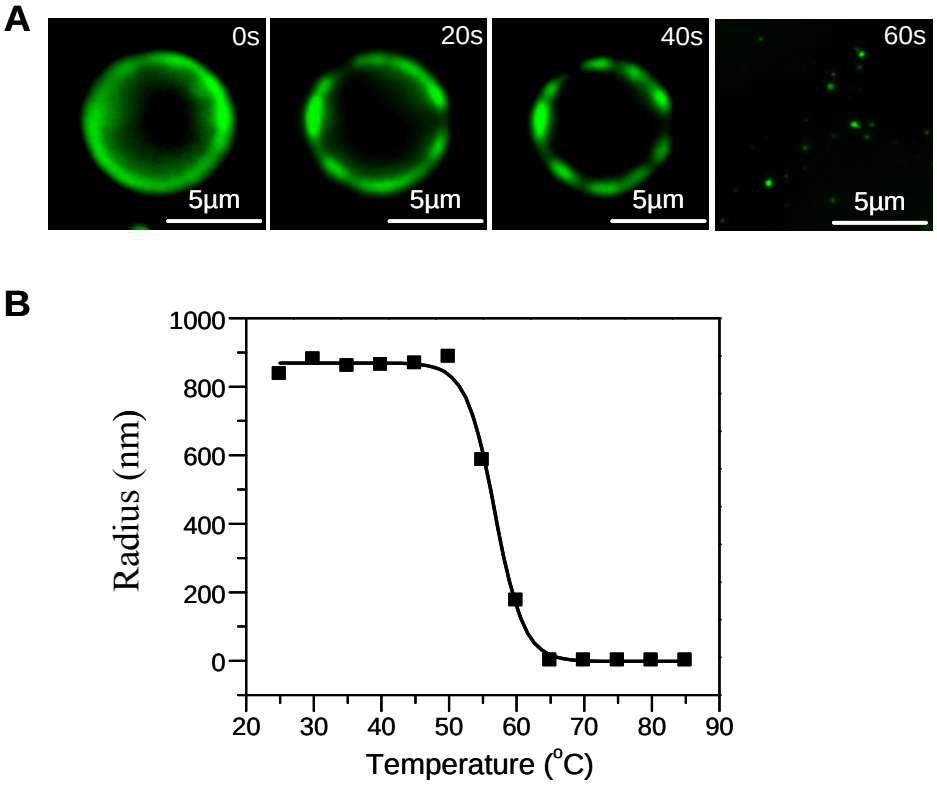

Figure 4.6 Imaging of disassembly of emulsion-templated dendrimer capsules. **(A)** salt-bridge bound emulsion-templated dendrimer capsules with the addition of EDTA; **(B)** Temperature triggered disassembly of hydrogen-bonded emulsion-templated dendrimer capsules.

4.4 Conclusion

In summary, we demonstrate that dendrimers as molecular nanospheres are able to spontaneously adsorb onto the emulsion droplet surface, just like solid nanoparticles. The highly-branched periphery of dendrimers allows them to cooperatively bind into multiple-layers of close-packed shells, which are stable and robust. The emulsion-templated dendrimer self-assembly expands the capsule to a broad range of micron sizes, which allows for versatile and

efficient encapsulation of a wide variety of materials. The micron-scaled emulsion-templated dendrimer capsules also have the advantages of ease in controlling disassembly and release of the encapsulant with external stimuli, such as the addition of EDTA or heat.

4.5 Experimental information

4.5.1 Materials

G4-Fréchet-32COOH, G2-Newkome-36COOH, G4-Fréchet-32OH, G2-Newkome-36OH were synthesized as described in Chapter 2 and 3.

Emulsion-templated dendrimer capsules formations were performed by using either water in oil (W/O) or oil in water (O/W) emulsions. To use the W/O emulsion as template, 10mg dendrimer, G4-Fréchet-32COOH or G2-Newkome-36COOH, was suspended in 200μL mineral oil. 100μL water was added, followed by shaking or vortexing for 5min. W/O emulsion droplets were densely covered by dendrimers to form dendrimers capsules. Then 100 μL $CaCl_2$ (pH=7.2), was carefully added to the bottom of the vial by a micropipette. The capsules (1-100μm) were moved from oil phase to aqueous phase by centrifuge at 600rmp for 30s. The capsules were collected by carefully taking the aqueous phase. W/O emulsion was also applied to template the self-assembly of G2-Newkome-36OH by vortexing 100μL water and 200μL mineral oil to form emulsion, and dendrimer was added while vortexing until droplets were densely covered. The capsules (1-100μm) were collected by centrifuge. To use the O/W emulsion as template, 100μL octanol was added into 200μL water, followed by shaking or vortexing. 10mg dendrimer was added into the emulsion solution while vortexing until droplets (1-100μm) were densely covered. The capsules (1-100μm) were collected by centrifuge.

Dual-drug Encapsulation: Doxorubicin hydrochloride (Dox) and Paclitaxel, Oregon Green® 488 conjugate were purchased from Sigma-Aldrich and Invitrogen, respectively. Dox

was encapsulated by adding 100μL Dox aqueous solution (1mg/mL) into the dendrimers oil suspension, followed by vortexing for 5min until the Dox droplets were densely covered by dendrimers. In order to lock the dendrimers together, 100 μL $CaCl_2$ (pH=7.2) was carefully added to the bottom and centrifuged at 600rmp for 30s to move capsules from oil phase to aqueous phase. 50μL aqueous phase was then taken. 5μL Paclitaxel (10^{-6} M, ethanol) was added into the aqueous capsules solution to stain dendrimers hydrophobic core. The capsules with dual-drug loaded were then observed under FM, with encapsulated Dox as red and Paclitaxel as green in membrane. Nanometer-sized dual-drug loaded capsules were obtained by extrusion. 2mL aqueous capsule solution was loaded in Extruder (LIPEX ™) with double-layered filtration membrane (PC, 25mm, 0.1μM, Whatman). Nitrogen gas flow with 800psi was applied. Multiple filtrations may be performed to reach monodisperse**.**

Encapsulation of protein/enzyme: Alexa Fluor® 488 FluoroNanogold-Streptavidin were purchased from Nanoprobes, and used as received. 100μL Streptavidin aqueous solution (2μg/mL) was mixed with 200μL mineral oil, followed by vortexing. 10mg G2-Newkome-36OH dendrimer was added while vortexing.

Encapsulation of cell: 2mL 293H cells in media solution was obtained by centrifuge at 1800rmp for 1min to remove the media, followed by washing for three times with PBS to fully remove the media. The live cells were stained by incubating with 1μL Calcein for 20min. To encapsulate live cells in dendrimer capsules, 100μL cell/PBS solution was mixed 200μL mineral oil. Then 10mg G2-Newkome-36OH dendrimer was added with gentle shaking.

4.5.2 Methods

Fluorescent and Light Microscopy Imaging: Dendrimer capsules were directly visualized under bright-field without dye labeling, using the Olympus IX71 inverted microscope.

Dendrimer capsules were also imaged on the Olympus IX71 inverted fluorescence microscope with a 60X objective and a Cascade CCD camera. A hydrophobic fluorophore dye (PKH 26) was used to label dendrimers in aqueous solution. The dual-drug loaded capsules were imaged by fluorescence microscope with encapsulated Dox as red and Paclitaxel as green in membrane. In both methods, 3μL dendrimer capsule solution was pipetted onto a glass slide (3″×1″×1mm, Premium Microscope Slides, Fisher) and the coverslip(25×25×0.13~0.17mm, Premium Cover Glass, Fisher) was carefully placed on. The glass slides and coverslips were rinsed with ethanol and dried with N_2 before using.

Scanning Electron Microscopy (SEM) measurement was obtained on a FEI Inspect F FEG-SEM at an accelerating voltage of 5kV. The surface of silicon wafer substrate was methylated following the previous publication. A drop of dendrimer capsule solution was suspended on to the substrate. The sample was dried in a desicator, and then sputtered with gold before imaging.

Dynamic Light Scattering (DLS) measurement was carried to measure the hydrodynamic diameter and size distribution of the capsules in solution by using ZETASIZER Nano-S90, Malvern, with a 633nm laser and scattering angle fixed at 90°. The cuvette was filled with dendrimer capsule solution and was equilibritated at set temperature for 10min before measurement. The dis-assembly of Newkome-OH dendrimer capsules in aqueous solution was record at 25°C, 35°C, 45°C, 47°C, 50°C, 55°C, 65°C, 75°C.

4.6 References

(1) Newkome, G. R.; Moorefield, C. N.; Vogtle, F. *Dendritic Macromolecules: Concepts, Synthesis, Perspectives*; VCH, Wenheim, Germany, 2001.

(2) Frechet, J. M. J.; Tamalia, D. A. *Dendrimers and Other Dendritic Polymers*; Whiley,: Chichester, UK, 2001.

(3) Zimmerman, S. C.; Lawless, L. J. *Dendrimers Iv* **2001**, *217*, 95-120.

(4) Tomalia, D. A.; Brothers, H. M.; Piehler, L. T.; Durst, H. D.; Swanson, D. R. *Proc. Natl. Acad. Sci. U. S. A.* **2002**, *99*, 5081-5087.

(5) Amabilino, D. B.; Ashton, P. R.; Balzani, V.; Brown, C. L.; Credi, A.; Frechet, J. M. J.; Leon, J. W.; Raymo, F. M.; Spencer, N.; Stoddart, J. F.; Venturi, M. *J. Am. Chem. Soc.* **1996**, *118*, 12012-12020.

(6) Zimmerman, S. C.; Zeng, F. W.; Reichert, D. E. C.; Kolotuchin, S. V. *Science* **1996**, *271*, 1095-1098.

(7) Wang, P.; Moorefield, C. N.; Jeong, K. U.; Hwang, S. H.; Li, S.; Cheng, S. Z. D.; Newkome, G. R. *Adv. Mater.* **2008**, *20*, 1381-+.

(8) Vanhest, J. C. M.; Delnoye, D. A. P.; Baars, M. W. P. L.; Vangenderen, M. H. P.; Meijer, E. W. *Science* **1995**, *268*, 1592-1595.

(9) Ungar, G.; Liu, Y. S.; Zeng, X. B.; Percec, V.; Cho, W. D. *Science* **2003**, *299*, 1208-1211.

(10) Ju, R.; Tessier, M.; Olliff, L.; Woods, R.; Summers, A.; Geng, Y. *Chem. Commun.* **2011**, *47*, 268-270.

(11) Ju, R.; Haley, J.; Geng, Y. *submitted*.

(12) Lanza, R.; Langer, R.; Vacanti, J. P. *Principles of Tissue Engineering*; Academic Press: San Diego, 2007.

(13) Gibbs, B. F.; Kermasha, S.; Alli, I.; Mulligan, C. N. *Int. J. Food Sci. Nutr.* **1999**, *50*, 213-224.

(14) Read, T. A.; Sorensen, D. R.; Mahesparan, R.; Enger, P. O.; Timpl, R.; Olsen, B. R.; Hjelstuen, M. H. B.; Haraldseth, O.; Bjerkvig, R. *Nat. Biotechnol.* **2001**, *19*, 29-34.

(15) Lim, Y. T.; Kim, J. K.; Noh, Y. W.; Cho, M. Y.; Chung, B. H. *Small* **2009**, *5*, 324-328.

(16) Soon-Shiong, P. *Adv. Drug Delivery Rev.* **1999**, *35*, 259-270.

(17) Pierre, A. C. *Biocatal. Biotransform.* **2004**, *22*, 145-170.

(18) Chaikof, E. L. *Annu. Rev. Biomed. Eng.* **1999**, *1*, 103-127.

(19) Cohen, I.; Li, H.; Hougland, J. L.; Mrksich, M.; Nagel, S. R. *Science* **2001**, *292*, 265-267.

(20) Loscertales, I. G.; Barrero, A.; Guerrero, I.; Cortijo, R.; Marquez, M.; Ganan-Calvo, A. M. *Science* **2002**, *295*, 1695-1698.

(21) Willaert, R. G.; Baron, G. V. *Rev. Chem. Eng.* **1996**, *12*, 5-205.

(22) Caruso, F.; Caruso, R. A.; Mohwald, H. *Science* **1998**, *282*, 1111-1114.

(23) Grigoriev, D. O.; Bukreeva, T.; Mohwald, H.; Shchukin, D. G. *Langmuir* **2008**, *24*, 999-1004.

(24) Velev, O. D.; Furusawa, K.; Nagayama, K. *Langmuir* **1996**, *12*, 2374-2384.

(25) Velev, O. D.; Furusawa, K.; Nagayama, K. *Langmuir* **1996**, *12*, 2385-2391.

(26) Dinsmore, A. D.; Hsu, M. F.; Nikolaides, M. G.; Marquez, M.; Bausch, A. R.; Weitz, D. A. *Science* **2002**, *298*, 1006-1009.

(27) Lin, Y.; Boker, A.; Skaff, H.; Cookson, D.; Dinsmore, A. D.; Emrick, T.; Russell, T. P. *Langmuir* **2005**, *21*, 191-194.

(28) Kralchevsky, P. A.; Nagayama, K. *Adv. Colloid Interface Sci.* **2000**, *85*, 145-192.

(29) Binks, B. P.; Clint, J. H. *Langmuir* **2002**, *18*, 1270-1273.

(30) McGorty, R.; Fung, J.; Kaz, D.; Manoharan, V. N. *Materials Today* **2010**, *13*, 34-42.

CHAPTER 5

CONCURRENT Π-Π STACKING IN COOPERATIVE DENDRIMER CAPSULE FORMATION

5.1 Introduction

Previously, we revealed the unique architectural features of dendrimers as highly-branched nanometer-sized spheres, and demonstrated their ability on maximizing cooperativity towards constructing supramolecular dendrimers capsules.[1,2] These capsules have the advantage of ease in controlling disassembly, which can be utilized to carry and release guest materials in a controllable fashion. In addition, the emulsion templated capsule formation provides more encapsulation versatilities. However, in order to further advance the functionality of these supramolecular dendrimer capsules, more sophisticated self-assembly mechanisms are yet to be exploited. In this chapter, we explored the feasibility of combining π-π stacking at dendrimers' core with the periphery cooperative bindings to construct functional dendrimer capsules. This work will provide the mechanistic foundation for further incorporating functional groups into dendrimers core to generate dendrimer capsules with built-in pores/channels, which can spontaneously and selectively encapsulate or release certain materials.

Π-π interactions, and combined with other non-covalent interactions, such as hydrophobic interactions, hydrogen bonding, electrostatic interactions, and metal ion coordination, have been widely utilized to construct functional supramolecular architectures.[3-9] Among numerous π-conjugated systems, the simplest arene-benzene has attracted increasing interest as an elementary building block to stack into molecular wires or 1-D nanostructures.[10-19]

Typically, the interactions between arenes are fairly weak due to the electrostatic repulsion between the electron rich π-surfaces. To increase the affinity between molecules within the 1-D stacking, the most commonly seen approach is to design arenes, especially benzene rings, with amide substituents. The hydrogen bondings between amides will enforce the co-facial π-π stacking between arenes. In this chapter, the benzene ring was utilized as the dendrimer core, and the benzene ring is hexasubstituted with amide to ensure the π-π stacking. The 1→3 C-branching COO^- dendritic motif was attached to the crowned benzene to provide periphery salt-bridging. Such dendrimers can cooperatively self-assemble into capsules, while the dendrimers stack vertically in membrane, Figure 5.1.

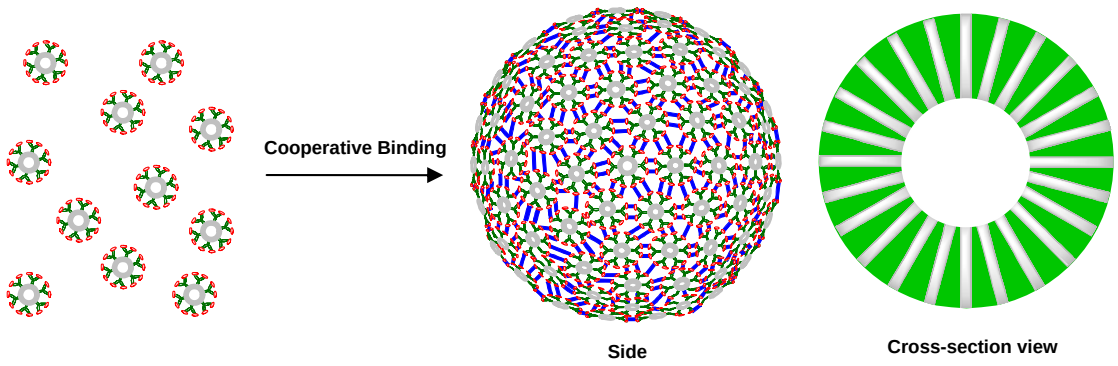

Figure 5.1. Schematic illustration of the concurrent π-π stacking combined with periphery cooperative binding of dendrimers into supramolecular capsules.

5.2 Results and Discussion

To investigate the potential applicability of combining π-π stacking with periphery cooperative bindings in the construction of functional supramolecular self-assemblies, two types of dendrimers, which has exactly the same 1→3 C-branching COO^- dendritic motif as periphery but completely different cores – *i.e.* the un-stackable carbon and stackable crowned benzene ring,

were synthesized and their self-assemble behaviors were studied, Figure 5.2. Upon dissolution in water at neutral pH, both dendrimers dispersed as individual molecules, and the periphery carboxyl groups completely dissociated into negatively charged carboxylates. With the addition of Ca^{2+}, both types of dendrimers can self-assemble into capsules via cooperative salt bridging. TEM imaging of G1-carbon tetraacid-12COO^- dendrimers with the addition of Ca^{2+} revealed hallow capsules with 20~30nm diameter and 3~4nm thickness, Figure 5.2A. In contrast, G1-benzene hexaacid-18COO^- dendrimers self-assemble into larger capsules with a much thicker and denser membrane. TEM imaging showed they form capsules with 420nm diameter and 140nm thickness, Figure 5.2B. The larger generation benzene-cored dendrimer - G2-benzene hexaacid-54COO^- also showed to self-assemble into capsules via Ca^{2+} bridging. However, instead of large size and thick membrane as assembled by the same type but lower generation dendrimer, the capsules are only 30~40 nm in diameter and 4~5nm in thickness, Figure 5.3C.

G1-carbon tetraacid-12COO^- and G1-benzene hexaacid-18COO^- are both first generation dendrimers, which results in similar molecular size ~2.5 nm[1], and comparable periphery groups. However, because of the difference in their core structure, the self-assembled capsules differ significantly in size, membrane thickness and denseness. Based on the membrane volumes, capsules assembled by G1-carbon tetraacid-12COO^- were estimated to have 1~2 layers dendrimers packing in the membrane. While, the capsules assembled by G1-benzene hexaacid-18COO^- are packed with more than 50 layers dendrimers, and these dendrimers were densely packed within membrane, shown as the dark membrane in TEM. This distinctive difference indicates that the stackable benzene ring core can enhance the vertical packing of dendrimers within membranes. Compared to G1-carbon tetraacid-12COO^-, the capsules self-assembled by G1-benzene hexaacid-18COO^-, have much larger cavity and overall diameter. In Chapter 2, we

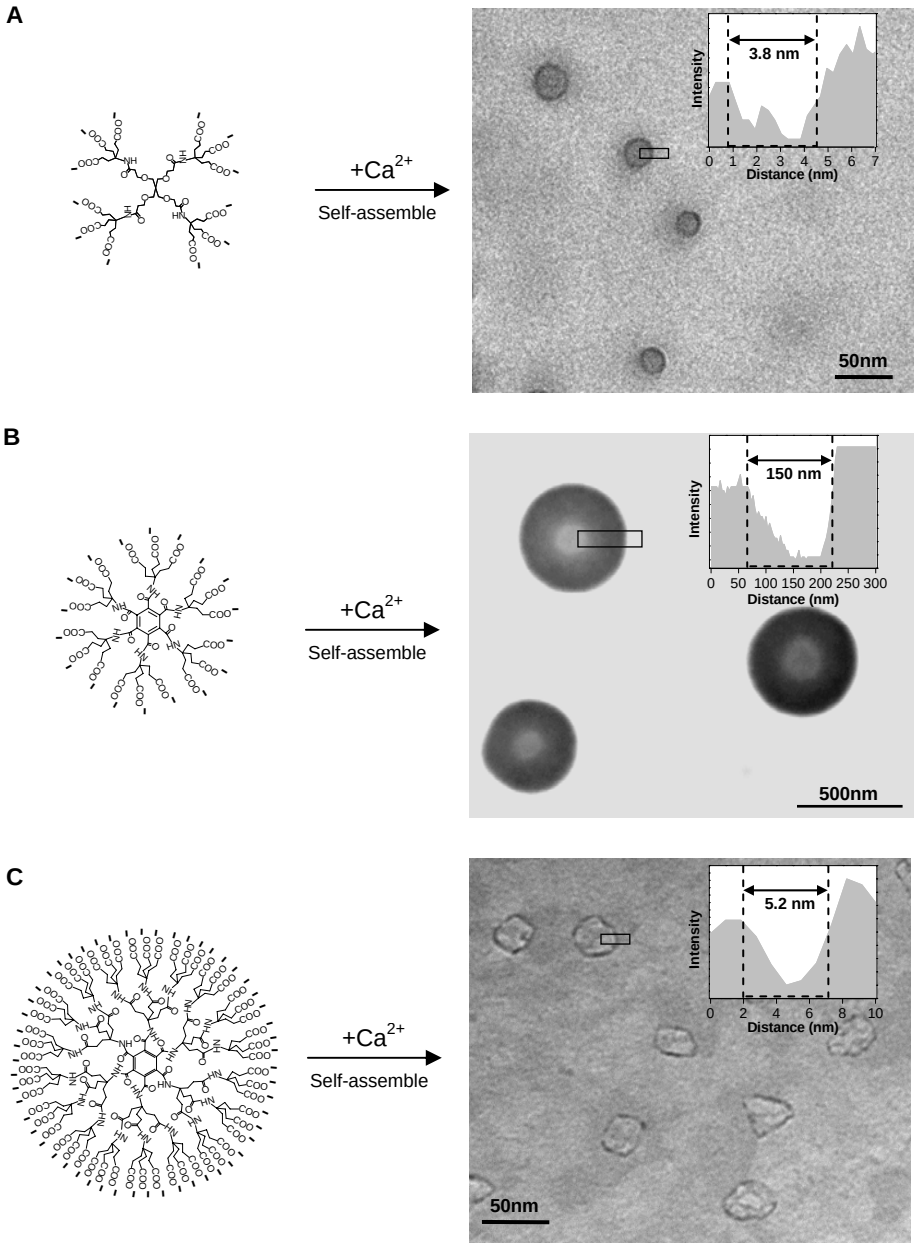

Figure 5.2 Ca^{2+} induced self-assembly of carbon tetraacid and benzene hexaacid type COO^- dendrimers into supramolecular capsules in water. **(A)** G1-carbon tetraacid-12COO^- dendrimers; **(B)** G1-benzene hexaacid-18COO^- dendrimers; **(C)** G2-benzene hecxaacid-54COO^- dendrimers. I. Molecular structure; II. TEM imaging of capsules. Inset, illustration of the capsule thickness by intensity mapping.

discussed that rigid dendrimers tend to form larger capsules than flexible dendrimers. The stacking could significantly reduce the flexibility of each individual dendrimers, which lead to larger membrane curvatures. The size and thickness of the benzene hexaacid-COO^- type dendrimer capsules are also depended on the generation of the dendrimers. Previously, we revealed that larger generation dendrimer tend to form larger capsules with thicker membrane.[1] However, capsules assembled by G2-benzene hexaacid-$54COO^-$ were more similar towards G1-carbon tetraacid-$12COO^-$ rather than G1-benzene hexaacid-$18COO^-$, which shows the stacking of benzene ring core is generation depended. The high generation surrounding dendritic groups prevents dendrimers from arranging themselves within van der Waals radii for the π-π interactions to happen, which prohibit the stacking in dendrimers' core.

The π-π stacking within dendrimer capsules was revealed by UV-Vis absorbtion and Photoluminescene (PL). Figure 5.3 showed the UV-Vis spectras of the monomer and capsules for the benzene hexaaid-COO^- type dendrimers. Upon the addition of Ca^{2+}, the absorption of G1-benzene hexaacid-$18COO^-$ capsules was red shifted relative to the monomer, which indicated the π-π stacking of benzene-rings within capsule membrane.[17] The G2 dendrimer capsules showed no such red shift, indicating again the absence of π-π stacking.

The normalized PL spectras on monomers and capsules of the benzene hexaacid-COO^- type dendrimers were shown in Figure 5.4. For G1-benzene hexaacid-$18COO^-$ dendrimer, both monomer and capsules solutions were excitated at 300nm. Before the addition of Ca^{2+}, the monomers showed emission at 405nm. Upon the addition of Ca^{2+}, the formation of capsules caused a red shifting of ca. 20nm, Figure 5.4A I. While, for G2-benzene hexaacid-$54COO^-$ dendrimer, both monomer and capsules solutions showed the same emission, Figure 5.4B I. In PL, the excited state of monomers is only localized on a single molecule. When the conjugated

systems co-facially stack together via π-π interactions, the energy of the excited state is lowered by localizing among multiple molecules, which causes red-shifted emissions.[11,17,19] The red-shifted emission on the capsules assembled by the first generation benzene hexaacid-COO^- type dendrimers indicated that within the capsule membrane, the π-π interactions between the benzene rings co-facially stack dendrimers together. While, for G2-benzene hexaacid-$54COO^-$ dendrimers, there is no such π-π stacking. The co-facial π-π stacking within the capsule membrane was further confirmed by collecting PL spectras as the excitation wavelengths increase. For G1-benzene hexaacid-$18COO^-$ dendrimer capsules, the emissions were red-shifted as the excitations were moved to a longer wavelength, which indicated that the stacked chromophores were restricted in a condensed media – capsules membrane. For the second generation dendrimer capsules, no shift was observed, which was consistent with the thin membrane observed.

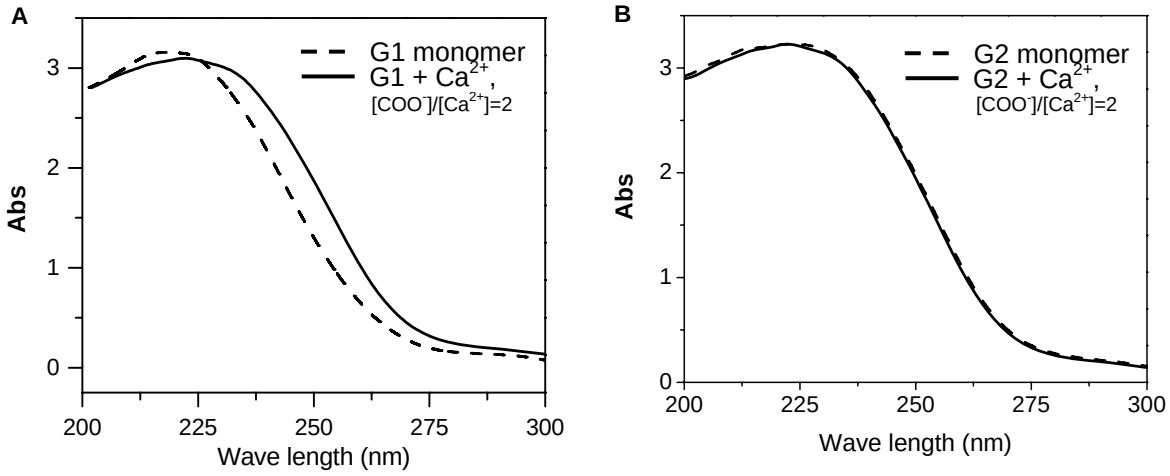

Figure 5.3 UV-Vis measurements of the benzene hexaacid-COO^- type dendrimer monomers and Ca^{2+} induced capsules. **(A)** G1-benzene hexaacid-$18COO^-$; **(B)** G2-benzene hexaacid-$54COO^-$.

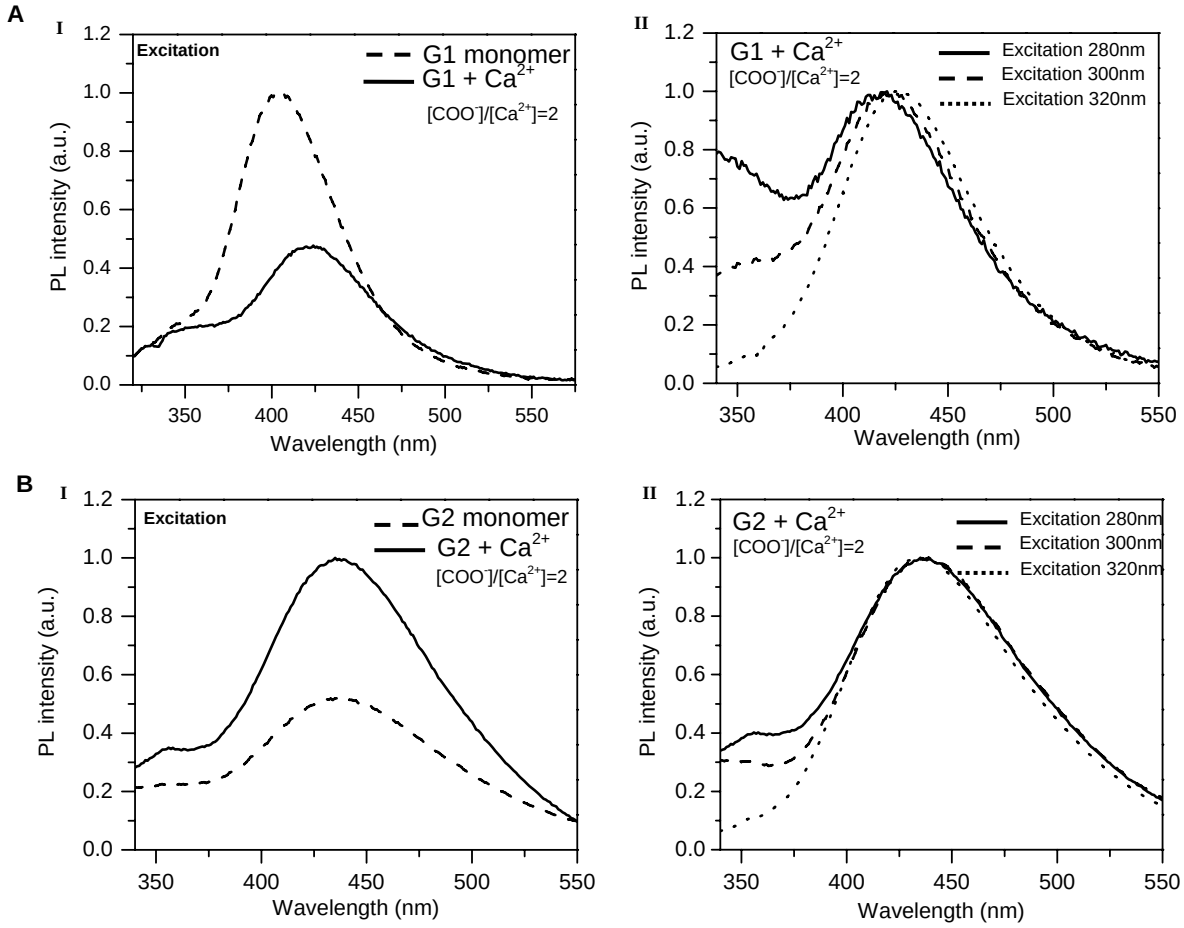

Figure 5.4 Normalized PL spectra analysis of benzene hexaacid-COO^- type dendrimer monomers and capsules. **(A)** G1-benzene hexaacid-$18COO^-$; **(B)** G2-benzene hexaacid-$54COO^-$. I. The emission of dendrimer monomers and Ca^{2+} induced capsules, excitation 300nm; II. The emission of capsules collected at different excitation wavelength.

To understand this new self-assembly strategy in more detail, FT-IR was employed to study the role of hydrogen bonding in this π-π stacking combined cooperative dendrimer capsule formation. In the case of G1-benzene hexaacid-$18COO^-$, the N-H stretching for dendrimer monomer showed at 3475 cm^{-1}, which is typical for non-hydrogen bonded amide. Upon the addition of Ca^{2+}, the N-H stretching for dendrimer capsules was present at 3189 cm^{-1}, and the IR

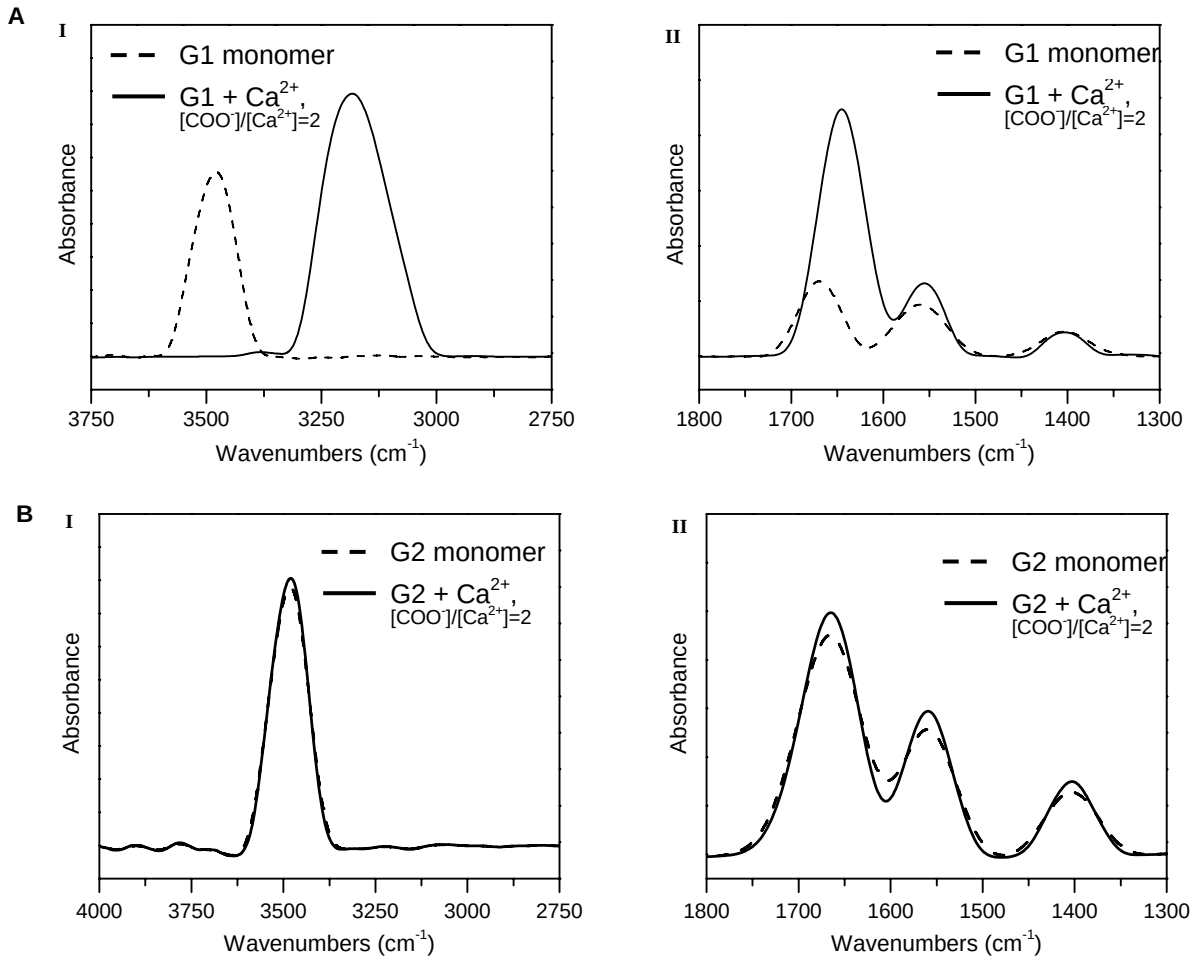

Figure 5.5 FT-IR analysis on benzene hexaacid-COO^- type dendrimer monomers and Ca^{2+} induced capsules. **(A)** G1-benzene hexaacid-$18COO^-$; **(B)** G2-benzene hexaacid-$54COO^-$. I. N-H stretching region; II. C=O stretching region.

absorption intensity significantly increased, indicating the existence of hydrogen bonds, Figure 5.5A I.[14,16,19] Similarly, as the formation of capsules, the C=O stretching for dendrimer shifted from 1665 cm^{-1} to 1649 cm^{-1}, associated with the increasing of intensity, showing again the present of hydrogen bondings in capsules formation, Figure 5.5A II.[14,16,19] As comparison, the

FTIR spectra of G2 dendrimer monomer and capsules showed the absence of hydrogen bondings, Figure 5.5B I II. Generally, for π-π interactions to happen, the distance between two conjugated systems have to be less than 2 Å. Therefore, for dendrimers' core to co-facially stack together, the system have to not only overcome the electrostatic repulsion between the electron rich π-surfaces of benzene rings,[10] but also arrange the crowded dendritic periphery groups cleverly to get the benzene ring cores close enough for π-π stacking to happen. For G1-benzene hexaacid-18COO^-dendrimer, the six amide substituents on the benzene ring core G1 form intermolecular hydrogen bondings. These hydrogen bondings helped bring and arrange the dendrimers' core close enough to enforce the co-facial stacking of benzene rings. Further more, such hydrogen bonding enforced π-π stacking is shown to stack arenes helically when the arenes are substituted at their 1,3,5-position with amides.[20,21] However, CD analysis on the G1-benzene hexaacid-18COO^- capsules solution revealed no detectable signals, indicating dendrimers were arranged in a pallet stacking fashion rather than helical fashion. Such preferred packing is most likely due to the fact that the benzene ring in G1-benzene hexaacid-18COO^- dendrimer ring is fully substituented. The crowded periphery dendritic periphery groups make the pallet stacking energetically preferred than helical stacking.

To better understand the π-π stacking combined cooperative Ca^{2+}/COO^- binding that underlies the capsule formation, ITC was used to study the energetics of the binding process. Ca^{2+} titrations were performed with G1-benzene hexaacid-18COO^- dendrimer and G1-carbon tetraacid-12COO^- dendrimer as comparison, and the isothermals were plotted in Figure 5.6. Both isothermals have the same doublephasic pattern and were best fitted with the two independent binding site model. In case of G1-benzene hexaacid-18COO^-, the parameters were $K_1 = 3.0\times10^3$ M^{-1}, $\Delta H_1 = 5.97$ kcal/mol, $T\Delta S_1 = 10.7$ kcal/mol, $\Delta G_1 = -4.8$ kcal/mol; and $K_2 = 3.5 \times 10^4$ M^{-1},

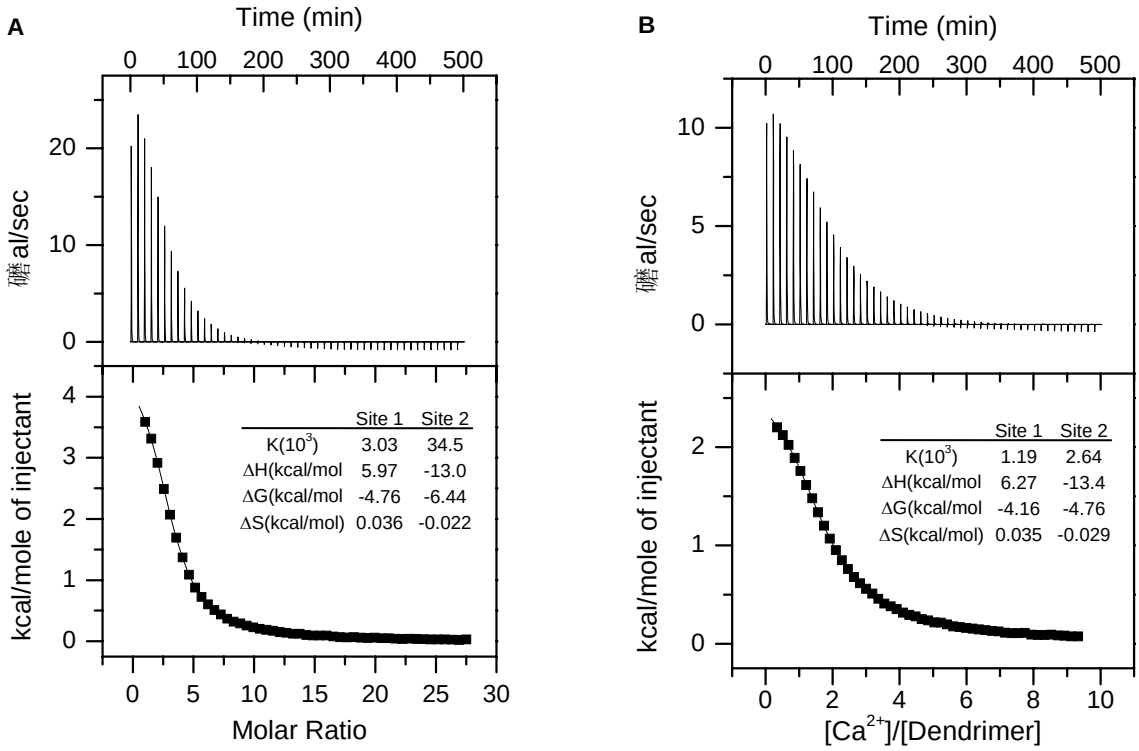

Figure 5.6 ITC analysis on Ca^{2+} binding to G1 carbon tetraacid and benzene hexaacid type COO^- dendrimers. **(A)** G1-benzene hexaacid-18COO^- and **(B)** G1-carbon tetraacid-12COO^- dendrimers. Upper panels show the calorimetric titrations; Lower panels display the integrated heat values as a function of molar ratio. The solid line represents the curve fitting to a two independent binding site model.

ΔH_2 = -13 kcal/mol, $T\Delta S_2$ = - 6.56 kcal/mol, ΔG = -6.4 kcal/mol. On the other hand, for G1-carbon tetraacid-12COO^-, the parameters were $K_1 = 1.2\times10^3\ M^{-1}$, ΔH_1 = 6.27 kcal/mol, $T\Delta S_1$ = 10.7 kcal/mol, ΔG_1 = -4.8 kcal/mol; and $K_2 = 3.5 \times 10^4\ M^{-1}$, ΔH_2 = -13 kcal/mol, $T\Delta S_2$ = - 6.56 kcal/mol, ΔG = -6.4 kcal/mol. In both systems, the first process is endothermic and entropically driven, which is energetically consistent with disruption of the ordered water solvation shell upon individual Ca^{2+}-COO^- counterion binding.[22] In addition, the average binding constant K_1

for these two systems are both similar to the previously reported Ca^{2+}-COO^- counterion binding constant[23]. For both system, the second process is exothermic and enthalpically driven, which is referred as COO^--Ca^{2+}-COO^- salt-bridge formation following the Ca^{2+}-COO^- counterion binding to assemble dendrimers together, and the average K_2 is greater than K_1 as an indication of the positive cooperativity in both systems. However, unlike the similar K_1 value, K_2 for G1-benzene hexaacid-18COO^- is more than ten times greater than K_2 for G1-carbon tetraacid-12COO^-. This is largely because of the participation of intermolecular hydrogen bonding and π-π stacking in the self-assembly of G1-benzene hexaacid-18COO^- dendrimers. Such hydrogen bonding enforced π-π stacking assists the proximity of dendrimers, which practically facilitate the formation of COO^--Ca^{2+}-COO^- salt-bridges as reflected by the greater binding affinity.

5.3 Conclusion

In summary, we showed that π-π stacking at dendriemers' core can be combined concurrently with the cooperative dendrimer capsule formation, and the π-π interaction between dendrimers' core can stack dendrimers vertically within the capsule membrane. This work demonstrate the mechanistic foundation for further advancing the functionality of supramolecular dendrimer capsules, such as incorporating functional groups into dendrimers core to generate dendrimer capsules with built-in pores/channels, which can spontaneously and selectively encapsulate or release certain materials.

5.4 Experimental information

5.4.1 Materials

G1-carbon teraacid-12COOH **:** The detailed synthetic route was described in Chapter 2, Figure 2.10, 2.11, 2.12. ^{1}H NMR([H_6]-H_2O) of G1-carbon teraacid-12COOH: δ(ppm) = 1.75 (br,

24H, **a**, C**H**$_2$CH$_2$COO), 1.98 (br, 24H, **b**, C**H**$_2$COO), 2.32 (br, 8H, **c**, C**H**$_2$CONH), 3.22 (br, 8H, **d**, CH$_2$C**H**$_2$O)4.95 and 3.49 (br, 8H, **e**, OC**H**$_2$)**,** Figure 5.7.

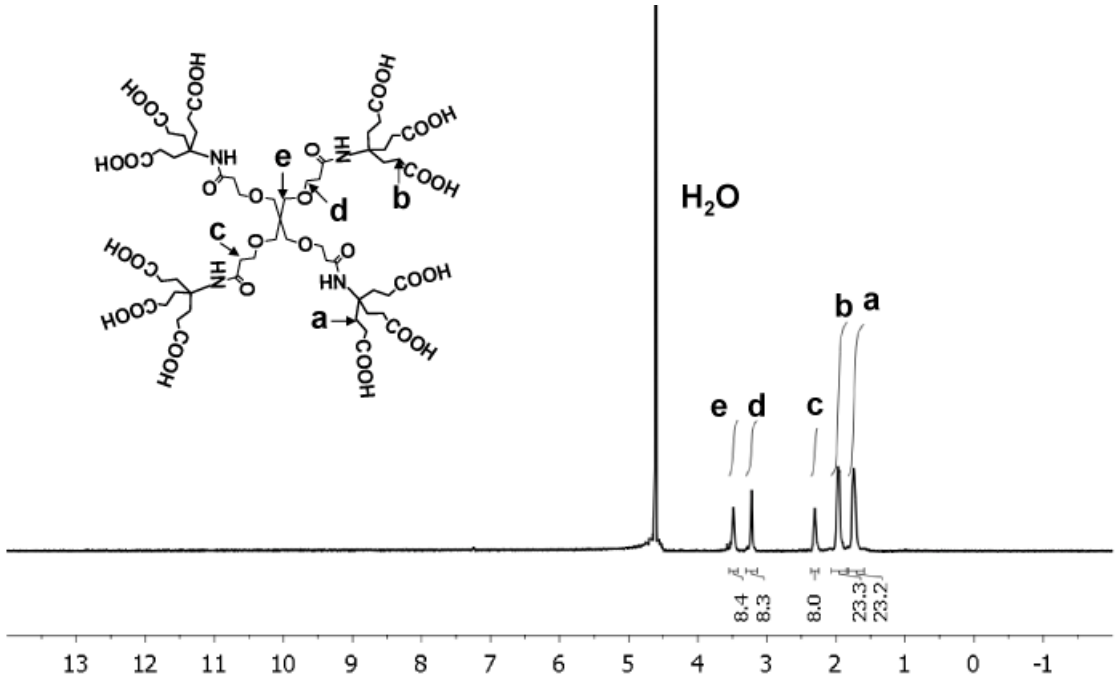

Figure 5.7 NMR spectra of G1-carbon teraacid-12COOH.

G1-Benzene hexaacid-18COOH and G2-Benzene hexaacid-54COOH were synthesized by the reported divergent approach, Figure 5.8. The benzene hexaacid core is commercial available. The tri-branched amine dendritic monomer was synthesized following previous publications, Figure 2.10. The first generation dendrimer G1-Benzene hexaacid-18COOH was synthesized by reacting benzene hexaacid with the tri-branched amine monomer under DCC/1-HBT peptide coupling condition, followed by removal of the t-Butyl protecting group with formic acid [24,25]. The second generation dendrimer G2-Benzene hexaacid-54COOH was synthesized by coupling the tri-bachched amine monomer with the first generation dendrimer

under DCC/1-HBT, followed by removal of the t-Butyl protection group. ^{1}H NMR(D_2O) of G1-Benzene hexaacid-18COOH: δ(ppm) = 1.75 (br, 36H, **a**, C**H**$_2$CH$_2$COO), 1.98 (br, 36H, **b**, C**H**$_2$COO), Figure 5.9. ^{1}H NMR(D_2O) of G2-Benzene hexaacid-54COOH: δ(ppm) = 1.75 (br, 36H, **a**, C**H**$_2$CH$_2$COO), 1.98 (br, 36H, **b**, C**H**$_2$COO), Figure 5.10.

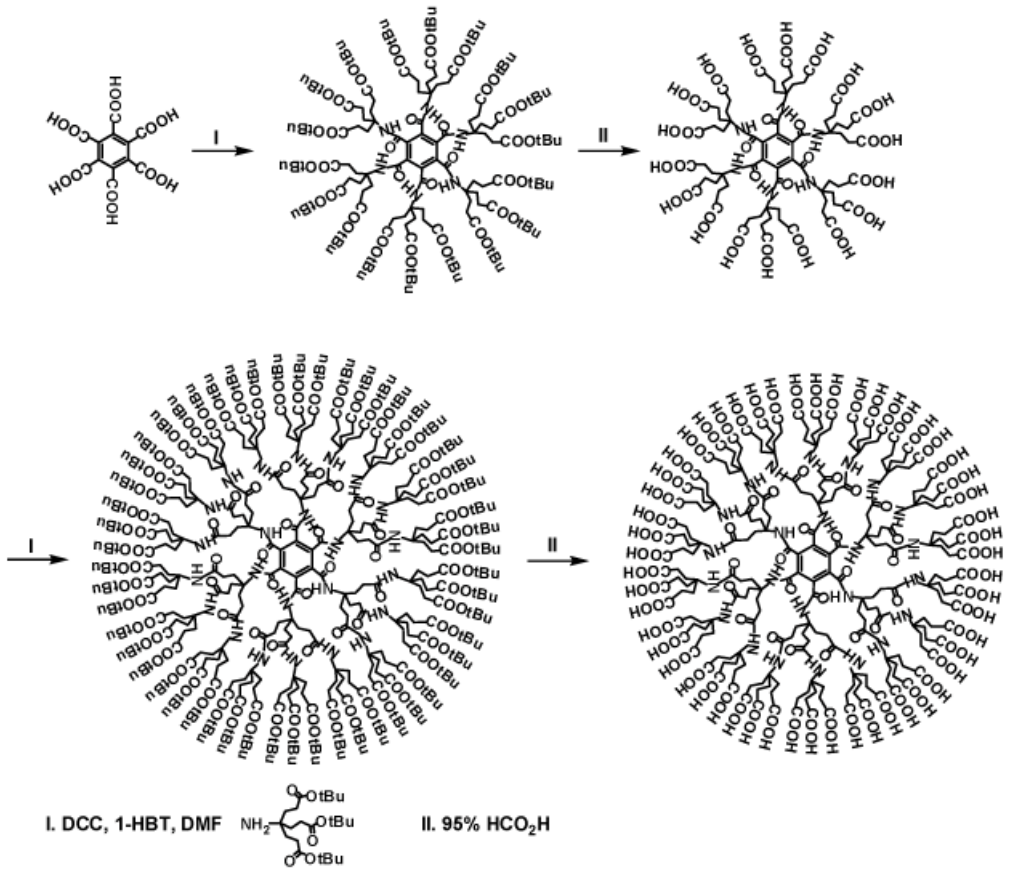

Figure 5.8 Reaction scheme for the preparation of G1-Benzene hexaacid-18COOH and G2-Benzene hexaacid-54COOH.

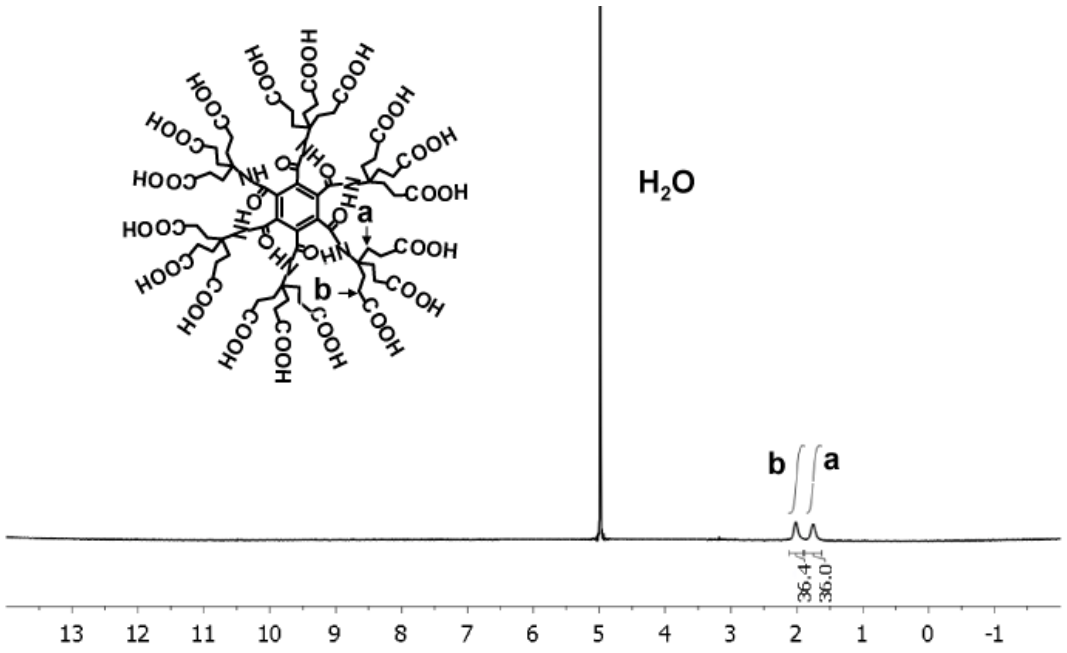

Figure 5.9 NMR spectra of G1-benzene hexaacid-18COOH.

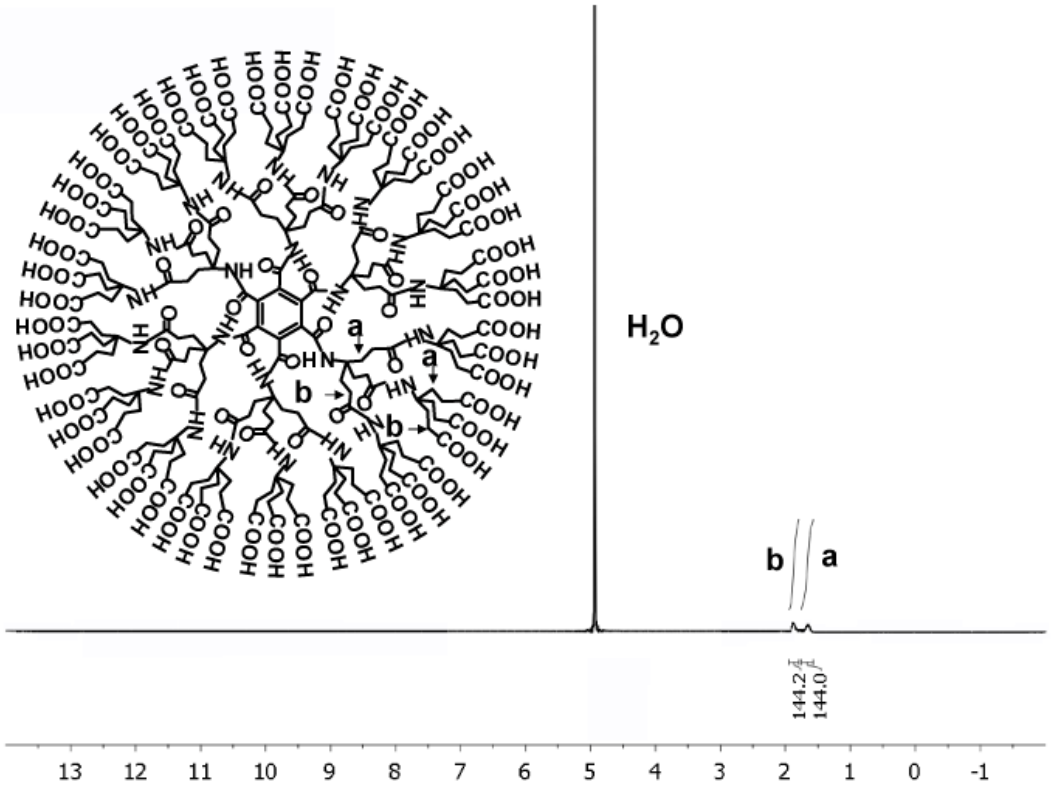

Figure 5.10 NMR spectra of G2-benzene hexaacid-54COOH.

Capsule solution preparation: Water was purified by PURELAB Plus® High Purity Water Polishing System from U.S.Filter, and then filtrated through syringe filters with 0.45μm sized pore and polypropylene filter media purchased from Whatman®. Dendrimer was dissolved in water, and pH was adjusted to 7.2 with NaOH. Then $CaCl_2$ solution was added, followed by vortexing for 30s and placing still for 5min before further testing. The concentrations and mixing ratios between dendrimer and Ca^{2+} were listed in Table S1.

Table 5.1 Dendrimer capsule solution preparation

Sample Name	Dendrimer Concentration	$[COO^-]/[Ca^{2+}]$
G1-carbon teraacid-12COOH-1mM-2-1-Ca	1mM	2
G1-Benzene hexaacid-18COOH-0.125mM	0.125mM	N/A
G1-Benzene hexaacid-18COOH-10mM	10mM	N/A
G1-Benzene hexaacid-18COOH-0.125mM-2-1-Ca	0.125mM	2
G1-Benzene hexaacid-18COOH-10mM-2-1-Ca	10mM	2
G2-Benzene hexaacid-54COOH-0.125mM	0.125mM	N/A
G2-Benzene hexaacid-54COOH-2.5mM	2.5mM	N/A
G2-Benzene hexaacid-54COOH-0.125mM-2-1-Ca	0.125mM	2
G2-benzene hexaacid-54COOH-2.5mM-2-1-Ca	2.5mM	2

5.4.2 Methods

*TEM, Negatively-stained TEM and Cryo-TEM measurement:*The cross-section view of capsules formed by G1-Benzene hexaacid-18COOH with $CaCl_2$ ($[COO^-]/[Ca^{2+}]$=2/1) were imaged by TEM. 3μL G1-Benzene hexaacid-18COOH-10mM was pipetted onto a carbon coated copper grids, followed by removal of the excess liquid with a piece of filter paper. The sample grid was then dried before imaging. In order to image the surface topologies, the dried sample grid was negatively stained with 2% uranyl acetate in ethanol. The TEM images were obtained on a FET TECNAI 20G Transmission Electron Microscopy operating at an acceleration voltage

of 200kV and at ambient temperature. The capsules formed by G1-carbon teraacid-12COOH with $CaCl_2$ ($[COO^-]/[Ca^{2+}]$=2/1) were imaged by Cryo-TEM. 3μL G1-carbon teraacid-12COOH-1mM-2-1-Ca solution was pipetted onto a lacey carbon copper grid (ESI), followed by removal excess liquid with a piece of filter paper. The specimen was then quickly plunged into liquid nitrogen to ensure vitrification. The specimen was stored under liquid nitrogen, and then transferred to a cryogenic sample holder (Gatan 626) in a FET TECNAI 20G TEM operating at -177°C for imaging.

DLS measurement : The hydrodynamic radius and the size distribution of the dendrimer capsules in solution were measured by ZETASIZER Nano-S90, Malvern, with a 633nm laser with scattering angle fixed at 90°. The cuvette was filled with dendrimer capsule solution and was equilibritated at set temperature for 10min before measurement.

UV-Vis spectrometry measurements were carried with a Cary 100 UV-Vis spectrophotometer. The UV-Vis spectras of dendrimer monomer solutions, G1-Benzene hexaacid-18COOH-0.125mM and G2-Benzene hexaacid-54COOH-0.125mM, also the capsule solutions, G1-Benzene hexaacid-18COOH-0.125mM-2-1-Ca and G2-Benzene hexaacid-54COOH-0.125mM-2-1-Ca were recorded at room temperature. The absorption peak of benzene ring was monitored.

Photoluminescence (PE) Spectroscopy measurements were obtained using a Jobin Yvon FluoroMax-3 Fluorimeter. Dendrimer monomer solutions, G1-Benzene hexaacid-18COOH-0.125mM and G2-Benzene hexaacid-54COOH-0.125mM, were excitated at 300nm, and the emission spectras were recorded from 340nm to 550nm. The capsule solutions, G1-Benzene hexaacid-18COOH-0.125mM-2-1-Ca and G2-Benzene hexaacid-54COOH-0.125mM-2-1-Ca

were excited at different wavelength (280nm, 300nm, 320nm) and the emission spectras from 340nm to 550nm were recorded.

FT-IR Spectroscopy measurements were performed by using a Thermo Scientific Nicolet Is10 FT-IT Spectrometer, equipped with a diamond Smart ATR accessory. 5μL sample solution was pipetted onto the diamond sample stage and the FT-IR spectra were recorded at room temperature. Interferograms were collected at $4cm^{-1}$ resolution and apodized with a NB (Norton-Beer) Function. The FT-IR spectra of the following samples: G1-Benzene hexaacid-18COOH-10mM, G1-Benzene hexaacid-18COOH-10mM-2-1-Ca, G2-Benzene hexaacid-54COOH-2.5mM, and G2-Benzene hexaacid-54COOH-2.5mM-2-1-Ca were recorded, and the spectra of water was also recorded and subtracted as background.

CD measurements were recorded on Jasco J-715 spectropolarimeter. All the spectras were obtained at 25ºC, from 600 to 190 nm with a scanning speed of 50 nm min^{-1}, and a total of 3 individual scans were accumulated, with subtracting the background absorbance from water. The CD spectrum of G1-Benzene hexaacid-18COOH-0.125mM, G1-Benzene hexaacid-18COOH-0.125mM-2-1-Ca, G2-Benzene hexaacid-54COOH-0.125mM, and G2-Benzene hexaacid-54COOH-0.125mM-2-1-Ca were recorded.

ITC measurements were recorded on a VP-ITC MicroCalorimeter (MicroCal, Inc). The dendrimers solution, 0.35mM G1-Benzene hexaacid-$18COO^-$ or 1mM G1-carbon teraacid-$12COO^-$ aqueous solution (pH 7.2) were loaded into the titration cell, and the reference cell was filled with deionized water. Fifty injections of 50 mM Ca^{2+} were titrated into the dendrimer sample cell in 5 μL increments at 10 min interval with stirring at 310 rpm to ensure complete equilibration. The heat of dilution was measured by making identical injections in the absence of dendrimers. The net binding reaction heat was obtained by subtracting the heat of dilution from

the measured total heat of reaction. The titration data were then fitted using the MicroCal Origin software and least-square algorithm, and these data were best fit to a two independent binding site model. The binding enthalpy ΔH, binding constant K, and the binding stoichiometry n were permitted to float during the least-square minimization process and taken as the best-fit value.

5.5 References

(1) Ju, R.; Tessier, M.; Olliff, L.; Woods, R.; Summers, A.; Geng, Y. *Chem. Commun.* **2011**, *47*, 268-270.

(2) Ju, R.; Haley, J.; Geng, Y. *submitted*.

(3) Hoeben, F. J. M.; Jonkheijm, P.; Meijer, E. W.; Schenning, A. P. H. J. *Chem. Rev.* **2005**, *105*, 1491-1546.

(4) Claessens, C. G.; Stoddart, J. F. *J. Phys. Org. Chem.* **1997**, *10*, 254-272.

(5) Gazit, E. *Faseb J.* **2002**, *16*, 77-83.

(6) Vriezema, D. M.; Hoogboom, J.; Velonia, K.; Takazawa, K.; Christianen, P. C. M.; Maan, J. C.; Rowan, A. E.; Nolte, R. J. M. *Angew. Chem.,Int. Ed.* **2003**, *42*, 772-776.

(7) Song, B.; Wei, H.; Wang, Z. Q.; Zhang, X.; Smet, M.; Dehaen, W. *Adv. Mater.* **2007**, *19*, 416-+.

(8) Song, B.; Wang, Z. Q.; Chen, S. L.; Zhang, X.; Fu, Y.; Smet, M.; Dehaen, W. *Angew. Chem., Int. Ed.* **2005**, *44*, 4731-4735.

(9) Engelkamp, H.; Middelbeek, S.; Nolte, R. J. M. *Science* **1999**, *284*, 785-788.

(10) Bushey, M. L.; Nguyen, T. Q.; Zhang, W.; Horoszewski, D.; Nuckolls, C. *Angew. Chem., Int. Ed.* **2004**, *43*, 5446-5453.

(11) Nguyen, T. Q.; Martel, R.; Avouris, P.; Bushey, M. L.; Brus, L.; Nuckolls, C. *J. Am. Chem. Soc.* **2004**, *126*, 5234-5242.

(12) Nguyen, T. Q.; Bushey, M. L.; Brus, L. E.; Nuckolls, C. *J. Am. Chem. Soc.* **2002**, *124*, 15051-15054.

(13) Bushey, M. L.; Nguyen, T. Q.; Nuckolls, C. *J. Am. Chem. Soc.* **2003**, *125*, 8264-8269.

(14) Bushey, M. L.; Hwang, A.; Stephens, P. W.; Nuckolls, C. *J. Am. Chem. Soc.* **2001**, *123*, 8157-8158.

(15) Bushey, M. L.; Hwang, A.; Stephens, P. W.; Nuckolls, C. *Angew. Chem., Int. Ed.* **2002**, *41*, 2828-+.

(16) Jang, W. D.; Aida, T. *Macromolecules* **2004**, *37*, 7325-7330.

(17) Jonkheijm, P.; Hoeben, F. J. M.; Kleppinger, R.; van Herrikhuyzen, J.; Schenning, A. P. H. J.; Meijer, E. W. *J. Am. Chem. Soc.* **2003**, *125*, 15941-15949.

(18) van Gorp, J. J.; Vekemans, J. A. J. M.; Meijer, E. W. *J. Am. Chem. Soc.* **2002**, *124*, 14759-14769.

(19) van Herrikhuyzen, J.; Jonkheijm, P.; Schenning, A. P. H. J.; Meijer, E. W. *Org. Biomol. Chem.* **2006**, *4*, 1539-1545.

(20) Lightfoot, M. P.; Mair, F. S.; Pritchard, R. G.; Warren, J. E. *Chem. Commun.* **1999**, 1945-1946.

(21) Nguyen, T. Q.; Martel, R.; Bushey, M.; Avouris, P.; Carlsen, A.; Nuckolls, C.; Brus, L. *Phys. Chem. Chem. Phys.* **2007**, *9*, 1515-1532.

(22) Linton, B. R.; Goodman, M. S.; Fan, E.; van Arman, S. A.; Hamilton, A. D. *J. Org. Chem.* **2001**, *66*, 7313-7319.

(23) Joseph, N. R. *The J. Biol. Chem.* **1946**, 529-541.

(24) Young, J. K.; Baker, G. R.; Newkome, G. R.; Morris, K. F.; Johnson, C. S. *Macromolecules* **1994**, *27*, 3464-3471.

(25) Newkome, G. R.; Weis, C. D. *Org. Prep. Proced. Int.* **1996**, *28*, 242-244.

CHAPTER 6

INDUCTION OF SUPER-HELICES BY BREAKING NANO-MOLECULAR SHAPE SYMMETRY

Rong Ju, Yan Geng.

To be submitted to *Chem. Comm.*

6.1 Abstract

Chiral supramolecular structures, most commonly helices, are typically constructed from chiral molecule subunits, and their handedness is generally governed by the configuration of monomeric chiral centers. Here, we introduce nanometer scale shape-asymmetry into dendrimers by coupling two different-sized but chemically identical achiral dendritic fragments. We found that with smaller magnitude of size difference, the asymmetric dendrimers form simple achiral fibrils which self-assemble into parallel bundles. In comparison, greater shape-asymmetry directs dendrimer self-assembly into helical fibrils which form higher-order coiled-coil bundles and spontaneously loop into supercoiled double-helices. Thus, when combined with cooperative non-covalent self-assembly forces, sufficient shape-asymmetry rather than classical monomeric chiral centers can generate complex and unusual chiral supramolecular structures. Our finding offers a new systematic design principle for constructing chiral supramolecular structures of potential interest in optoelectronic and other materials applications.

6.2 Introduction

Symmetry is an important structural motif that influences the functions and properties of objects at all scales, ranging from molecules and nano/micro-particles to macroscopic matters. Symmetry elements range from reflection planes, rotation axes to inversion centers. The extreme case of asymmetry is chirality, where an object has no symmetry elements on its mirror image. The most familiar molecular example of chirality occurs when four chemically different groups are bonded to a carbon atom. Chiral centers in molecules can further induce chirality at supramolecular level, most commonly as helices.[1-5] The handedness of supramolecular helix is typically governed by the configuration of chiral centers within the molecular components.[1-5] However, chiral structure formation from achiral molecules has also been observed, such as

chiral liquid crystal formation from the achiral banaba-shaped bent-core mesogens, which indicates the possibility of other principles independent of chiral centers in constructing chiral supramolecular structures.[6,7] Recent study on larger micron-sized colloidal particles under magnetic field show that simple overall shape non-symmetry can force the colloidal self-assembly chain to coil.[8] Although the micron-scale dimension of solid colloidal particles and the external force directed assembly mechanism are distinctively different from molecules and their non-covalent interactions, such finding nonetheless suggested shape non-symmetry could also be exploited for inducing chiral structure formation. Here, we break the shape symmetry of dendrimer molecules at the nanometer scale and reveal the profound impact of simple molecular shape non-symmetry on supramolecular self-assembly processes. We show that with cooperative non-covalent interactions, increasing molecular shape non-symmetry can transform dendrimer supramolecular self-assembly from achiral parallel fibrillar bundles to surprising hierarchical supercoiled double-helices. Our finding not only provides new insights into supramolecular chirality, but also offers a new systematic design principle for constructing novel chiral supramolecular structures that maybe of interest for optoelectronic applications, or as functional nanoparticle templates for chiral catalysis and sensor applications.

Dendrimers are highly-branched, three-dimensionally globular, and nanometer-sized molecules, which have attracted broad interest due to their unique architectures and interesting properties.[9-13] Here, we break the spatial symmetry of dendrimer molecules by coupling two different-sized but chemically identical dendritic fragments together to reveal the effect of molecular shape symmetry on supramolecular self-assembly process, Figure 6.1. Since dendrimer size increases with generations, *i.e.* number of branching layers, the size difference between the linked two dendritic fragments can be easily controlled by generations. For example,

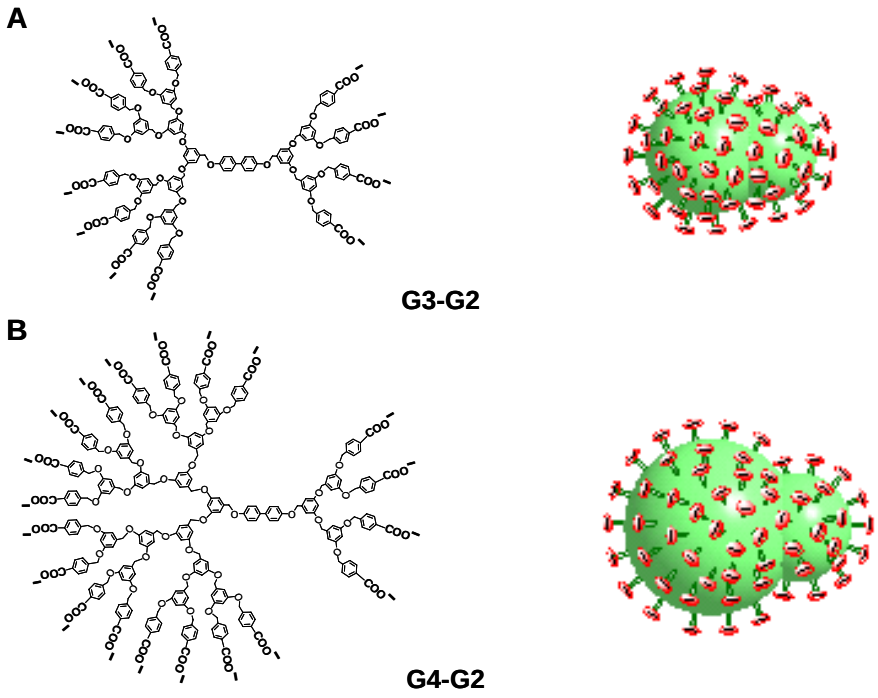

Figure 6.1 Molecular structure and schematic representation of (**A**) **G3-G2** and (**B**) **G4-G2** non-symmetrical Fréchet dendrimers, functionalized with carboxylate terminal groups.

the diameters of second-generation (**G2)**, third-generation (**G3**) and fourth-generation (**G4**) of carboxyl-terminated Fréchet dendrimers in water have been measured as ca. 3nm, 4nm, and 5nm respectively.[14] We then employed the reported convergent synthetic route[15,16] and coupled **G2** Fréchet-COOH dendritic fragment with **G3** and **G4** fragments respectively to produce the non-symmetrical **G3-G2** and **G4-G2** dendrimers. Fréchet-type dendrimers are well-known as unimolecular micelles in water, where the highly hydrophobic benzyl ether interior collapses into rigid spherical core, surrounded by closely-packed polar surface groups.[15] Thus non-symmetrical **G3-G2** and **G4-G2** dendrimers will have dumbbell-shaped architecture with two different sized compact spherical lobes upon dissolution in water. One should note that **G3-G2** and **G4-G2** dendrimers are essentially the same in all chemical aspects, except **G4-G2** has greater shape non-

symmetry than **G3-G2**. These shape non-symmetrical dendrimers are nonetheless achiral – *i.e.* there is no chiral center and each has an internal symmetry plane as well as rotational axes that go through the two lobes.

6.3 Results and Discussion

Upon dissolution in water at neutral pH, the non-symmetrical **G3-G2** and **G4-G2** dendrimers dispersed as free individual molecules, as the carboxyl surface groups completely dissociate into negatively-charged carboxylates (-COO^-), Figure 6.2. Previously, we showed that

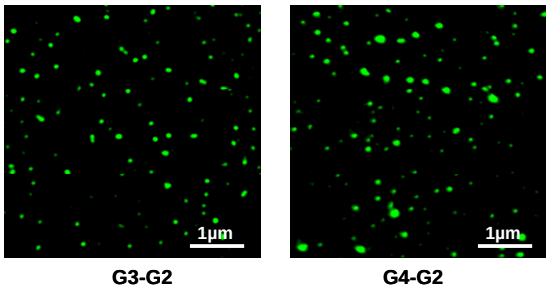

Figure 6.2 Direct FM visualization of the dispersed carboxylate-terminated **G3-G2** and **G4-G2** dendrimer monomers in aqueous solution.

with the addition of divalent cations (M^{2+}), such as Ca^{2+}, spherically symmetrical Fréchet-COO^- dendrimers cooperatively self-assemble into enclosed capsules via COO^--M^{2+}-COO^- salt bridges.[14] In contrast, here at equilibrium, the non-symmetrical dendrimers had self-assembled as cylindrical structures with the addition of M^{2+}, Figure 6.3, 6.5. Direct fluorescent microscopy imaging of dye-labeled **G3-G2** and **G4-G2** dendrimers in aqueous solution showed they formed short cylinders at Ca^{2+} concentration well below stoichiometry of total carboxylates, *i.e.* Ca^{2+}:COO^- ~ 1:10. The cylinder length increased with Ca^{2+} concentration and could reach a maximum of 15µm. Further Transmission electron microscopy (TEM) analysis revealed distinct

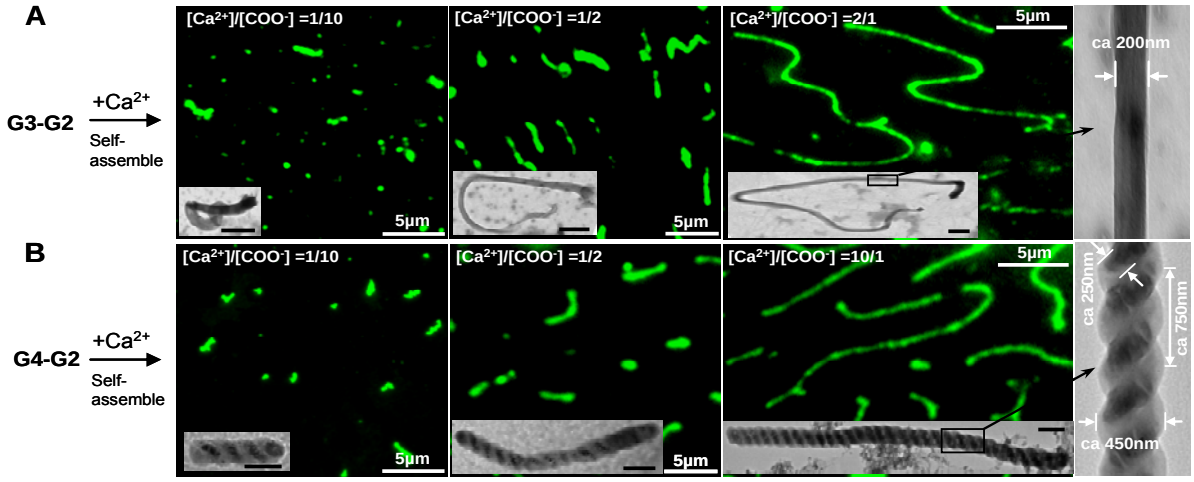

Figure 6.3 Ca^{2+} induced self-assembly of carboxylate-terminated asymmetric (**A**) **G3-G2** and (**B**) **G4-G2** dendrimers in aqueous solution (scale bar in TEM insets: 500nm). Right panels at the far end: magnified TEM micrographs.

nano-scale structural differences between the **G3-G2** and **G4-G2** equilibrium cylinder structures, insets in Figure 6.3. The **G3-G2** cylinders are fibrillar bundles aggregated parallelly, Figure 6.3A, insets and right panel. In contrast, the **G4-G2** cylinders appear to be close-ended supercoiled double-helices, Figure 6.3B.

The distinctive differences between the **G3-G2** and **G4-G2** equilibrium cylinder structures were also reflected in their CD measurements, Figure 6.4. Before the addition of Ca^{2+}, **G3-G2** and **G4-G2** monomeric dendrimers are achiral and no Cotton effect was observed, Figure 6.4 a, b. However, a strong positive Cotton effect at ~220 nm, *i.e.* absorbance wavelength of benzene, was produced by **G4-G2** after reaching equilibrium with the addition of Ca^{2+}, indicating chirality in the structures formed, Figure 6.4 d,e,f. The signal intensity also systematically increases with the observed elongation of the supercoiled **G4-G2** double-helices at higher Ca^{2+} concentrations. In contrast, no Cotton effect was observed on **G3-G2** with the

addition of Ca^{2+}, Figure 6.4c, indicating that the formed **G3-G2** cylinder structures are achiral, consistent with the parallel fibrillar bundle morphology observed by TEM.

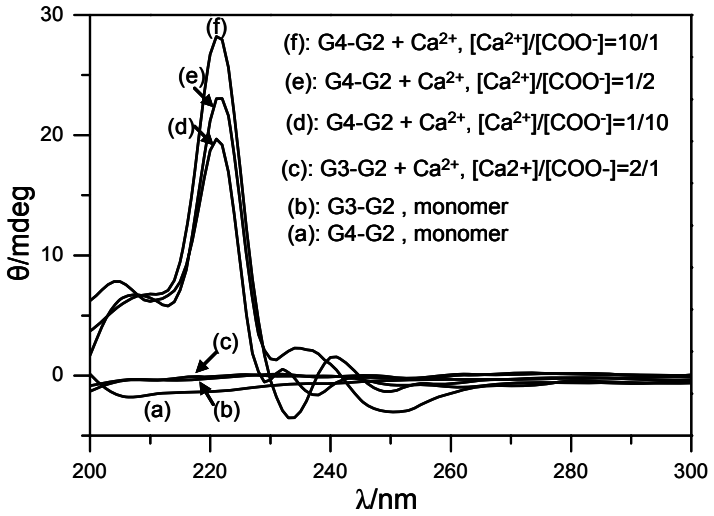

Figure 6.4 CD analysis of asymmetric **G4-G2** and **G3-G2** dendrimers and their self-assemblies in aqueous solution. (a,b) – dendrimer monomer; (c-f) equilibrated self-assembly with the addition of Ca^{2+}.

Compared to spherically symmetrical dendrimers, which prefer isotropic expansion and close-packing into enclosed capsules, breaking their shape symmetry notably shifts the dendrimer self-assembly pathway to anisotropical elongation into cylindrical fibrils that can further assemble into higher-order superstructures, such as achiral fibrillar bundles (**G3-G2**) or supercoiled double-helices (**G4-G2**). Since **G3-G2** and **G4-G2** are the same molecules, differing only in the nanometer-scaled relative sizes of their two dendritic fragment halves, the spontaneous formation of drastically different supramolecular self-assembly structures is rather intriguing. With highly-branched peripheral binding sites and smaller size difference between the two lobes, it seems **G3-G2** dendrimers allow for initial spontaneous head-to-head binding via

COO^{-}-M^{2+}-COO^{-} salt bridges into single fibrils, followed by shoulder-to-shoulder parallel binding between fibrils into bundles. In contrast, the formation of the close-ended supercoiled double-helices in achiral **G4-G2** dendrimers cannot be so easily explained. Typically, in order to form close-ended, supercoiled helices, some prerequisite conditions have to be met. For example, in double-stranded helical DNA, supercoils form when the two component strands are not free to unwind. This condition exists when they are in a covalently closed circle, such as a bacterial plasmid, or in a linear chromosome where rotation of strands is constrained by proteins, such as histones. Here, there are no covalently closed circular strands, and the formation of the close-ended supercoiled double-helices is spontaneous without any assistance from proteins or external physical force manipulations.

These asymmetrical dendrimers can also self-assemble into cylindrical shaped supramolecular structures with the addition of other divalent alkaline earth metal ions, Figure 6.5. Upon the addition of Mg^{2+}, G4-G2 self-assembled into close-ended supercoiled double-helices, *i.e.* Mg^{2+}:COO^{-}~1:4. Unlike Ca^{2+}, the Mg^{2+} induced double-helices were much loosely coiled, which can be directly imaged by fluorescent microscopy with dye-labeling, Figure 6.5A. Compared with Ca^{2+}, Mg^{2+}, Ba^{2+} driven self-assembly showed different morphologies. Instead of double helix, the addition of Ba^{2+} leads to more stiff smooth cylinders, as revealed by both fluorescent microscopy and TEM, Figure 6.5B. The morphological differences were also reflected in the CD measurements, Figure 6.5 C. After reaching equilibrium, G4-G2 showed a strong positive cotton effect with the addition of either Ca^{2+}or $Mg^{2+.}$ However, the cotton effect produced by the addition of Mg^{2+} shifted towards lower wavelength comparing with Ca^{2+}. The addition of Ba^{2+}, not surprisingly, showed no cotton effect, which were constant with the microscopy imaging.

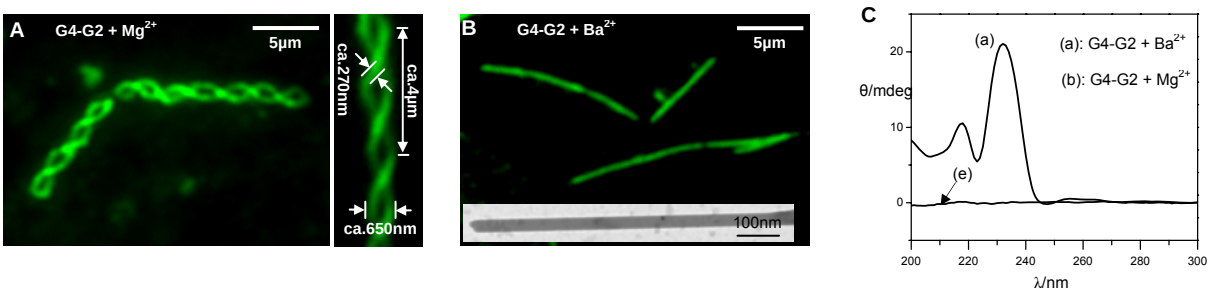

Figure 6.5 The self-assembly of **G4-G2** dendrimers induced by Mg^{2+} and Ba^{2+} in aqueous solution. **(A)** Mg^{2+} and **(B)** Ba^{2+}, **(C)** CD spectra of equilibrated **G4-G2** self-assembly in aqueous solution with the addition of (a) Ba^{2+}, (b) Mg^{2+}.

To unravel the mechanism behind the surprising close-ended supercoiled double-helice formation, we studied the kinetics of the non-symmetrical **G4-G2** dendrimer self-assembling process with the addition of Ca^{2+}, Figure 6.6. Before reaching the final equilibrium super-structures, several levels of structural self-organization were observed. Initially, single helical fibrils of ~5nm in diameter instantaneously formed upon the addition of Ca^{2+}, Figure 6.6A. In contrast to **G3-G2**, the much more pronounced size difference between the two lobes of the **G4-G2** dendrimers here causes helical formation. This is probably due to the steric effect imposed by the size difference, in synergy with the long range electrostatic repulsions along the fibril axis, that forces the single fibril spontaneously twist into helix as the negatively charged **G4-G2** dendrimer molecules bind head-to-head via COO^{-}-M^{2+}-COO^{-} salt bridges into single fibrils. Interestingly, we found the twist direction of these self-assembling **G4-G2** dendrimers is quite sensitive to directional external force. We found applying counter-clockwise vortex had led to predominant left-handed fibrils, whereas clockwise vortex led to predominant right-handed fibrils. One should note that the origin of the helical formation is not governed by vortex, but

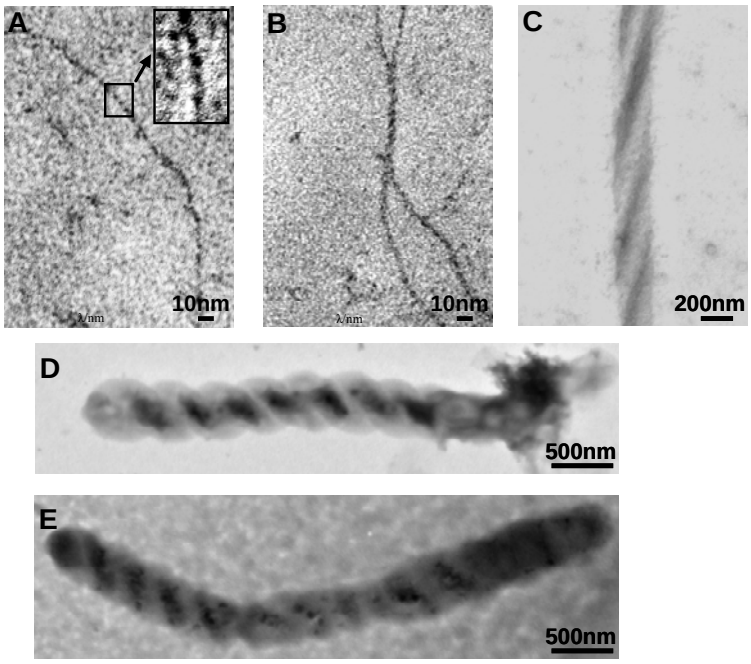

Figure 6.6 Kinetics of the supercoiled double-helice formation from the non-symmetrical **G4-G2** dendrimers with the addition of Ca^{2+}. (**A**) 30 sec after mixing; Inset: magnified TEM micrograph. (**B**) 5 min after mixing; (**C**) 2 hours after mixing; (**D**) 8 hours after mixing; (**E**) 12 hours after mixing.

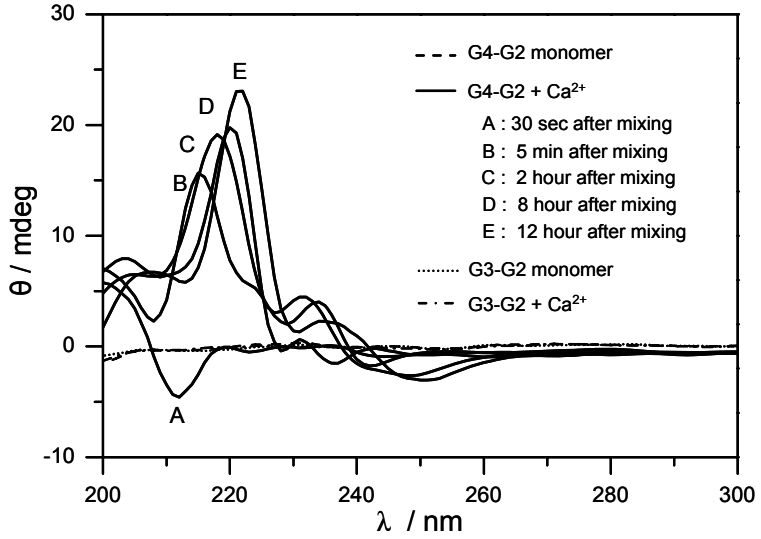

Figure 6.7 CD analysis of the kinetics of the supercoiled double-helice formation.

rather by the sufficient size difference in the non-symmetrical dendrimers. With **G3-G2** dendrimers that have smaller size difference, no helical formation can be generated, whereas for **G4-G2** dendrimers that have sufficiently larger size difference, helical formation is spontaneous, either with or without vortex. Vortex, however, can influence the direction of the **G4-G2** fibril handedness and help achieve chiral resolution. Compared to seeding and other methods typically used in spontaneous resolution,[17] using external vortex to achieve chiral resolution in the self-assembling non-symmetrical dendrimer system here has the advantages of free of impurity and ease in control. Using counter-clockwise vortex as example, corresponding CD measurements showed a marked negative Cotton effect on achiral **G4-G2** dendrimer solutions upon the immediate addition of Ca^{2+}, Figure 6.7 (A), confirming the helical chirality of the formed single fibrils with a preferred handedness. Otherwise, a racemic mixture of helices with the opposite handedness would cancel out the CD signal. As a comparison, no CD signal was observed for **G3-G2** dendrimers under the same condition, consistent with their nature in producing achiral fibrils instead of chiral helices.

After the formation of the initial single helical fibrils, dimers of helical fibrils coiling around each other started to form within minutes, Figure 6.6B. Like many natural biopolymers,[18,19] the coiling of the helical fibrils here was of opposite handedness. Using counter-clockwise vortex system as example, predominantly right-handed dimer coils of the left-handed single fibrils were observed by TEM, Figure 6.6B. The corresponding CD measurements showed the flipping of the Cotton effect from negative to positive, Figure 6.7 (B). The absorption band also slightly shifted to longer wavelength, which is typical for further aggregation. Coiling of fibrils continued for hours and had produced thicker right-handed coiled-coil bundles, Figure 6.6C. The coiled bundles could reach up to ca. 250nm in thickness, containing about 50 fibrils.

Eventually, the accumulating torsional force along the coiling bundles led to spontaneous looping in the center and positive supercoiling upon themselves. Predominant right-handed supercoiled double-helices with a loop on one end and open on the other end were observed by TEM, Figure 6.6D. In the final step, the open ends of the superoiled double-helice appear to gradually close, presumably to stabilize the supercoiled structures, Figure 6.6E. Positive supercoiling in biology, such as in DNA systems, requires assistance from scaffold proteins and/or topoisomerases, and the spontaneous positive supercoiling observed here is quite intriguing. Due to the unique branched feature of dendrimers, the hierarchical self-assembly of the **G4-G2** dendrimers with the addition of M^{2+} here is likely to be a highly cooperative process, which may play a critical role in the production of sufficient torsional force that can induce spontaneous looping and positive supercoiling.

We used Isothermal Titration Calorimetry (ITC) to further study the cooperativity of the Ca^{2+} binding that underlies the self-assembly process of the **G4-G2** dendrimers. The titration was exothermic and best fitted to two distinct binding sites, Figure 6.8. Unlike spherical dendrimers, the non-symmetrical dendrimers start to self-assemble via COO^{-}-Ca^{2+}-COO^{-} salt-bridge bindings at Ca^{2+} stoichiometry as low as Ca^{2+}: COO^{-} ~ 1:10, indicating a negligible contribution from any individual COO^{-}-Ca^{2} counterion bindings on the ITC titration. The two most likely COO^{-}-Ca^{2+}-COO^{-} salt-bridge binding sites are the sites responsible for assembling **G4-G2** dendrimers into the initial individual helical fibrils and those responsible for fibril coiling. The much later stage of the spontaneous looping and supercoiling should have minimal impact on the ITC titration, since they are mostly resulted from the accumulating torsional force, rather than any further Ca^{2+} binding. The formation of the ordered single helical fibrils from large numbers of **G4-G2** monomers is most likely responsible for the first highly exothermic phase

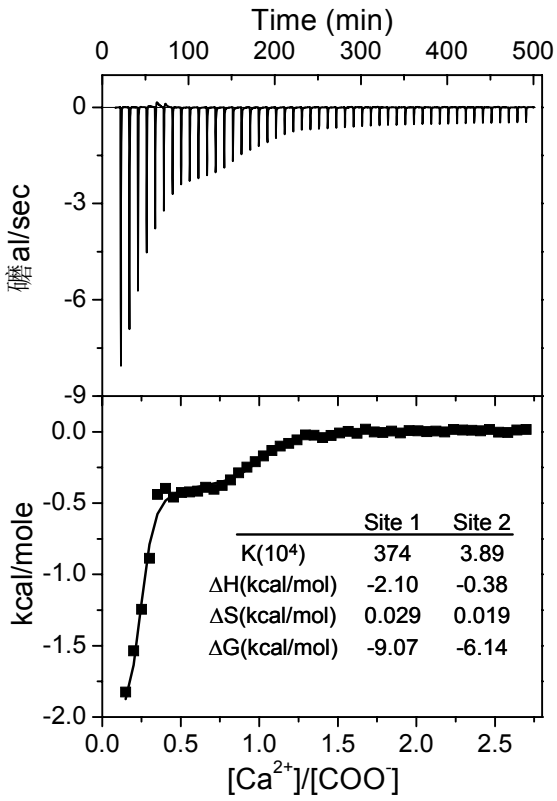

Figure 6.8 ITC analysis on Ca^{2+} binding to non-symmetrical **G4-G2** Fréchet-COO^- dendrimer. Upper panel shows the calorimetric titrations; Lower panel displays the integrated heat values as a function of molar ratio. The solid line represents the curve fitting to a two independent binding site model.

observed from ITC. The second less exothermic phase, on the other hand, better reflects the process of fibril coiling, where additional salt-bridges between individual strands of helical fibrils form coiled-coil bundles. For both processes, the entropic change is rather trivial, due to the offset between the entropic gain in solvent disorder and entropic loss in degree of structural freedom. The average binding constant for the two events was estimated as $K_1 \sim 3.74 \times 10^6\ M^{-1}$ and $K_2 \sim 3.89 \times 10^4\ M^{-1}$ respectively. Both are significantly larger than the published values for individual Ca^{2+}/COO^- counterion binding[20], indicating the highly positive cooperative nature of

the two self-assembling processes. In addition, both phases of the titration have sigmoidal characters, also suggesting cooperativity.

6.4 Conclusion

In summary, we show that introducing nano-scaled molecular shape non-symmetry can profoundly affect the supramolecular self-assembly process. Specifically, as the magnitude of shape non-symmetry increases**,** the supramoleualr dendrimer self-assembly formation is shifted from parallel achiral fribrillar bundles to surprising supercoiled double-helices. Thus, we have demonstrated that with cooperative non-covalent self-assembly conditions, molecular shape non-symmetry rather than traditional chrial centers can generate unusual and complex chiral supramolecular structures. In addition, we can also conveniently achieve chiral resolution by using directional external force, such as vortex. Our results provide new insights into supramolecular chirality and we also expect this finding will lead to new systematic design principle for constructing novel chiral supramolecular structures that maybe of interest for optoelectronic applications or as functional nanoparticle templates for chiral catalysis and sensor applications.

6.5 Experimental Information

6.5.1. Materials

Methyl ester protected G4, G3 and G2 Fréchet dendritic fragments were synthesized following the reported convergent route,[15] using 3,5-dihydroxybenzyl alcohol as the monomer unit and the step-wise growth consisting of activation by bromination and coupling by alkylation, Figure 2.7. G3 and G4 Fréchet dendritic fragments were then coupled with G2 fragment by a stepwise coupling to a difunctional core, 4,4′-dihydroxy-biphenyl[16], followed by hydrolysis of the methyl ester protecting groups, Figure 6.9. All synthesized dendrimers were characterized by

NMR before use. ^{1}H NMR ([H_6]-DMSO) of the synthesized G3-G2: δ(ppm) = 4.94 and 5.05 (m,44H,OCH_2), 6.4-6.7(m, 30H, ArH), 6.91(m,4H, core ArH), 7.44 and 8.00(m, total 52H, 48 PhH and 4 core ArH). ^{1}H NMR ([H_6]-DMSO) of the synthesized G4-G2: δ(ppm) = 4.95 and 5.10 (m,76H,OCH_2), 6.49-6.70 (m,54H,ArH), 6.91(m,4H,core ArH), 7.50 and 7.98 (m, total 84H, 80PhH and 4 core ArH).

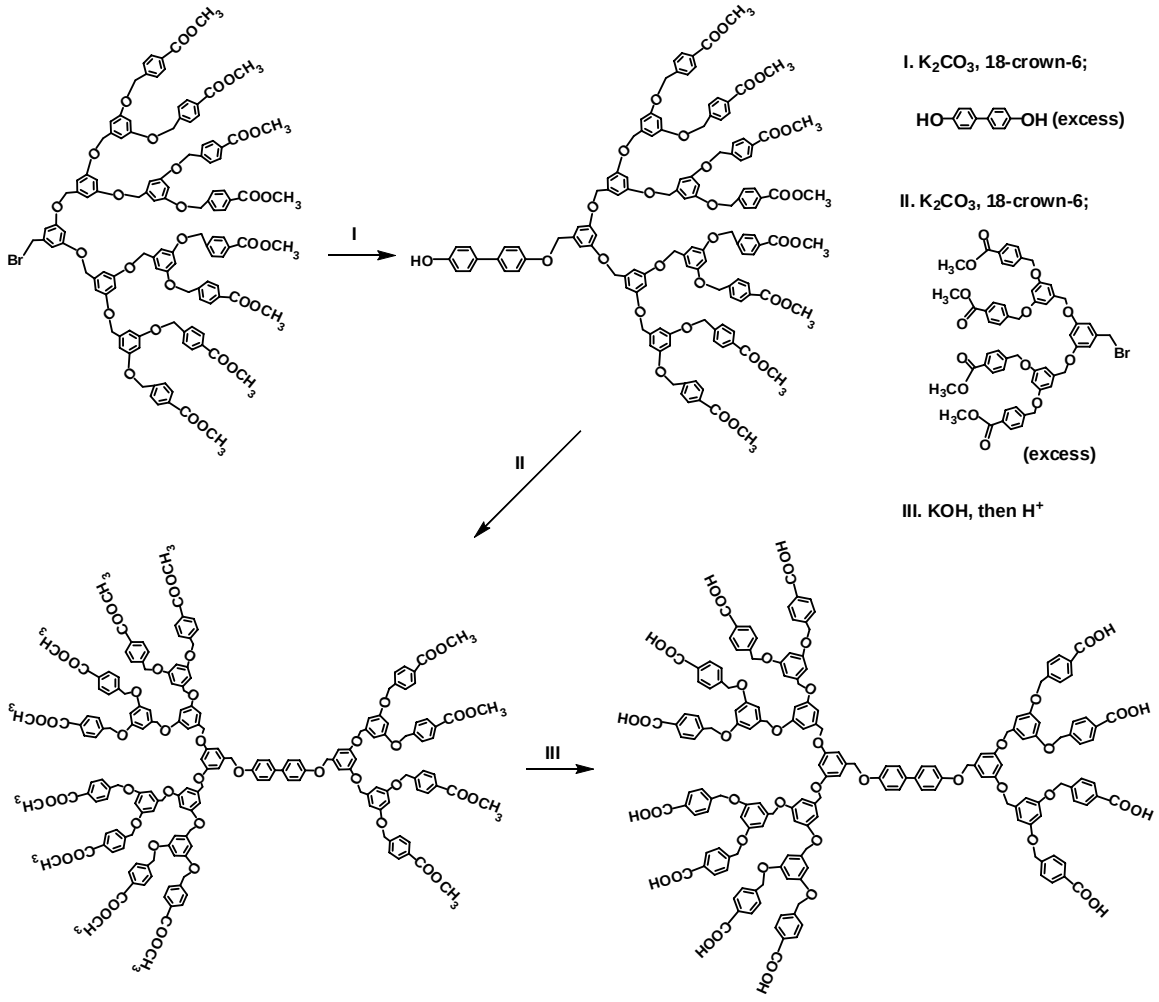

Figure 6.9. Reaction scheme for coupling G3 and G2 Fréchet dendritic fragments.

6.5.2. Methods

Fluorescent Microscopy Imaging was obtained by using a hydrophobic fluorophore dye (PKH 26) to label the **G3-G2** and **G4-G2** Fréchet-carboxylate dendrimers in aqueous solution. 3 μL samples were used in the chamber formed between glass slide and cover slip for imaging. The dipersed asymmetric dendrimer monomers and their self-assembly with the addition of Ca^{2+} in aqueous solution were directly observed on an Olympus IX71 inverted fluorescence microscope with a 60X objective and a Cascade CCD camera.

Transmition Electron Microscopy (TEM) measurements were carried by pipetting 2μL of dendrimer self-assembly aqueous solution onto a carbon coated copper grids. A piece of filter paper was then used to quickly remove the excess liquid, leaving a thin film of solution spanning the grid. The sample copper grids were then freeze dried before imaging. TEM images were obtained on a FET TECNAI 20G Transmission Electron Microscopy operating at an acceleration voltage of 200kV and at ambient temperature.

Circular Dichroism (CD) measurements of dendrimer aqueous solutions were recorded on Jasco J-715 spectropolarimeter with a scanning speed of 50 nm per min at 25ºC. The background absorbance from water was then subtracted from the recorded spectra before analysis.

Isothermal Titration Calorimetery (ITC) measurement were recorded on a VP-ITC MicroCalorimeter (MicroCal, Inc). Aqueous solution of 0.2 mM **G4-G2** dendrimer at pH 7 was loaded into the titration cell, and the reference cell was filled with deionized water. Fifty successive injections of 28 mM Ca^{2+} were made into the dendrimer sample cell in 5 μL increments at 10 min interval with stirring at 310 rpm to ensure complete binding equilibration. Control experiments to determine the heat of dilution were carried out by making identical

injections in the absence of dendrimers. The net binding reaction heat was obtained by subtracting the heat of dilution from the measured total heat of reaction. The titration data were then fitted using the MicroCal Origin software and least-square algorithm, and these data were best fit to a two independent binding site model. The binding enthalpy ΔH, binding constant K, and the binding stoichiometry n were permitted to float during the least-square minimization process and taken as the best-fit value.

6.6 References

(1) Engelkamp, H.; Middelbeek, S.; Nolte, R. J. M. *Science* **1999**, *284*, 785-788.

(2) Cornelissen, J. J. L. M.; Fischer, M.; Sommerdijk, N. A. J. M.; Nolte, R. J. M. *Science* **1998**, *280*, 1427-1430.

(3) Hirschberg, J. H. K. K.; Brunsveld, L.; Ramzi, A.; Vekemans, J. A. J. M.; Sijbesma, R. P.; Meijer, E. W. *Nature* **2000**, *407*, 167-170.

(4) Palmans, A. R. A.; Vekemans, J. A. J. M.; Havinga, E. E.; Meijer, E. W. *Angew. Chem.,Int. Ed.* **1997**, *36*, 2648-2651.

(5) Bae, J.; Choi, J. H.; Yoo, Y. S.; Oh, N. K.; Kim, B. S.; Lee, M. *J. Am. Chem. Soc.* **2005**, *127*, 9668-9669.

(6) Lin, S. C.; Lin, T. F.; Ho, R. M.; Chang, C. Y.; Hsu, C. S. *Adv. Funct. Mater.* **2008**, *18*, 3386-3394.

(7) Pelzl, G.; Diele, S.; Weissflog, W. *Adv. Mater.* **1999**, *11*, 707-724.

(8) Zerrouki, D.; Baudry, J.; Pine, D.; Chaikin, P.; Bibette, J. *Nature* **2008**, *455*, 380-382.

(9) Frechet, J. M. J.; Tamalia, D. A. *Dendrimers and Other Dendritic Polymers*; Whiley,: Chichester, UK, 2001.

(10) Newkome, G. R.; Moorefield, C. N.; Vogtle, F. *Dendritic Macromolecules: Concepts, Synthesis, Perspectives*; VCH, Wenheim, Germany, 2001.

(11) Zeng, F. W.; Zimmerman, S. C. *Chem. Rev.* **1997**, *97*, 1681-1712.

(12) Tomalia, D. A.; Brothers, H. M.; Piehler, L. T.; Durst, H. D.; Swanson, D. R. *Proc. Natl. Acad. Sci. U. S. A.* **2002**, *99*, 5081-5087.

(13) Ungar, G.; Liu, Y. S.; Zeng, X. B.; Percec, V.; Cho, W. D. *Science* **2003**, *299*, 1208-1211.

(14) Ju, R.; Tessier, M.; Olliff, L.; Woods, R.; Summers, A.; Geng, Y. *Chem. Commun.* **2011**, *47*, 268-270.

(15) Hawker, C. J.; Wooley, K. L.; Frechet, J. M. J. *J. Chem. Soc., perkin Trans. 1* **1993**, 1287-1297.

(16) Wooley, K. L.; Hawker, C. J.; Frechet, J. M. J. *J. Am. Chem. Soc.* **1993**, *115*, 11496-11505.

(17) Pérez-Garcíaa, L.; Amabilino, D. B. *Chem. Soc. Rev.* **2002**, *31*, 342-356.

(18) Eyre, D. R. *Science* **1980**, *207*, 1315-1322.

(19) Mclachlan, A. D. *Annu. Rev. Biophys. Bioeng.* **1984**, *13*, 167-189.

(20) Joseph, N. R. *J. Biol. Chem.* **1946**, 529-541.

CHAPTER 7

CONCLUSION AND OUTLOOK

7.1 Conclusion

In this dissertation, we exploited the unique feature of dendrimers as nano-sized macromolecules with highly-branched peripheral binding sites and demonstrated their ability to maximize cooperative binding as a novel modular self-assembly approach to design and construct functional supramolecular assemblies.

This cooperative binding self-assembly approach has the advantage of generality and versatility. Two classic types of dendrimers, Fréchet type and Newkome type dendrimers, which differ significantly in composition, branching motif and rigidity, can self-assemble into capsules via cooperative salt-bridging and hydrogen bondings, when they were functionalized with –COOH and –OH peripheral groups, respectively. Dendrimers with –COOH peripheral groups formed capsules in aqueous solutions with the addition of divalent metal ions. Such dendrimer capsules are tunable in size and thickness, controllable in disassembly, and can potentially be used for a wide variety of encapsulation applications. The cooperative feature of dendrimers showed more intriguing ability in regulating supramolecular self-assemblies via hydrogen bondings in highly-competitive solvents, *e.g.* water. The cooperative formation of multiple H-bonding networks can significantly enhance the strength and stability of H-bonding, which allows for dendrimer self-assembly into capsules even in highly competitive and disruptive aqueous solutions. These H-bonded dendrimer capsules have the advantage of the thermo-responsiveness to trigger controlled disassembly and release of encapsulated materials. Further

more, the utilization of emulsions in templating the cooperative self-assembly of dendrimers expands the capsule to a broad range of micron sizes, which allows for versatile and efficient encapsulation of a wide variety of materials. The micron-scaled emulsion-templated dendrimer capsules also have the advantages of ease in controlling disassembly and release of the encapsulant with external stimuli.

To further advance the functionality of dendrimer capsules, we combined other more directed interactions, such as hydrogen bondings and π-π interactions at dendrimers' core with the periphery cooperative bindings. Dendrimers with arene ring as the core self-assembled into capsules via periphery cooperative bindings, meanwhile the π-π interactions at dendrimers' core help stack them co-facially in membrane. This work serves as the foundation for incorporating functional groups into the core to generate dendrimer capsules with built-in pores/channels, which can spontaneously and selectively encapsulate or release certain materials.

Further more, we showed that introducing nano-scaled molecular shape non-symmetry can profoundly affect the supramolecular self-assembly process. Via periphery cooperative binding, the non-symmetric dendrimers showed to assemble into cylindrical superstructures, from parallel fibrillar bundles to supercoiled double-helices. This study not only provides new insights into supramolecular asymmetry, but also offers a new systematic design principle that with cooperative non-covalent self-assembly conditions, molecular shape non-symmetry rather than traditional chrial centers can generate unusual and complex chiral supramolecular structures.

7.2 Outlook

Our studies focused on fully exploring the unique multivalency feature of dendrimers on maximizing cooperative bindings. It demonstrated a modular self-assembly approach to design and construct functional supramolecular assemblies. So far, we showed that dendrimers can self-

assemble into capsules, fibrillar bundles and supercoiled double-helices via the cooperative Ca^{2+} bridging. However, other than Ca^{2+}, Mg^{2+} and Ba^{2+} also showed the ability to assemble dendrimers. With spherical dendrimers, Mg^{2+}, Ba^{2+} can assemble them into capsules with different size and thickness. Especially with the asymmetric dendrimers, Mg^{2+} can induce double-helices with a looser pitch, while Ba^{2+} can form rigid cylinders. If the effect of different ion can be better understand, it will further enrich our ability on manipulating dendrimer self-assemblies.

Secondly, other than simple benzene ring, more functional groups can be incorparatied as dendrimers' core, such as porphyrin, cyclodextrin, cyclic peptide and phenylacetyline macrocycles. These functional groups were shown to stake into columns via π-π interaction or hydrogen bonding, and they have the ability to specifically bind with a variety of guests into their cavity, ranging from metal ions, gases, to biomolecules. Capsules assembled by these core-functionalized dendrimers will have built-in selective pores/channels, which may spontaneously and selectively encapsulate or release certain materials.

Finally, we studied the cooperative self-assembly of spherical and asymmetric dendrimers, and revealed that the dendrimers shape can profoundly affect the supramolecular self-assembly process. In order to pursue more functional supramolecular structures, other geometric dendrimers and their self-assemblies will be further explored. These studies will greatly extend the versatility of this new modular self-assembly approach, and provide additional insight into the designing principle for supramolecular assemblies with sophisticated functionalities.